Kinetic study of copolymerization and terpolymerization of *N*-Carboxyanhydrides of Ornithine, Glycine and Aspartic acid

By

Siyasanga Mbizana

Thesis presented in fulfilment of the requirements for the degree of Masters of Science (Polymer Science)

at

Stellenbosch University

Supervisor: Prof. Bert Klumperman
Co-supervisor: Dr Rueben Pfukwa

Department of Chemistry and Polymer Science

Faculty of Science

December 2014

Declaration

By submitting this thesis electronically, I declare that the entirety of the work contained therein is my own, original work, that I am the owner of the copyright thereof (unless to the extent explicitly otherwise stated) and that I have not previously in its entirety or in part submitted it for obtaining my qualifications.

Siyasanga Mbizana December 2014

Abstract

Kinetic studies on polymerization of *N*-Carboxyanhydrides (NCAs) of ornithine, glycine and aspartic acid are described in this report. The studies involved the synthesis of protected amino acid derivatives which are subsequently phosgenated to afford the respective NCAs. Kinetic studies of homo and copolymerization of the NCAs were conducted via *in situ* ^{1}H NMR spectroscopy through monitoring the decrease of relevant proton intensities. NCA homopolymerization studies revealed the effect of side chains on NCA monomers, with NCAs bearing larger side chain groups being less reactive as observed on derivatives of aspartic acid and ornithine in comparison to glycine.

In subsequent kinetic copolymerization studies, it was observed that glycine (Gly) NCA incorporated more readily in the growing copolymer chain when copolymerized with β-benzyl-L-aspartate (Bz-Asp) NCA. In contrast, when Bz-Asp was copolymerized with protected ornithine NCAs, it was observed that Bz-Asp incorporated into the growing chain at a high rate compared to the Orn-based NCAs. Upon copolymerization of Gly NCA with N_{δ}-9-fluorenylmethyloxycarbonyl-L-ornithine (f-Orn) NCA, it was observed that the protons used to monitor the kinetics of Gly NCA were overlapping with those of f-Orn NCA protecting group. To overcome this problem, the carbobenzyloxy (Z) group was introduced as a protecting group on the ornithine side chain to afford Z-Orn NCA. The effect of the side chain protecting group on reactivity of ornithine NCAs (f-Orn and Z-Orn NCAs) was minimal as seen in the copolymerization with Bz-Asp. On the basis of binary copolymerizations, kinetic parameters were determined with the Contour software program, which uses the nonlinear least squares methodology in conjunction with the terminal unit copolymerization model and were found to be $r_g = 2.51$ and $r_a = 0.46$ for Gly/Bz-Asp system, $r_a = 3.92$ and $r_{of} = 0.40$ for Bn-Asp/f-Orn system and $r_a = 3.27$ and $r_{oz} = 0.48$ for Bz-Asp/Z-Orn system. The reported reactivity ratios were calculated by plotting copolymer composition versus feed composition and the experimental data fitted with constant relative error.

A preliminary terpolymerization reaction at approximately equimolar fractions of Gly, Bz-Asp and Z-Orn NCAs was conducted. From the terpolymerization mixture, the behaviour of NCAs as a function of conversion agreed with the monomer reactivities observed in the binary copolymerizations. It was observed that the ternary mixture initially led to a high overall fraction of Gly in comparison to Bz-Asp and Z-Orn in the terpolymer, but with increase in conversion the incorporation of the latter two monomers gradually increased in

the terpolymer. The NCAs can be arranged in terms of their reactivities as follows, Gly ≥ Bz-Asp ≥ f-Orn ≈ Z-Orn.

Opsomming

Kinetiese studies van die polimerisasie van *N*-Karboksi-anhidriede (NCA) van ornitien, glisien en aspartiensuur was in hierdie studie ondersoek. Die sintese van beskermde aminosuur afgeleides was uitgevoer voor dit gefosgeniseerd was na die onderskeie NCA's. Kinetiese studies van homo- en kopolimerisasies van die NCA's is gedoen via *in situ* ^{1}H-KMR spektroskopie, deur die afname van die relevante proton intensiteite te monitor. NCA homopolimerisasie studies het die effek van sykettings op NCA monomere getoon; NCA's met groter sykettinggroepe is minder reaktief vir afgeleides van aspartiensuur en ornitien in vergelyking met glisien.

In daaropvolgende kinetiese kopolimerisasie studies, is daar waargeneem dat glisien (Gly) NCA makliker opgeneem word in die groeiende kopolimeer ketting as dit gekopolimeriseer word met β-bensiel-L-aspartaat (Bz-Asp) NCA. In teenstelling hiermee was bevind dat as Bz-Asp gekopolimeriseer word met beskermde ornitien NCA, was dit waargeneem dat Bz-Asp teen 'n hoër tempo opgeneem word in die groeiende ketting in vergelyking met die Orn-gebaseerde NCA. By kopolimerisasie van Gly NCA met N_{δ}-9-fluorenielmetieloksikarboniel-L-ornitien (f-ORN) NCA, is daar waargeneem dat die protone wat gebruik is om die kinetika van Gly NCA te monitor, oorvleuel met dié van f-Orn NCA beskermingsgroep. Om hierdie probleem te oorkom, is die karbobensieloksie (Z) groep gebruik om as 'n beskerming groep op die ornitien syketting Z-Orn NCA te dien. Die effek van die sykettingbeskermingsgroep op reaktiwiteit van ornitien NCA (f-Orn en Z-Orn NCA) was minimaal soos waargeneem in die kopolimerisasie met Bz-Asp. Op die basis van binêre kopolimerisasies is kinetiese parameters bepaal met die *Contour* sagteware program, wat gebruik maak van die lineêre kleinste kwadrate metode in samewerking met die terminale eenheid kopolimerisasie model en is bevind $r_g = 2.51$ en $r_a = 0.46$ vir Gly / Bz-Asp stelsel, $r_a = 3.92$ en $r_{of} = 0.40$ vir Bn-Asp / f-Orn stelsel en $r_a = 3.27$ en $R_{oz} = 0.48$ vir Bz-Asp / Z-Orn stelsel. Die reaktiwiteit verhoudings is bereken deur die eksperimentele data (met 'n konstante relatiewe fout) deur die kopolimeer samestelling teenoor die invoer samestelling te plot.

'n Voorlopige terpolimerisasie reaksie op ongeveer ekwimolêre fraksies van Gly, Bz-Asp en Z-Orn NCA is uitgevoer. In die terpolimerisasie mengsel, het die gedrag van NCA's as 'n funksie van die omskakeling ooreengekom met die monomeer reaktiwiteite vanaf die binêre kopolimerisasies. Dit is waargeneem dat die drieledige mengsel aanvanklik gelei het tot 'n hoë algehele inhoud van Gly in vergelyking met Bz-Asp en Z-Orn in die terpolimeer, maar

met toename in die omskakeling het die inkorporering van die twee laasgenoemde monomere geleidelik toegeneem in die terpolymer. Die NCA kan in terme van hul reaktiwiteit rangskik word soos volg, Gly ≥ Bz-Asp ≥ f-Orn ≈ Z-Orn.

Acknowledgements

I would like to thank my supervisor Prof. Bert Klumperman for giving me the opportunity to work in his lab, under his supervision and for the support he provided throughout my study and my cosupervisor Dr Rueben Pfukwa for his wise words and suggestion when I stumbled in the project.

Dr Lebohang "L" Hlalele I wish I had a word that can express my gratitude for the valuable advices on my study and for patiently going through all my chapters. Mpho Phiri I am grateful for all your assistance particularly in processing "my first" *in situ* ^{1}H NMR experiments. *Ke a leboha ntate le 'm'e ka thuso ea lona.(thank you guys for your assistance)*

I would also like to thank Elsa Malherbe and Jaco Brands for helping in running NMR experiments. I would like to give thanks to the staff of Department of Chemistry and Polymer Science, the University of Stellenbosch and NRF for funding my study

I am grateful to the free radical group members: Rueben, Lebohang, Sandile, Paul, Khotso, Alex, Elrika, Lehani, Ingrid, Nicole, Sthembile, Anna, Mpho, Johnel, Njabu, Welmarie, William, Rueben, Nusrat and Waled (for the funny but fruitful discusions) for the support, encouragements, cheerful discussions and condonations you gave me.

I hope my siblings (Bulelani and his family, Nolwando, Nandipha, Solomzi and Aphelele) will forgive me for being an absent brother and I am grateful for their support and love, to my deceased parents these are the fruits of your upbringing and nurturing. Am also grateful to the Mbizana and extended family members (particularly uncle Thembalethu's family and Nonkumpuza's family).

A big thank to friends (Sandile, Aron, Mvuyisi Sithandile and Khaya).

Above all I'd like to give thanks and praise to the omnipotent God and saviour.

Table of contents

List of Figures

List of Schemes

List of Tables

List of Equations

List of Abbreviations

ECM	Extra cellular matrix
RGD	Arginine, Glycine and Aspartic acid tripeptide
LDV	Leucine, Aspartic acid and Valine tripeptide sequence
SPPS	Solid phase peptide synthesis
PLA	Polylactic acid
NHS	*N*-hydroxysuccinimide
ROP	Ring opening polymerization
NCAs	*N*-Carboxyanhydrides
NAM	Normal amine mechanism
AMM	Activated monomer mechanism
MWD	Molecular weight distribution
DMF	Dimethyl formamide
HMDS	Hexamethyldisilazane
TMS-CBM	Trimethylsilyl Carbamate
TMS	Trimethylsilyl
HCl	Hydrochloride
HVT	High Vacuum Technique
MALDI-ToF MS	Matrix-assisted laser desorption/ionization Time of flight mass spectrometry
NALDI-TOF MS	Nano-assisted laser desorption-ionization Time of flight mass spectrometry
THF	Tetrahydrofuran

CO_2	Carbon dioxide
FTIR	Fourier transform infrared spectroscopy
LROP	Living ring opening polymerization
RAFT	Reversible addition fragmentation chain transfer
ATRP	Atom transfer radical polymerization
PBLG	Poly(γ-benzyl-L-glutamate)
MMA	Methyl methacrylate
PEG-NH_2	Amine end capped poly(ethylene glycol)
PMOx-NH_2	Amine end capped poly(2-methyl-2-oxazolidine)
PAA	Poly(amino acids)
UV	Ultraviolet
NMR	Nuclear magnetic resonance
HPLC	High performance liquid chromatography
Vs.	Versus
IR	Infrared
SPS	Sequential peptide synthesis
Bz-Asp	β-benzyl-L-Aspartate
Z-Orn	N_δ-Carbobenzyloxy-L-Ornithine
Gly	Glycine
f-Orn	N_δ-9-Fluorenylmethyloxycarbonyl-L-Ornithine
Lys	Lysine
Glu	Glutamine
DMSO-d_6	Deuterated dimethyl sulfoxide

Fmoc	9-fluorenylmethyloxycarbonyl
TFA	Trifluoroacetic acid
TFA-*d*	Deuterated Trifluoroacetic acid
NMP	*N*-Methylpyrrolidone
MHz	Megahertz
SEC	Size exclusion chromatography
EDTA	Ethylenediaminetetra-acetic acid

List of symbols

R_H	Hydrodynamic radii
X	Halogen
Z	Carbobenzyloxy group
$^{a}M_n$	Number average molar mass measured by SEC
$^{b}M_n$	Number average molar mass measured by ^{1}H NMR
M_w	Weight average molar mass
$Đ$	Molecular weight dispersity
$[M]_o$	Initial monomer concentration
[M]	Monomer concentration
f^0	Initial feed composition
f	Instantaneous feed composition
X	Individual monomer conversion
F	Instantaneous copolymer composition
cF	Overall or cumulative copolymer composition
X_t	Overall conversion
r	Reactivity ratio

Chapter I: Introduction

Synthetic biopolymers find use in biomedical and pharmaceutical applications. For example, hydrophobic polyesters are well known for their biocompatibility, low immunogenicity and good mechanical properties.[1] Their applications in tissue engineering, drug delivery systems and in various other medical applications however are limited by poor interaction with cells that may lead to foreign body reactions *in vivo*. The lack of functional groups in these polymer structures further rules out modification with biological moieties. Polyesters can be modified by the introduction of other polymer segments such as a hydrogel forming PEG block, or functionalization for targeted post-polymerization modifications, *e.g.* with polycarbonates and poly(amino acids).

Biopolymers can further be functionalized with specific proteins or peptides to enhance interactions with cells.[2] Although proteins by virtue of being natural materials offer general biocompatibility as well as enzyme degradation, their application is limited since proteins have to be isolated from organisms. In addition there is the need for purification due to degradation upon storage *i.e.* prior to application. Most of the challenges posed by proteins can be overcome by immobilising small peptides segments onto biopolymers. These segments are affordable, exhibit slow degradation, and they selectively target a particular type of cell adhesion receptors. Short peptide immobilization merges properties of proteins with those of synthetic polymers. One such peptide segment is a tripeptide sequence composed of amino acids of arginine, glycine and aspartic acid (RGD) (Figure 1-1) found in most proteins that promote cell adhesion in the extracellular matrix (ECM).[3]

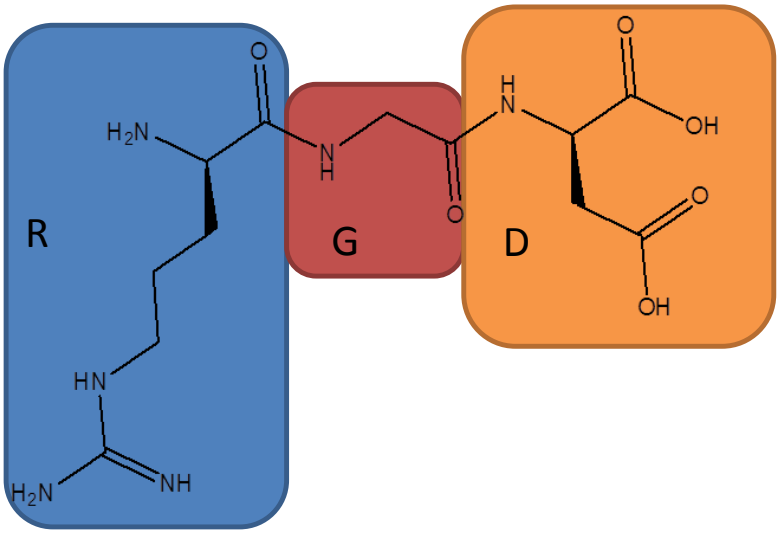

Figure 1-1 Arginine-glycine aspartic acid (RGD) sequence structure

1.1. RGD as an adhesive tripeptide sequence

The specific mechanism for adhesion of cells by RGD sequences is complex since RGD binds to a number of integrins and the receptor specificity varies among matrix molecules. The cell adhesion mechanism mediated by integrins on proteins can essentially be divided into four steps: cell attachment, cell spreading, formation of stress fibers through actin organization and formation of focal adhesions that link molecules of the ECM to stress fibers of the cell (actin cytoskeletons).[4] The role of the RGD sequence as a cell attachment site was illustrated by replacing one of the amino acids in the sequence with another possessing a similar functionality *e.g.* (alanine for glycine, glutamic acid for aspartic acid, lysine for arginine, etc.).[5,6] In all cases, it was observed that any amino acid substitution decreased cell attachment activity. Functionalization of synthetic biopolymers with RGD sequences improved cell attachment and cell proliferation.[7,8]

1.1. Synthesis of RGD sequence

Short peptides containing the RGD sequence can be prepared via enzymatic and chemical methods.[9,10] The advantages of an enzymatic method are mild conditions, high regioselctivity and stereospecificity. However, the low solubility of hydrophilic amino acids in organic solvents results in low yields with enzymatic method.[11] Short RGD peptides can be prepared

by solid phase peptide synthesis (SPPS).[12] SPPS is used to prepare peptides with a well-defined sequence of amino acids.[13,14] Its application for the preparation of higher molecular weight peptides is hampered by racemization and only short peptides can be prepared due to complexity of the technique.[15]

Facile synthesis of high molecular weight peptides without a specific amino acid sequence and subtle racemization proceeds via ring-opening polymerization (ROP) of α-amino acids *N*-carboxyanhydrides (NCAs). Traditionally, ROP of NCAs proceeds by initiation with either basic or nucleophilic initiators with release of CO_2 (Scheme 1-1). Termination reactions and other side reactions limit the ability of ROP to afford complex peptides structures. The development of living ROP (LROP) of NCAs countered this by suppressing the side reactions, therefore improving control over molecular weight distribution and polymer structures, hence allowing the preparation of advanced structures such as block, graft and hybrid copolypeptides. LROP of NCAs may proceed either by protecting the growing active chain ends from termination reactions or by tuning reaction conditions so as to decrease unintended reactions.

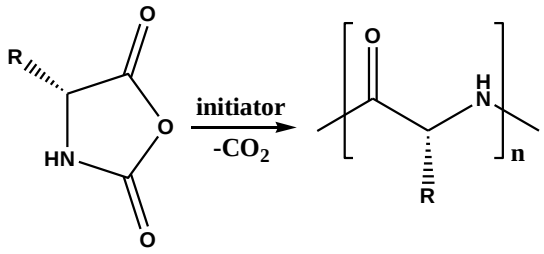

Scheme 1-1 Ring-opening polymerization of *N*-carboxyanhydrides

Statistical polypeptides that resemble natural proteins are prepared by simultaneous copolymerization of two or more NCAs. The average distribution or sequence of amino acids along the chain is understood by knowing reactivity ratios of NCAs. Statistical polypeptides retain natural peptide (protein) properties such as degradation by proteolytic enzymes and they adapt secondary structures, etc. Due to the variety of amino acids, the number of initiators available and effortlessness of the method, ROP of NCAs is an ideal lab scale method for preparation of higher molecular weight peptides.

Statistical or random copolymerization of NCAs are well documented where copolymerization parameters are used to express reactivity of NCAs and provide knowledge of the amino acid distribution along the polypeptide chain.[16] In earlier studies, the progress of

copolymerization reaction was followed by monitoring the released CO_2 or the decrease of NCA carbonyl intensity with IR, however both methods cannot selectively distinguish between different NCAs. As a consequence, little or no detailed kinetic information on copolymerization of NCAs is available. Recently, Zelzer *et al.* reported an the application of HPLC to describe the copolymerization kinetics of NCAs of benzyl-L-glutamate and carbobenzyloxy-L-lysine.[17] With the inclusion of benzyl-L-tyrosine as third monomer, the HPLC application was extended to the determination of terpolymerization kinetics.[18] The terpolymerization of NCAs of leucine, aspartic acid and valine, which act as interaction sites between $\alpha_4\beta_1$ integrin and ECM has been reported and copolymerization parameters were reported.[19] However up to this point, we are not aware of any report where kinetics of NCA co- and terpolymerization are monitored by *in situ* ^{1}H NMR. Similarly, to the best of our knowledge, post-polymerization treatment or modification of terpolymers for further applications such as cell activities, drug deliveries, etc. has not been reported.

1.2. Aim of the study

The focus of this study is to synthesize a terpolymer (terpolypeptide) that through modification may possess the RGD sequence. Simultaneous ROP of three different NCAs will be used to prepare the terpolypeptides. The study will involve synthesis of NCA monomers, kinetic studies of homopolymerization and copolymerizations to understand their reactivity. *In situ* ^{1}H NMR will be used to follow the kinetics of homo-, co- and preliminary terpolymerization of NCAs. As a remark, the results obtained here can be used as a build-up in understanding terpolymerization behaviour of the respective NCAs.

The amino acids of choice are glycine, aspartic acid and ornithine. Ornithine is used as a precursor for arginine. The two differ only by the pendant group (primary amine versus guanidine). Ornithine is a non-natural amino acid, which has been employed in synthetic procedures as arginine precursor due to the difficulties associated with handling the guanidine group of arginine. Therefore guanidination of ornithine side chains affords arginine segments in polypeptides.

1.3. Outline of the report

1.3.1. Chapter II: Literature Review

Chapter II deals with the methods employed in peptide synthesis with emphasis on the Ring Opening Polymerization of α-*N*-Carboxyanhydrides (ROP of NCAs) as the conventional route. The conventional methods as well as developments leading to living ROP of NCAs are well elucidated and techniques used to prepare polypeptides architectures

1.3.2. Chapter III: The synthesis of *N*-Carboxyanhydrides

Chapter III deals with a brief introduction into the methods commonly used in the synthesis and purification of amino acid NCAs. Details of the procedures used to synthesize protected amino acids derivatives and the corresponding NCAs used in this study will be described in conjunction with the relevant NMR analyses.

1.3.3. Chapter IV: Homopolymerization of *N*-Carboxyanhydrides

Chapter IV deals with Ring-Opening Polymerization (ROP) of *N*-Carboxyanhydrides (NCAs) for preparation of poly(β-benzyl-L-aspartate), polyglycine, poly(N_δ-carbobenzyloxy-L-ornithine) and poly(N_δ-fluorenylmethyloxycarbonyl-L-ornithine). Initial lab scale homopolymerizations were carried out as test for controlled homopolymerizations of the respective NCAs with *in situ* ^{1}H NMR measurements. The *in situ* ^{1}H NMR measurements were conducted to monitor NCA consumption with time. The *in situ* ^{1}H NMR homopolymerization were necessary as a build up for co- and a preliminary terpolymerization reaction studied in Chapter V.

1.3.4. Chapter V: Copolymerization and Terpolymerization of Ornithine, Glycine and β-benzyl-L-Aspartate *N*-Carboxyanhydrides

Chapter V deals with binary copolymerizations of NCAs of glycine, β-benzyl aspartate, and protected ornithine as a build up for future terpolymerization studies. Kinetic studies of various binary copolymerizations are conducted in order to determine their reactivity ratios. Similar to homopolymerizations in Chapter IV, the binary copolymerizations are initiated by *n*-butylamine in DMSO-d_6 at room temperature under vacuum and followed via *in situ* ^{1}H NMR spectroscopy. The conditions from the binary copolymerizations are subsequently used as a build-up to a preliminary terpolymerization reaction.

1.3.5. Chapter VI: Outlook

Chapter VI deals with future objectives *i.e.* discussion on how terpolymer synthesis can be optimized to maximize the frequency of RGD sequences, based on results obtained from copolymerization kinetics. It also went further as to give an idea of how the RGD sequence will be analysed and probably be quantified. Finally, the plans are discussed of how the prepared terpolymers will be immobilized on hydrogels and tested in contact with mammalian cells.

1.4. References

(1) Amass, W.; Amass, A.; Tighe, B. *Polym. Int.* **1998**, *47*, 89.

(2) Ishihara, K.; Ishikawa, E.; Iwasaki, Y.; Nakabayashi, N. *J. Biomater. Sci., Polym. Ed.* **1999**, *10*, 1047.

(3) Ruoslahti, E.; Pierschbacher, M. D. *Cell* **1986**, *44*, 517.

(4) LeBaron, R. G.; Athanasiou, K. A. *Tissue Engineering* **2000**, *6*, 85.

(5) Lu, X.; Rahman, S.; Kakkar, V. V.; Authi, K. S. *J. Biol. Chem.* **1996**, *271*, 289.

(6) Pierschbacher, M. D.; Ruoslahti, E. *Proc. Natl. Acad. Sci. U. S. A.* **1984**, *81*, 5985.

(7) Brandley, B. K.; Schnaar, R. L. *Anal. Biochem.* **1988**, *172*, 270.

(8) Zhu, J.; Beamish, J. A.; Tang, C.; Kottke-Marchant, K.; Marchant, R. E. *Macromolecules* **2006**, *39*, 1305.

(9) Aufort, M.; Gonera, M.; Chaignon, N.; Le Clainche, L.; Dugave, C. *Eur. J. Med. Chem.* **2009**, *44*, 3394.

(10) Yamada, K.; Nagashima, I.; Hachisu, M.; Matsuo, I.; Shimizu, H. *Tetrahedron Lett.* **2012**, *53*, 1066.

(11) Zhang, L.-Q.; Zhang, Y.-D.; Xu, L.; Li, X.-L.; Yang, X.-c.; Xu, G.-L.; Wu, X.-X.; Gao, H.-Y.; Du, W.-B.; Zhang, X.-T.; Zhang, X.-Z. *Enzyme Microb. Technol.* **2001**, *29*, 129.

(12) Chen, X.; Park, R.; Shahinian, A. H.; Bading, J. R.; Conti, P. S. *Nucl. Med. Biol.* **2004**, *31*, 11.

(13) DeGrado, W. F.; Kaiser, E. T. *J. Org. Chem.* **1980**, *45*, 1295.

(14) Merrifield, R. B. *Biochemistry* **1964**, *3*, 1385.

(15) Carpino, L. A.; El-Faham, A.; Albericio, F. *Tetrahedron Lett.* **1994**, *35*, 2279.

(16) Kumar, A. *CPR* **2011**, *1*, 219.

(17) Zelzer, M.; Heise, A. *Polym. Chem.* **2013**, *4*, 3896.

(18) Zelzer, M.; Heise, A. *J. Polym. Sci., Part A: Polym. Chem.* **2014**, n/a.

(19) Wamsley, A.; Jasti, B.; Phiasivongsa, P.; Li, X. *J. Polym. Sci., Part A: Polym. Chem.* **2004**, *42*, 317.

Chapter II: Literature Review

Summary

This chapter reviews methods employed in peptide synthesis with emphasis on the Ring Opening Polymerization of α-*N*-Carboxyanhydrides (ROP of NCAs) as the conventional route. The conventional methods as well as developments leading to living ROP of NCAs are elucidated as well as the techniques used to prepare polypeptide architectures.

Introduction

Proteins and peptides play a vital role in life. They possess fascinating properties, *e.g.* their self-assembly into secondary structures, biocompatibility, and their biodegradation via enzymatic processes. Natural proteins are composed of approximately 20 different L-amino acids, arranged in a perfectly controlled sequence that dictates their properties. In nature, proteins are synthesized by transcription from DNA and translation of RNA. Through this method, up to thousands of amino acids are linked in a specific order for every natural protein by peptide bonds.

There has been a growing interest in the development of synthetic routes for the preparation of polypeptides that mimic natural proteins. Prebiotic formation of poly(amino acids) originated from the idea that amino acids undergo polycondensation at high temperatures to yield proteins.[1,2] Heating two or more amino acids above the boiling point of water (110-200 °C), leads to formation of protein-like polymers (proteinoids). Due to the requirement of acid catalysis, this works best with amino acids that have dicarboxylic acid groups like aspartic acid and glutamic acid or in the presence of phosphoric acid.[2,3] The copolymerization of 18 amino acids for a few hours under the above mentioned conditions yields a panpolymer (*i.e.* a polymer obtained from condensation of eighteen amino acids).[4,5] The disadvantages of thermal polymerization are susceptibility to decomposition of starting materials and products, racemization, nonprotenoids products, crosslinking and mixed linkages.[6,7] Recently, mechanistic studies of thermal polymerization showed a variety of products.[8,9]

The synthesis of peptides with a well-defined predetermined amino acid sequence can be afforded by sequential addition of amino acids via solid-phase peptide synthesis (SPPS).[10-13] The growing peptide is immobilised on a solid support, to render the peptide insoluble, which allows for impurities to be easily washed off. SPPS is limited to relatively low molecular weight peptides, low yields, racemization[14] and the chemistry involved with coupling and protection-deprotection steps.

Synthetic procedures employed to minimize complexities involved in SPPS are carried out in solution, where the activated amino acid derivatives are grown to polymers. The synthesis of polypeptides of higher molecular weights which retain properties of proteins relies on ring-opening polymerization (ROP) of *N*-Carboxyanhydrides (NCAs) of amino acids that have been purified and isolated. The term used to describe these products is synthetic polypeptides

or poly(amino acids) as opposed to proteins, to emphasize that their lack a specific amino acid sequence.

Synthetic polypeptides mimic natural proteins, with applications in the biomedical field, *e.g.* tissue engineering. They are biocompatible and possess a tendency to form secondary structures, albeit to a lesser extent, not as well defined and sophisticated as in the case of proteins. It is important for synthetic polypeptides to be well-defined with high molecular weight, structural homogeneity and appropriate functionality in order to self-assemble into nanostructures. The establishment of living initiating systems for ROPs of NCAs of amino acids led to well-defined polypeptides and hybrids, with high molecular weights and structural homogeneity.

2.1. Conventional Ring Opening Polymerization of *N*-CarboxyAnhydrides of α-amino acids

The typical method employed for preparation of long chain-polypeptides is ROP of NCAs of α-amino acids. From simple reagents, polypeptides can be prepared in good yields, with high molecular weights and no detectable racemization. Different amino acid NCAs offer access to a wide range of polypeptides that can be prepared. However, these polypeptides have been either homopolymers or a variety of copolymers that lacked control over monomer sequence and over dispersity compared to natural proteins. ROP of NCAs proceeds with elimination of carbon dioxide, where the polymerization mechanism is dictated by the initiator (see Scheme 2-1). Conventionally, nucleophilic and basic initiators are used to initiate ROP of NCAs, giving rise to normal amine mechanism (NAM) and activated monomer mechanism (AMM), respectively. Below are the discussions of mechanisms involved in the NCA ROP and development to living ROP techniques.

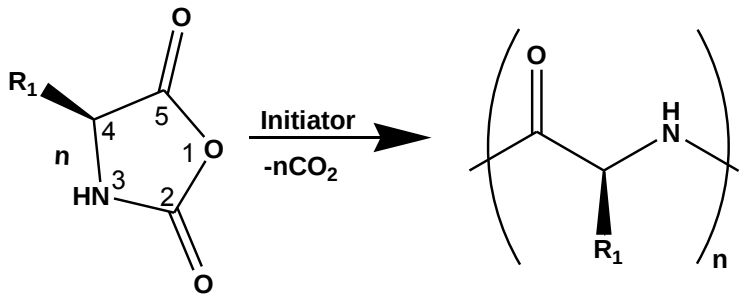

Scheme 2-1 Conventional ROP of NCAs of α-amino acids.

2.1.1. Normal Amine Mechanism

The NAM proceeds by nucleophilic attack of NCAs with initiators having at least a mobile hydrogen atom such as primary and secondary amines, water and alcohols. Primary amine initiators are preferred for their superior control over molecular weight as judged from the agreement between experimental and theoretical molecular weights.[15]

Upon nucleophilic attack (see Scheme 2-2) at the carbonyl carbon 5C of the NCA to cleave the 5C-1O bond, an intermediate carbamic (also carbamate) anion is formed that rapidly transforms to a carbamic acid by accepting a mobile hydrogen from the initiator, which then decarboxylates to form a primary amine that continues propagation.[16,17] By means of density functional theory calculations, Ling[17] showed that NAM is a three step mechanism, i.e. addition, ring opening and decarboxylation and further proved that the addition of initiator to the NCA is the rate determining step.

Primary amine initiators are more nucleophilic than the propagating ω-amino groups. Therefore, the initiation step is faster than the propagation step, leading to polypeptides with a narrow MWD and molecular weights in good agreement with predictions based on the monomer to initiator ratio. The use of primary amines ensures incorporation of initiator to the α-chain end.

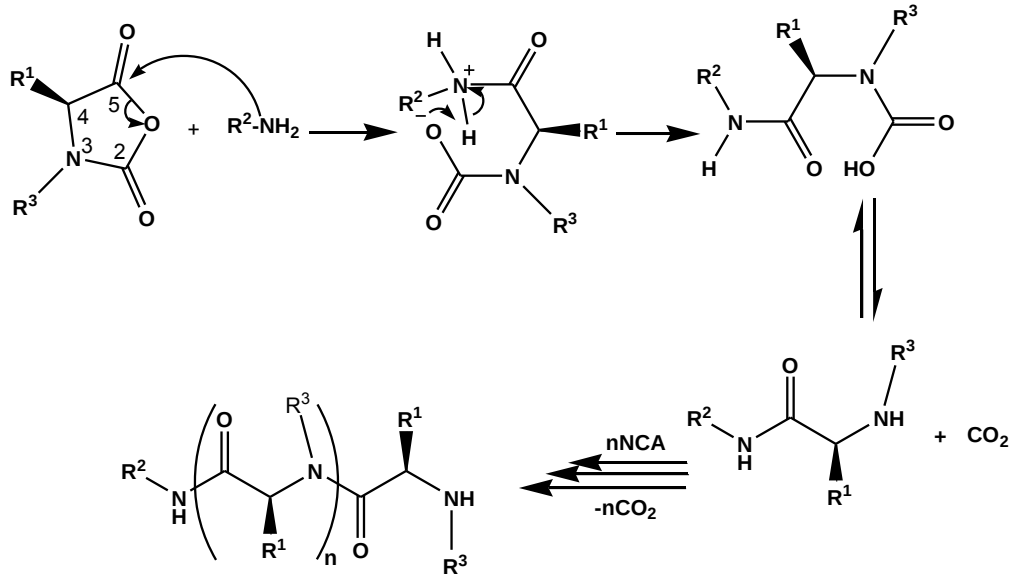

Scheme 2-2 The normal amine mechanism for the ROP of NCAs.

2.1.2. Activated Monomer Mechanism

The AMM is followed when basic species (mostly tertiary amines) initiate NCAs.[18,19] The basic initiator abstracts the hydrogen attached to the nitrogen atom of the NCA, forming an NCA anion (Scheme 2-3). In this case, the tertiary amine initiator acts as a catalyst that activates the NCA monomer, and is therefore not included in the final polymer in contrast to the initiator in NAM.[20-25] Initiation takes place by nucleophilic attack of an NCA anion to the 5C of neutral NCA to give a dimeric NCA anion, with release of carbon dioxide. Propagation proceeds by a similar attack of the dimeric NCA anion on a neutral NCA to give the trimeric NCA anion and so on. Bamford showed that the rate of propagation increases with increase in base strength of the initiator in AMM.[26] The initial step in AMM involves monomer activation before initiation and the initiation rate is lower than the propagation rate, leading to polymers with broad molecular weight distribution (MWD) and molecular weights that cannot be predicted from monomer/initiator ratio. As a consequence, tertiary amines are less frequently used as initiator/catalyst compared to primary amines.

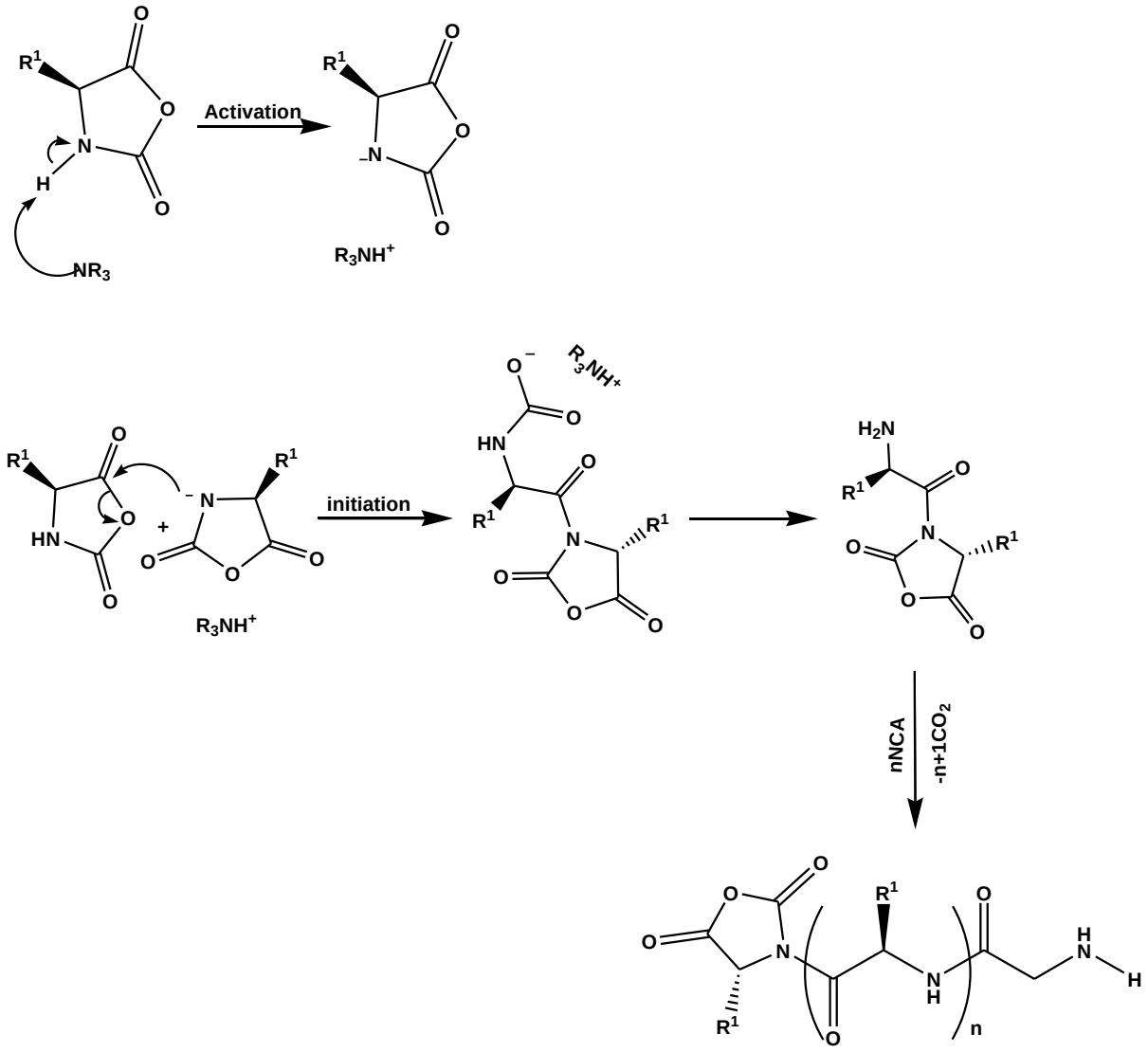

Scheme 2-3 Activation, initiation and propagation steps of the Activated Monomer Mechanism.

Primary amine initiators can polymerize NCAs with or without an H attached to the endocyclic nitrogen (R^3 = H) and ($R^3 \neq$ H) in contrast tertiary amine initiators operate by abstracting the H attached to the endocyclic N, *i.e.* it only applies when (R^3 = H) (see Scheme 2-2).[26] When secondary amines are employed for polymerization of NCAs both AMM and NAM can coexist.[24,27]

Abstraction of hydrogen at the α-carbon was reported when strong bases are used for polymerization of *N*-substituted NCAs. Since tertiary amines cannot initiate *N*-substituted NCAs and since the rate of polymerization cannot be explained in terms of primary amine initiation, it was concluded that propagation occurs by addition of the carbamate anion to an

NCA molecule to form a mixed anhydride. The unstable anhydride subsequently decomposes to a peptide bond. This was also demonstrated as neither free amines nor amide ions were available to the polymerization solution.[28]

Side reactions in ROP of NCAs may arise from impurities.[29-31] Termination reactions such as formation of ureido end groups occur when the propagating amino end group attacks the NCA at 2C instead of 5C.[32] (see Scheme 2-2 for numbering) Terminations can also occur due to propagating amine end groups reacting with solvents, *e.g.* DMF.[33] These side reactions limit the ability of conventional ROP of NCAs to produce polypeptides with end group functionality. Invention of living ROP of NCAs minimized side reactions that caused improper propagations and unwanted terminations.

2.2. Living ring-opening polymerization of *N*-CarboxyAnhydrides of α-amino acids

The presence of chain termination and side reactions in conventional ROP of NCAs, results in polypeptides with limited control over molecular weight and MWD, which hampers the preparation of well-defined polypeptides. An ideal ROP of NCA would be one with no chain-breaking reactions, *i.e.* the propagating active species remain intact throughout the polymerization process. The following section deals with the attempts made to gain control over ROP of NCAs.

2.2.1. Transition metal initiators

To minimise side reactions, Deming *et al.* pioneered the first living ROP of NCAs utilizing transition metal initiators.[34-37] This approach provided access to well-defined block copolymers, capable of being peptide biomaterials with potential application in drug delivery and tissue engineering.[35,38] Deming *et al.* found that zero-valent organometallic complexes bipyNi(COD) and $(PMe_3)_4Co$, polymerize NCAs via living ROP to high molecular weight polypeptides and narrow molecular weight distributions were obtained.

Mechanistic studies showed that both these metal complexes react identically with NCAs (Scheme 2-4), forming metallacyclic complexes by oxidative addition onto the NCA. These intermediates then react with a second NCA to yield 6-membered amido-alkyl metallacycles. The amido-alkyl metallacycles react with NCAs to yield larger metallacycles, which contract to generate the active species, *i.e.* 5-membered amido-amidate upon migration of proton to the metal-bound carbon. Propagation takes place by nucleophilic attack of the amido group

on the electrophilic carbonyl 5C of the NCA, generating a larger metallacycle which contract by elimination of carbon dioxide and proton transfer. In this way, the metal is able to migrate along the growing chain and is kept in place by chelation at the active chain end.

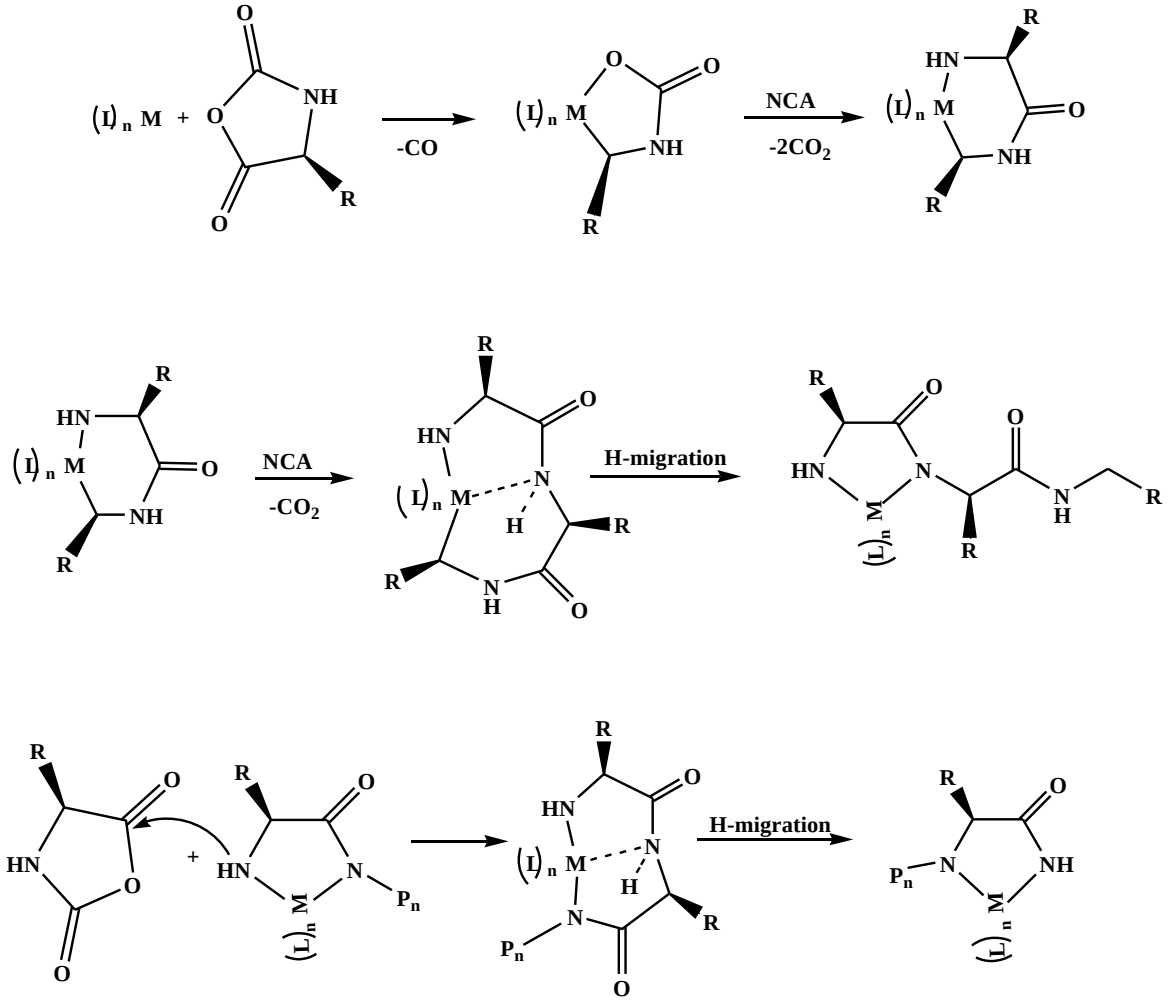

Scheme 2-4 Polymerization of NCAs with zero valent metals.

The requirement for living polymerizations with these transition metal-based initiators is the formation of chelating metallacyclic intermediates. Initiation with cobalt and nickel complexes is feasible and maintains the stereochemistry around chiral centres.[39]

The subsequent removal of metals poses extra work, whereas incomplete metal removal restricts biological applications. Furthermore, the metal-initiated polymerization is apparently only feasible with unsubstituted NCAs, as seen with proline (*N*-substituted) yielded no polymer, hence no ring contraction.[40] In addition, not all of the initiator used leads to the initiation of polymerization, as some portion complexes with carbon monoxide (released

during the first NCA addition). Hence, the observed average molecular weights are usually higher than predicted from initial monomer/initiator ratio.

2.2.2. Hexamethyldisilazane mediated living ROP of NCAs

Lu *et al.* reported the controlled living polymerization of NCAs mediated by hexamethyldisilazane (HMDS).[41] The initiation with HMDS showed quite a different behaviour to those initiated by conventional amines. As a secondary amine, HMDS (Scheme 2-5) is expected to have both nucleophilic and basic characters, which promote propagation by NAM and AMM respectively, whereby AMM is expected to prevail due to steric hindrance at the HMDS amine.

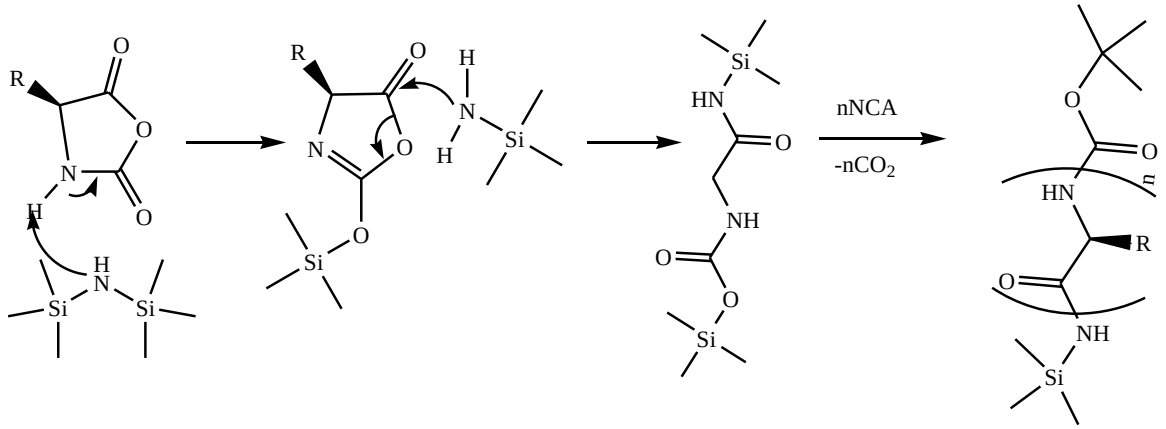

Scheme 2-5 Mechanism of Hexamethyldisilazane-mediated ROP of NCAs.

The first step involves deprotonation of the endocyclic 3NH by HMDS (Scheme 2-5**)**. The Si-N bond cleaves to form TMS-amine which ring-opens the NCA at 5CO resulting in a TMS-amide at the C-end, while the TMS group attaches to the N-end to form trimethylsilyl carbamate (TMS-CBM). Propagation then proceeds through transfer of TMS from TMS-CBM to the incoming monomer. It was confirmed later that TMS-CBM is the propagating species/group.[42,43] Polymers with molecular weights in agreement with the monomer/initiator ratio and with narrow molecular weight distributions, as well as block copolymers via sequential monomer addition were prepared with this method. Drawback of this method is that it applies only to unsubstituted NCAs, as the initiation step requires deprotonation of 3NH.

2.3. Improvements in normal amine mechanism and reaction conditions

All the above mentioned living polymerization techniques (Sections 2.2.1 and 2.2.2) require the addition of a species to protect the growing peptide from termination reactions and other side reactions. Since NAM ensures rapid initiation and efficient incorporation of the initiator to the growing chain, NAM possesses the ability to control ROP of NCAs if the propagating ω-amino group stays intact throughout the polymerization. Tuning reaction conditions for primary amine initiated NCA polymerizations in order to minimize side reactions, can result in controlled preparation of synthetic polypeptides. Reaction conditions such as temperature, pressure and pH of the reaction can bring about controlled polymerizations of NCAs. The following discussions focus on improving reaction conditions whereby NAM propagation is promoted.

2.3.1. Primary amine hydrochlorides

NAM is a nucleophilic ring-opening process, in which the polymer can grow linearly with increasing monomer conversion in the absence of side reactions. As mentioned earlier, NAM and AMM can co-exist in a given polymerization system. To circumvent this coexistence of mechanisms, Dimitrov *et al.*[44,45] used primary amine hydrochlorides to prevent the AMM, thereby enhancing the NAM (Scheme 2-6). The dormant hydrochloride chain ends dissociate to primary amines and HCl. The former propagate via the NAM and the HCl creates acidic conditions, in this way any NCA anion that could form is protonated thus preventing the AMM.

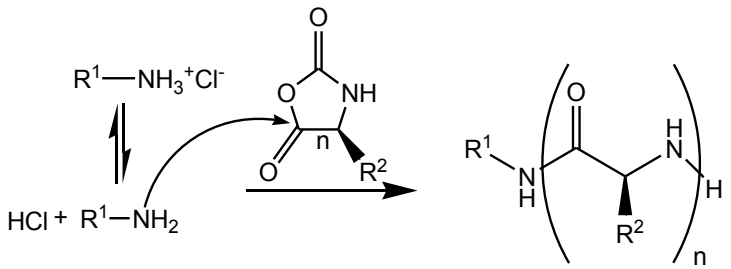

Scheme 2-6 Primary amine hydrochloride in the ROP of NCAs.

The use of this method at elevated temperatures, leads to preparation of hybrid block copolymers with molecular weights close to the predicted ones and narrow MWDs.[44-46] Since (synthetic) macroinitiators are used as ammonium hydrochlorides, synthetic polymers and

polypeptide components properties are linked. In this way hybrid block copolymers that self-assemble into nanostructures were prepared.[47]

Although involving elevated temperatures, the ROP of NCAs initiated with primary amine hydrochlorides is straightforward and can be applicable to any NCA in contrast to the above mentioned HMDS and metal-initiated living techniques.

2.3.2. NAM and low temperature

The effect of temperature on the polymerization of NCAs has been studied.[48-50] The results by capillary electrophoresis showed that about 99% of living polymers were retained when polymerization was conducted at 0 °C and 22% at room temperature.[48] Later, Habraken *et al.* used MALDI-ToF-MS to study polymerization of various NCAs at 0 °C, 20 °C and 60 °C. They found that side reactions/products started to show up at 20 °C and 60 °C. No side reactions were found at 0 °C. Side reactions included the formation of pyroglutamate for γ-benzyl-glutamate NCA and succinimide for β-benzyl-aspartate NCA, also formamide end-functionalized polymers, which were due to the reaction of propagating chains with the solvent *N*,*N*-dimethyl formamide.[50]

The decrease in termination reactions at lower reaction temperature can be attributed to the high activation energy barrier for these reactions, which was overcome at higher temperatures. Hence, at low temperature, the low activation energy propagation reaction was highly favoured over unwanted reactions.

2.3.3. NAM and High Vacuum Technique.

The first ROP of NCA using high vacuum technique (HVT),[51] made use of *n*-hexylamine and 1,6-diaminohexane as initiators which are strong nucleophiles that exclusively follow the NAM route. The group applied their expertise on HVT[52] to find the necessary reaction conditions for living ROP of NCAs. In essence these include purification of reactants, apparatus, solvents and reaction proceeding under vacuum. MALDI-TOF MS, Nano-assisted laser desorption-ionization mass spectrometry (NALDI-TOF MS) and ^{13}C NMR were used to confirm the end group structure of polymers that were prepared by both HVT and glove box techniques in DMF/THF. Preparation of poly(*O*-benzyl-L-tyrosine) via HVT yielded a polymer exclusively by NAM. The only termination observed, was reaction with DMF in

contrast to polymers prepared in the glove box, where initiation took place by NAM and AMM, and other termination products were observed.[53]

HVT relies on removing volatile components from the reaction system, and also allows CO_2 released during NCA ROP to escape from the reaction mixture. This creates the necessary conditions for living ROP of NCAs. The CO_2 produced during polymerization is removed from reaction solution to fill up the vacuum. This eliminates the possibility of CO_2 complexing with amine end groups. Decarboxylation increases the rate of propagation as more primary amines become available. The effect of CO_2 was particularly seen when the reaction vessels had a smaller volume than that occupied by the amount of CO_2 to be released. In such cases, incomplete polymerization and a slow rate of polymerization were observed in contrast to the case where vessels with volumes larger than the amount of released CO_2 were used.[54]

Tedious HVT is the price one has to pay for the synthesis of living polypeptides, which gives access to interesting hybrid architectures.[55] The versatility of HVT was shown by synthesis of well-defined homo- and copoly-L-prolines,[56] with *N*-substituted proline NCA i.e. *N*-substituted NCAs are not polymerized by AMM but by NAM.

The combination of low temperature and HVT could be optimized to provide living polymerization conditions.[57] It was observed that living polypeptides were prepared faster with HVT than under ambient pressure at the same temperature. Some monomers were found to best polymerize at 20 °C under high vacuum, others at 0 °C and high vacuum due to the different side reactions. Therefore optimized polymerization conditions for various NCAs were realized by compromising HVT and temperature.

Copolypeptides with well-defined structures were hardly accessed prior to living polymerizations, because of the earlier mentioned side reactions. Also, block copolypeptides were not easily prepared, due to contaminations with monomer and homopolymer. Therefore, complete separation/fractionation was required. Establishment of living ROP (LROP) of NCAs helped to synthesize well-defined polypeptides. Below we discuss copolypeptides that were prepared by LROP of NCAs.

2.4. Copolypeptides

Copolypeptides prepared by ROP of NCA can be categorised into two classes, one in which a single chain consists of single amino acid repeating units linked to another chain *i.e*. block copolypeptides. In the second group, the polypeptide consists of two or more amino acids randomly distributed along the chain. Research has been devoted mostly to the applications of the former class and it has served as a study tool for living polymerization techniques mentioned above.

2.4.1. Complex polypeptide architectures

Prior to development of LROP of NCAs, controlled synthesis of polypeptides was a challenge, except via SPPS. Conventional chain growth methods led to heterogeneous polypeptides with respect to end group functionality. As mentioned, one of the prerequisites for LROP technique of NCAs is its ability to prepare block copolypeptides.[38,41,50,56] Block copolypeptides are prepared by first polymerizing the first monomer via LROP (now macroinitiator) and subsequent addition of the second monomer, which is then initiated by the active chain ends. Because of the diverse functionality of different amino acids, the versatility of NCA ROP to prepare non-linear copolypeptides widens. Graft copolymers can be synthesized by first deprotecting the appropriately chosen side chains of the backbone polymer, then direct initiation if primary amines are on side chains, as in the case of grafting γ-benzyl glutamate NCA on lysine containing copolymers.[50] Alternatively, modification of protected side groups, as in the case of the aminolysis of poly(γ-benzyl-L-glutamate).[58] Deming's initiator was used to initiate both polymerizations of the backbone and of the side chains to prepare brushes with controlled segment length and high-density brush copolypeptides.[59] Recently, proteins have also been grafted on polypeptides prepared by NCA LROP, using click chemistry as with DNA[60] and Solid Phase Peptide Synthesis.[61]

The applications of polypeptides prepared by LROP of NCAs extend to the use of star copolypeptides in drug delivery systems. Star copolypeptides can be prepared by initiation either with low molecular weight multifunctional initiators (compounds with 3 or more primary amines),[54,62,63] or with macromolecular initiators[55,64] with 3 or more reactive sites.

2.4.2. Hybrid copolypeptides

Advanced polymer architectures can be prepared, by combining the properties of synthetic polymers with those of natural polymers such as proteins or polypeptides.[65] Hybrid copolypeptides consist of a synthetic polymer block linked to a polypeptide block. The non-peptide block can be prepared via synthetic pathways such as RAFT-mediated polymerization followed by modification of the end groups into ones capable of initiating ROP of NCAs.[66,67] Polypeptides can also be used as macroinitiators to prepare hybrid copolypeptides.[68,69] The first step involves the preparation of a polypeptide block that is subsequently used as a macroinitiator for polymerization of vinyl monomers. Stieg *et al.* prepared a bifunctional initiator comprising Deming's initiator and an ATRP initiator moiety, the Deming moiety was used to prepare poly(γ-benzyl glutamate) (PBLG) of high molecular weight and low dispersity. Then PBLG was used as a macroinitiator for ATRP of MMA to afford rod-coil hybrid block copolypeptides.[68]

Solubility properties from synthetic polymers maybe combined with secondary structures from polypeptides resulting in self-assembling hybrid copolymers.[70,71] As an illustration, biocompatible and water-soluble amino end-capped poly(ethylene glycol) PEG-NH_2 and poly(2-methyl-2-oxazolidine) PMOx-NH_2 were used for ROP of NCAs of γ-benzyl-L-glutamate and *S*-benzyloxycarbonyl-L-cysteine to afford poly(amino acid) (PAA) blocks and hydrogels. The self-assembly of these amphiphilic polymers in water was studied with dynamic light scattering and fluorescence spectroscopy. In aqueous solutions, the block copolymers associate into particles with hydrodynamic radii (R_H) ranging from 70 to 130 nm. Larger R_H was observed for copolymers containing poly(*S*-benzyloxycarbonyl-L-cysteine) in contrast to the analogues of poly(*γ*-benzyl-L-glutamate). FTIR analysis showed that poly(γ-benzyl-L-glutamate) blocks adopt a helical conformation while poly(*S*-benzyloxycarbonyl-L-cysteine) blocks prefer *β*-sheets.[70]

2.4.3. Random copolypeptides

All the above mentioned polypeptides are prepared by sequential polymerization of monomers. Simultaneous polymerization of monomers however, results in a statistical distribution of monomer residues along the polypeptide chain. The distribution may either be random, alternating or blocky in nature. This can be described or predicted from knowledge of the reactivity ratios, which simply indicate the relative tendency of monomers to be incorporated in the polymer chain. To fully understand monomer sequence distribution, linear[72] and non-linear least squares methods[72,73] are used to determine reactivity ratios of NCA comonomers. Residual monomer and copolymer compositions can be determined at low conversion using FTIR, UV-Vis and NMR spectroscopy.

Conformational studies on aqueous solutions of random copolypeptides have been published.[74-76] Studies on degradation of random copolypeptides by proteolytic enzymes showed that the chains were cleaved/degraded randomly, rate of degradation follows Michealis-Menten rate law and was first order in enzyme concentration.[77,78]

Reactivity ratios can be influenced by solvent, initiator and reaction conditions. As a consequence of reactivity ratios, comonomer ratios in the copolymer and in the residual monomer may change towards higher conversion due to so-called composition drift. The composition and distribution of comonomers along the chain dictate copolymer properties.

Kumar *et al*. reviewed earlier studies on NCA binary copolymerization and the associated reactivity ratios.[79] Recently, Zelzer *et al.*[80] developed a method using HPLC to monitor consumption of N_{ε}-benzyloxy-L-lysine and γ-benzyl-L-glutamate NCAs initiated by *n*-hexylamine under N_2 in DMF. The polymerization samples were quenched by acid hydrolysis (HCl), filtered and analysed by HPLC relying on the UV absorption of the aromatic protection groups at 254 nm for detection of the amino acids. The HPLC method provided monomer concentrations at specific time-points during polymerization. When the normalised concentrations obtained from HPLC chromatograms were compared with normalised IR data, the overall shape of the curves matched well from both measurements throughout the polymerization. The use of linear graphical methods (Kelen-Tüdös) showed that γ-benzyl-L-glutamate was incorporated more readily in the random copolymer with a small composition drift.[80]

Few reports on copolymerization of 3 or more amino acid monomers are available. Terpolymerization and copolymerizations of L-leucine, L-valine and β-benzyl-L-aspartate NCAs,[81] were investigated to determine the random nature of terpolymers and ^{1}H NMR spectroscopy was used to determine the actual monomer compositions of the copolymers obtained at low conversion. The conversion was estimated by monitoring the CO_2 released. Random copolymers were prepared from binary copolymerizations and the terpolymer composition was predicted using reactivity ratios obtained from binary copolymerization with the Alfrey-Goldfinger equations and experimentally verified. There was no statistical difference between predicted compositions and actual experimental composition, from the above discussion, there is a need to develop a robust method in which individual comonomer consumption will be immediately monitored.

In this study an *in situ* ^{1}H NMR protocol was developed to monitor polymerization of NCA monomers. During copolymerization, individual comonomer consumptions were directly monitored and copolymerization parameters were determined. In addition since the resonance peaks used to monitor monomer consumption were well resolved, the *in situ* ^{1}H NMR protocol was successfully applied to monitor a preliminary terpolymerization reaction.

2.5. References

(1) Nakashima, T.; Fox, S. W. *BioSysterns* **1981** *14* 151

(2) Harada, K.; Fox, S. W. *Arch. Biochem. Biophys.* **1965**, *109*, 49.

(3) Melius, P. *BioSystems* **1982**, *15*, 275.

(4) Fox, S. W.; Harada, K. **1960**, *82*, 3745.

(5) Hayakawa, T.; Windsor, C. R.; Fox, S. W. *Arch. Biochem. Biophys.* **1967**, *118*, 265.

(6) Fox, S. W.; Suzuki, F. *BioSystems* **1976**, *8*, 40.

(7) Kokufuta, E.; Suzuki, S.; Harada, K. *BioSystems* **1977**, *9*, 211.

(8) Kricheldorf, H. R.; Lossow, C. V.; Lomadze, N.; Schwar, G. *J. Polym. Sci., Part A: Polym. Chem.* **2008**, *46*, 4012.

(9) Mita, H.; Nomoto, S.; Terasaki, M.; Shimoyama, A.; Yamamoto, Y. *Int. J. Astrobiol.* **2005**, *4*, 145.

(10) DeGrado, W. F.; Kaiser, E. T. *J. Org. Chem.* **1980**, *45*, 1295.

(11) Merrifield, R. B. *J. Am. Chem. Soc.* **1963**, *85*, 2149.

(12) Merrifield, R. B. *J. Am. Chem. Soc.* **1963**, *86*, 304.

(13) Merrifield, R. B. *Biochemistry* **1964**, *3*, 1385.

(14) Carpino, L. A.; El-Faham, A.; Albericio, F. *Tetrahedron Lett.* **1994**, *35*, 2279.

(15) Aoi, K.; Tsutsumiuchi, K.; Okada, M. *Macromolecules* **1993**, *27*, 875.

(16) Deanna, P. L.; Politakos, N.; Avgeropoulos, A.; Messman, J. M. *Macromolecules* **2009**, *42* 7781.

(17) Jun, L.; Huang, Y. *Macromol. Chem. Phys.* **2010**, *211*, 1708.

(18) Goodman, M.; Arnok, U. *J. Am. Chem. Soc.* **1964**, *86*, 3384.

(19) Idelson, M.; Blout, E. R., 2387.

(20) Peggion, E.; Terbojevich, M.; Cosani, A.; Colombini, C. *J. Am. Chem. Soc.* **1966**, *88*, 3630.

(21) Peggion, E.; Terbojevich, M.; Cosani, A.; Colombini, C. *J. Am. Chem. Soc.* **1966**, *88*, 3630.

(22) Murray, G.; Hutchison, J. *J. Am. Chem. Soc.* **1966**, *88*, 3627.

(23) Ballard, D. G. H.; Bamfor, C. H. *J. Am. Chem. Soc.* **1956**, 1926

(24) Bamford, C. H.; Block, H. *J. Am. Chem. Soc.* **1961**, 4992.

(25) Bamford, C. H.; Block, H.; Pug, A. C. P. *J. Am. Chem. Soc.* **1961**, 2057.

(26) Bamford, C. H.; Block, H. *J. Am. Chem. Soc.* **1961**, 4989.

(27) Sekiguchi, H. *Pure Appl. Chem.*, *53*, 1689.

(28) Goodman, M.; Arnok, U. *J. Am. Chem. Soc.* **1964**, *86*, 3384.

(29) Doty, P.; Lundberg, R. D. *J. Am. Chem. Soc.* **1957** *79*, 2338.

(30) Lundberg, R. D.; Doty, P. *J. Am. Chem. Soc.* **1957**, *79*, 3961.

(31) Idelson, M.; Blout, E. R. *J. Am. Chem. Soc.* **1957** *79*, 3948.

(32) Sela, M.; Berger, A. *J. Am. Chem. Soc.* **1955**, *77*, 1893.

(33) Habraken, G. J. M.; Peeters, M.; Dietz, C. H. J. T.; Koning, C. E.; Heise, A. *Polym. Chem.* **2010**, *1*, 514.

(34) Deming, T. J. *J. Am. Chem. Soc.* **1997**, *119*, 2759.

(35) Deming, T. J. *Nature* **1997**, *390*, 386.

(36) Deming, T. J. *J. Am. Chem. Soc.* **1998**, *120*, 4240.

(37) Deming, T. J. *Macromolecules* **1999**, *32*, 4500.

(38) Brzezinska, K. R.; Deming, T. J. *Macromolecules* **2001**, *34*, 4348.

(39) Cheng, J.; Deming, T. J. *Macromolecules* **1999**, *32*, 4745.

(40) Deming, T. J.; Curtin, S. A. *J. Am. Chem. Soc.* **2000**, *122*, 5710.

(41) Lu, H.; Cheng, J. *J. Am. Chem. Soc.* **2007**, *129*, 14114.

(42) Lu, H.; Cheng, J. *J. Am. Chem. Soc.* **2008**, *130*, 12562.

(43) Lu, H.; Wang, J.; Lin, Y.; Cheng, J. *J. Am. Chem. Soc.* **2009**, *131*, 13582.

(44) Dimitrov, I.; Schlaad, H. *Chem. Commun. (Cambridge, U. K.)* **2003**.

(45) Dimitrov, I.; Kukula, H.; Cölfen, H.; Schlaad, H. *Macromol. Symp.* **2004**, *215*, 383.

(46) Lutz, J.-F. o.; Schu¨t, D.; Kubowicz, S. *Macromol. Rapid Commun.* **2005**, *26*, 23.

(47) Huang, C.-J.; Chang, F.-C. *Macromolecules* **2008**, *41*, 7041.

(48) Vayaboury, W.; Giani, O.; Cottet, H.; Deratani, A.; Schue, F. *Macromol. Rapid Commun.* **2004**, *25*, 1221.

(49) Vayaboury, W.; Giani, O.; Cottet, H.; Bonaric, S.; Schue, F. *Macromol. Chem. Phys.* **2008**, *209*, 1628.

(50) Habraken, G. J. M.; Peeters, M.; Dietz, C. H. J. T.; Koning, C. E.; Heise, A. *Polym. Chem.* **2010** *1*, 514.

(51) Aliferis, T.; Iatrou, H.; Hadjichristidis, N. *Biomacromolecules* **2004**, *5*, 1653.

(52) Hadjichristidis, N.; Iatrou, H.; Pispas, S.; Pitsikalis, M. *J. Polym. Sci., Part A: Polym. Chem.* **2000**, *38*, 3211.

(53) Pickel, D. L.; Politakos, N.; Avgeropoulos, A.; Messman, J. M. *Macromolecules* **2009**, *42*, 7781.

(54) Aliferis, T.; Iatrou, H.; Hadjichristidis, N. *J. Polym. Sci., Part A: Polym. Chem.* **2005**, *43*, 4670.

(55) Karatzas, A.; Iatrou, H.; Hadjichristidis, N. *Biomacromolecules* **2008**, *9*, 2072.

(56) Gkikas, M.; Iatrou, H.; Thomaidis, N. S.; Alexandridis, P.; Hadjichristidis, N. *Biomacromolecules* **2011**, *12*, 2396.

(57) Habraken, G. J. M.; Wilsens, K. H. R. M.; Koning, C. E.; Heise, A. *Polym. Chem.* **2011**, *2*, 1322.

(58) Sugimoto, H.; Nakanishi, E.; Hanai, T.; Yasumura, T.; Inomata, K. *Polym. Int.* **2004**, *53*, 972.

(59) Rhodes, A. J.; Deming, T. J. *J. Am. Chem. Soc.* **2012**, *134*, 19463−1946.

(60) Chen, P.; Li, C.; Liu, D.; Li, Z. *Macromolecules* **2012**, *45*, 9579−9584.

(61) Enomoto, H.; Nottelet, B.; Halifa, S. A.; Enjalbal, C.; Dupre´, M.; Tailhades, J.; Coudane, J.; Subra, G.; Martinez, J.; Amblard, M. *Chem. Commun. (Cambridge, U. K.)* **2013**, *49*, 409.

(62) Li, J.; Xu, S.; Zheng, J.; Pan, Y.; Wang, J.; Zhang, L.; He, X.; Liu, D. *Eur. Polym. J.* **2012**, *48* 1696.

(63) Klok, H.-a.; Hernández, J. R.; Becker, S.; Mûllen, K. *Journal of Polymer Science: Part A: Polymer Chemistry* **2001**, *39*, 1572.

(64) Thornton, P. D.; Billah, S. M. R.; Cameron, N. R. *Macromol. Rapid Commun.* **2013**, *34*, 257−262.

(65) Li, J.; Wang, T.; Wu, D.; Zhang, X.; Yan, J.; Du, S.; Guo, Y.; Wang, J.; Zhang, A. *Biomacromolecules* **2008**, *9*, 2670.

(66) Fan, Y.; Chen, G.; Tanaka, J.; Tateishi, T. *Biomacromolecules* **2005**, *6*, 3051.

(67) Thornton, P. D.; Brannigan, R.; Podporska, J.; Quilty, B.; Heise, A. *J. Mater. Sci.: Mater. Med.* **2012**, *23*, 37.

(68) Steig, S.; Cornelius, F.; Witte, P.; Staal, B. B. P.; Koning, C. E.; Heise, A.; Menzel, H. *Chem. Commun. (Cambridge, U. K.)* **2005**, 5420.

(69) Liu, Y.; Chen, P.; Li, Z. *Macromol. Rapid Commun.* **2012**, *33*, 287−295.

(70) Obeid, R.; Scholz, C. *Biomacromolecules* **2011**, *12*, 3797.

(71) Markland, P.; Zhang, Y.; Amidon, G. L.; Yang, V. C. *J. Biomed. Mater. Res., Part A* **1999**, *47*, 595.

(72) Ishiwari, K.; Hayashi, T.; Nakajima, A. *Polym. J. (Tokyo, Jpn.)* **1978**, *10*, 87.

(73) Ishiwari, K.; Hayashi, T.; Nakajima, A. *Bull. Inst. Chem. Res., Kyoto Uni* **1977**, *55*, 366.

(74) Nylund, R. E.; Miller, W. G. *J. Am. Chem. Soc.* **1965**, *87*, 3537.

(75) Ishiwari, K.; Nakajima, A. *Bull. Inst. Chem. Res., Kyoto Uni* **1976** *54*, 72.

(76) Miller, W. G.; Nylund, R. E. *J. Am. Chem. Soc.* **I965**, *87*, 3542.

(77) Miyachi, Y.; Jokei, K.; Oka, M.; Hayashi, T. *Eur. Polym. J.* **1999**, *35*, 395.

(78) Miyachi, Y.; Jokei, K.; Oka, M.; Hayashi, T. *Eur. Polym. J.* **1999**, *35*, 607.

(79) Kumar, A. *CPR* **2011**, *1*, 219.

(80) Zelzer, M.; Heise, A. *Polym. Chem.* **2013**, *4*, 3896.

(81) Wamsley, A.; Jasti, B.; Phiasivongsa, P.; Li, X. *J. Polym. Sci., Part A: Polym. Chem.* **2004**, *42*, 317.

Chapter III: The synthesis of *N*-Carboxyanhydrides

Summary

This chapter deals with a brief introduction into the methods commonly used for synthesis and purification of amino acid NCAs. Details of the procedures used to synthesize protected amino acids derivatives and the corresponding NCAs used in this study will be described in conjunction with relevant NMR analyses.

Introduction to α-*N*-CarboxyAnhydrides of Amino Acids

A facile synthesis of polypeptides with high molecular weights[1-4] and self-assembling properties[5] employs ring opening polymerization (ROP) of cyclic α-*N*-CarboxyAnhydrides (NCAs) of amino acids. Basic or nucleophilic initiators are used to initiate ROP of NCAs that propagate by elimination of CO_2. Preparation of polypeptides with potential applications in biomaterials requires the use of pure NCA monomers. Several methods are used for the synthesis of NCAs.[6,7] Below an overview will be presented of the two commonly used methods to prepare NCAs, *i.e*. Leuchs' method and the Fuchs-Farthing method.

Leuchs was working on Sequential Peptide Synthesis (SPS) when he accidentally discovered NCAs of amino acids (later known as Leuchs' anhydride), whilst purifying *N*-alkoxycarbonyl amino acid chlorides.[8-10] In this method as shown in Scheme 3-1, α–*N*-alkoxy-protected amino acids react with halogenating agent to produce *N*-alkoxycarbonyl amino acid halides, which ring close to cyclic NCAs,[11-15] at higher temperatures and/or longer reaction times. The leaving halide and alkyl groups (Scheme 3-1) influence the ease of *N*-alkoxycarbonylamino acid halide cyclization. It was found that the required temperature for cyclization decreases in the order X = Cl > Br > I and also when a benzyl group is used instead of an alkyl group.[16,17] The general synthesis of NCAs via Leuchs' method is illustrated in Scheme 3-1.

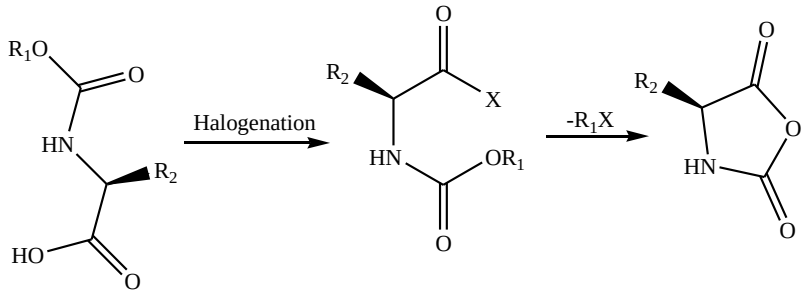

Scheme 3-1 Schematic illustration of the NCA synthesis according to Leuchs' method.

Fuchs-Farthing method proceeds by direct phosgenation of α-*N*-unprotected amino acids to produce NCAs as shown in Scheme 3-2.[18] Phosgene gas is bubbled through the suspension of amino acid, in a dry aprotic solvent.[19] The toxic, gaseous phosgene is hard to handle and excess amount is needed to complete the reaction. Liquid diphosgene (trichloromethyl chloroformate)[20] was used as substitute to supply 2 equivalents of phosgene per molecule of diphosgene.[21] To minimize toxicity, an easy to handle crystalline phosgene substitute, bis(trichloromethyl) carbonate (triphosgene), was evaluated.[22] Triphosgene decomposes at a

temperature of 50-60 °C into three equivalents of phosgene, which improves the stoichiometry and makes NCAs readily accessible in less than three hours.[22,23] The solid phosgene trimer is the most frequently used source of phosgene for NCA synthesis.[24,25]

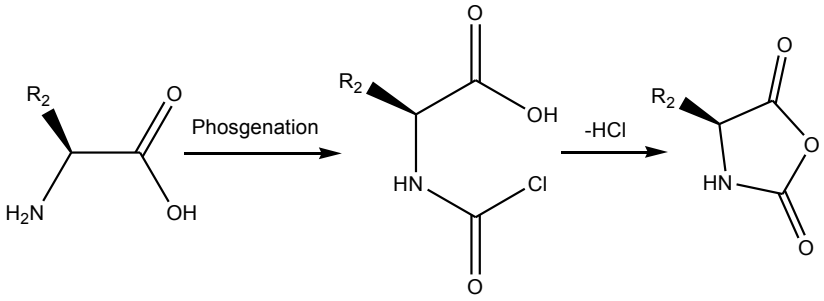

Scheme 3-2 Direct phosgenation of amino acids NCA synthesis.

NCA purification

For use in the controlled synthesis of polypeptides, NCAs must be free of contaminants that might disturb living propagation. NCAs are mostly purified by multiple recrystallizations under anhydrous conditions to remove impurities formed during synthesis (chloride compounds).[26] By repeated recrystallizations Lundberg *et al.* showed that the chloride content can be brought to very low concentrations (0.01 weight %). However, the HCl effect on polymerization was observed even at this concentration.[27] A clean synthesis of NCAs relies on removal of HCl produced during the NCA synthesis, in order to avoid side reactions caused by HCl contamination.[28] HCl is often removed with bases and scavengers. A facile and most frequently used method for removal of HCl employs α-pinene as HCl scavenger. The scavenger takes HCl to form bornyl chloride which is soluble in solvents that are used to precipitate NCAs.[28]

Purification of NCAs using flash chromatography on silica gel was suggested to be applicable and advantageous for purification of oily NCAs by Kramer *et al*. Flash chromatography method afforded NCAs with very low impurities and no need for repeated recrystallization.[29]

NCAs provide both activation of α–carbonyl and protection of α–amino moieties in one step. Since amino acids may possess different side chain-functional groups capable of interfering with NCA synthesis and polymerization, it is necessary to protect those side chain-functional groups to prevent unwanted reactions. Amino acid side chain protection groups, protection

strategies and removal conditions are well documented.[30] When choosing a protecting group, many aspects are considered, *e.g.* affordability, easy coupling and removal with no side reactions, high yields of amino acid derivative obtainable upon protection and deprotection reactions, and stability of the protecting group throughout its application period.

In this work the NCAs of glycine, aspartic acid and ornithine were prepared successfully, with the latter two amino acids' pendant groups protected prior to NCA synthesis. The β-carboxylic acid group of aspartic acid was selectively protected to benzyl ester according to a reported method.[31,32] Ornithine is a non-natural amino acid that can be used as a modifier[33] and as a precursor to aid complex work with amino acids, *e.g.* arginine and citrulline derivatives. Polyarginine is often prepared by guanidation of the side chain amino groups of polyornithine.

Selective protection of the δ-amino ornithine side chain, involves masking both α-carboxyl and α-amino functional groups via a copper complex, followed by acylation of the δ-amino side chain.[34,35] Copper is then removed from the amino acid-copper complex to yield the N_{δ}-protected ornithine derivative.[36,37]

3.1. Experimental

3.1.1. Materials

Glycine (assay 99.6%), L-aspartic acid (reagent grade ≥ 98%, Sigma), L-ornithine hydrochloride (assay ≥ 99%, Sigma), (+)-α-pinene (98%, Aldrich), benzyl alcohol (99-100.5%(GC), Sigma-Aldrich), benzyl chloroformate (technical grade 95%, Aldrich), 9-fluorenylmethyloxycarbonyl chloride (97%, Aldrich), bis(trichloromethyl) carbonate (purum ≥ 99%), diphosphorus pentoxide (extra pure assay ≥ 97%, Merk), trifluoroacetic acid (99%, Sigma-Aldrich), deuterium oxide (99.8%, Acros organics), pyridine (99.8%, Aldrich), glacial acetic acid (min 99.8%, SaarChem), ethylenediaminetetra-acetic acid disodium salt dehydrate (99-101%, SaarChem), copper(II)carbonate basic (purum ≥ 95%, Sigma-Aldrich), trifluoroacetic acid-D 99 Atom% D.

3.1.2. Analysis

In this work the amino acid NCAs and their protected derivatives were prepared successfully according to reported literature procedures. Hence ^{1}H NMR and ^{13}C NMR were solely used to confirm structure and to assure purity of the compounds.

3.1.3. Synthesis of Glycine *N*-CarboxyAnhydride (Gly NCA)

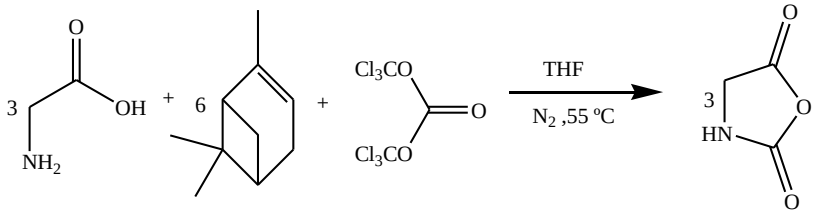

Scheme 3-3 Synthesis of Glycine NCA by phosgenation method.

The NCA of glycine was prepared according to a modified phosgenation procedure.[18,23] Glycine (5.0 g, 0.067 mol) which had been dried in vacuum and α-(+)-pinene (21.1 mL, 0.1329 mol) were added to a dry 3-necked 250 mL flask and refluxed in anhydrous THF (50 mL) at 55 ºC under nitrogen for an hour. Triphosgene (6.62 g, 0.0223 mol) in anhydrous THF (20 mL) was slowly added to the reaction mixture. The reaction was allowed to proceed for further 2 hours. The resulting reaction mixture was decanted to pentane (150 mL) and the product was kept at 0 ºC for 12 hours to complete precipitation. The white precipitate was filtered and washed three times with pentane and recrystallized twice from 1:8 THF: pentane

mixture. After several washings with pentane, the white crystals were vacuum-dried and stored in a refrigerator over phosphorous pentoxide. Yield 55%, ^{1}H NMR (DMSO-d_6, ppm): 4.19 (s, 2H, CH_2), 8.83 (s, 1H, NH). ^{13}C NMR (DMSO-d_6, ppm): 169.39 (COO), 152.98 (HNCOO), 46.26 ($HNCH_2$).

3.1.4. Synthesis of Aspartic acid *N*-CarboxyAnhydride

3.1.4.1. Preparation of β-benzyl-L-aspartate

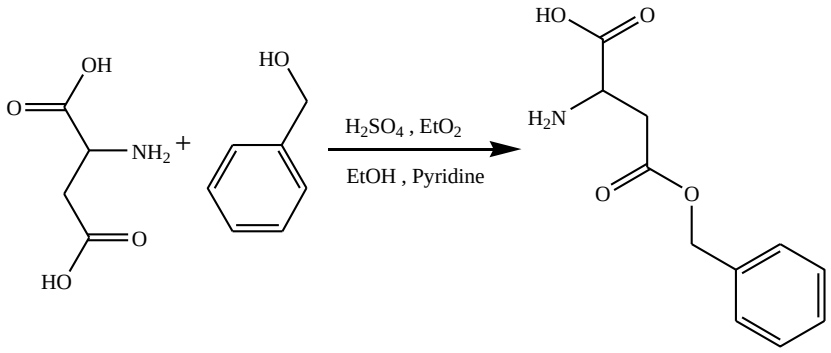

Scheme 3-4 Illustration of β-benzyl aspartate synthesis.

The β-carboxylic acid group of aspartic acid was protected following a reported procedure.[31,32] Sulfuric acid (10.5 mL) was added slowly in a 1-neck 500 mL flask chilled with diethyl ether (105 mL) in an ice bath, followed by drop wise addition of benzyl alcohol (105 mL). Diethyl ether was then removed under reduced pressure, followed by slow addition of L-aspartic acid (15.0 g, 0.113 mol) to the clear solution. The reaction was allowed to proceed for 24 hr. at 15 °C. Ethanol (21 mL) was slowly added to the reaction mixture with stirring, followed by drop wise addition of pyridine (54 mL) until opalescent. The slurry was kept overnight at ~ 0 °C, centrifuged and recrystallized from water by addition of pyridine drops, then centrifuged to give white odorless crystals. Yield 64%, ^{1}H NMR (TFA-*d*, ppm): δ 7.43 – 7.09 (m, 5H, ArH), 5.24 (q, J = 11.9 Hz, 2H, $ArCH_2$), 4.67 (s, 1H, CH), 3.54 – 3.17 (m, 2H, CH_2), 2.31 (s, 2H, NH_2). ^{13}C NMR (TFA-*d*, ppm): 175.29 (COOH), 174.69 (COO), 136.50 (Ar), 132.20 (Ar), A131.71 (Ar), 131.26 (Ar), 72.79 (Ar CH_2), 53.58 (H_2NCH), 36.00 (CH_2).

3.1.4.2. Preparation of β-benzyl-L-aspartate *N*-CarboxyAnhydride (Bz-Asp NCA)

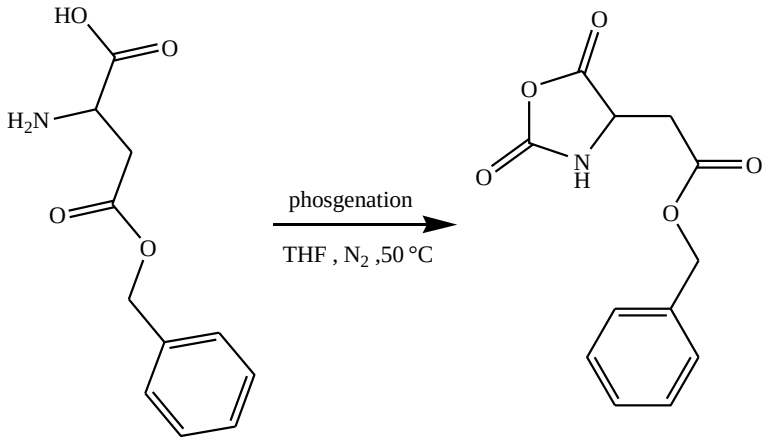

Scheme 3-5 Illustration of β-Benzyl-L-aspartate NCA synthesis.

The procedure for the synthesis of β-benzyl-L-aspartate *N*-carboxyanhydride (Scheme 3-5, Bz-Asp NCA) was the same as that followed for Glycine NCA synthesis (Section 3.1.2). Yield 84%, ^{1}H NMR (DMSO-d_6, ppm): δ 8.99 (s, 1H, NH), 7.37 (s, 5H, ArH), 5.13 (s, 2H, $ArCH_2$), 4.69 (t, J = 4.1 Hz, 1H, CH), 3.08 (dd, J = 17.7, 4.8 Hz, 1H, CH_2), 2.90 (dd, J = 17.8, 4.2 Hz, 1H, CH_2). ^{13}C NMR (DMSO-d_6, ppm): 170.98 (HCCOO), 169.27 (H_2CCO), 152.13 (HNCOO), 135.52 (Ar), 128.45 (Ar), 128.20 (Ar), 128.12 (Ar), 66.31 ($ArCH_2$), 53.62 (α-CH), 34.68 (βCH_2).

3.1.5. Preparation of ornithine (Orn) *N*-Carboxyanhydride

3.1.5.1. Synthesis of acylated-ornithine-copper complexes

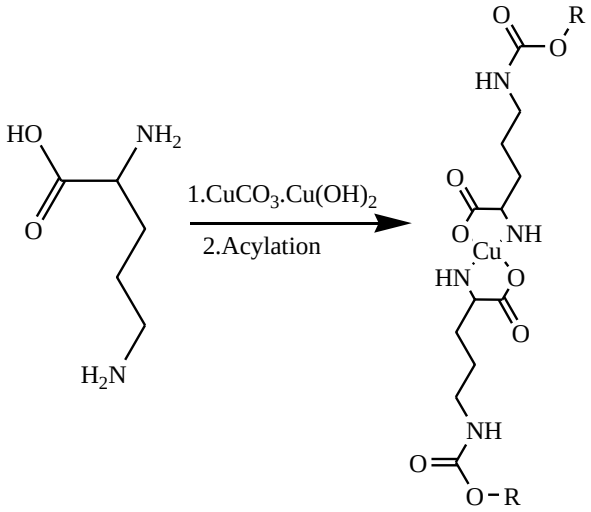

Scheme 3-6 Synthesis of ornithine–copper complex and acylation.

Masking of both α-carboxylic acid and α-amino acids proceeded according to a reported method.[38] Basic copper carbonate (8.40 g, 38.0 mmol) was added in portions to a refluxing 100 mL aqueous solution of ornithine hydrochloride (5.0 g, 37.0 mmol) in a 3-neck 500 mL round bottom flask equipped with magnetic stirrer at 100 °C. The solution was refluxed for additional 30 minutes. Unreacted copper carbonate was filtered off and the solution was cooled to 0 °C. Sodium hydroxide (30 mL, 2 N) was then added, followed by a 30 minutes drop wise addition of acylating compound (i.e. benzyl chloroformate or 9-fluorenylmethyloxycarbonyl chloride) in 1.5 equivalents. The reaction was allowed to run at 0 °C for 40 minutes then additional 30 minutes at 25 °C. The blue protected ornithine-copper complex precipitate was filtered, washed with water, ethanol and dried under vacuum. Yield 75%.

3.1.5.2. Synthesis of N_δ-Acylated Ornithine

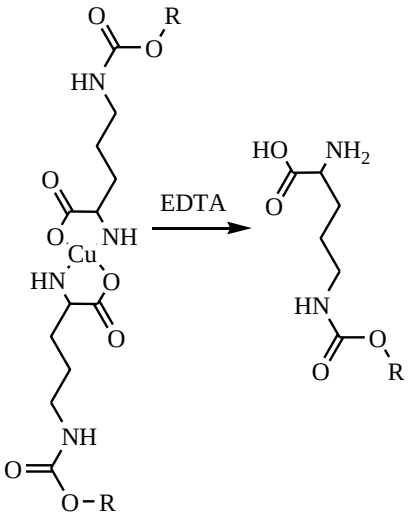

Scheme 3-7 Illustration of the synthesis of δ-acylated ornithine derivatives.

Removal of copper from the complex proceeded by the modified method of Kuwata.[39] for the illustration of N_δ-carbobenzyloxy(Z) ornithine derivative (Scheme 3-8): Copper complex was suspended in aqueous EDTA solution of pH 9 at 50 °C, a white *Z*-ornithine precipitated out of the pale blue aqueous solution. The precipitate was filtered out, refluxed in aqueous EDTA repeatedly to a complete white precipitate and clear aqueous solution. The precipitate was subsequently suspended in 50% acetic acid, filtered, washed with water and dried under vacuum. Yield 97%, ^{1}H NMR. (D_2O/TFA, ppm): 7.35-7.25 (m, 5H, ArH), 4.99 (s, 2H, $ArCH_2$), 3.97 (t, 1H, α-CH), 3.06 (t, 2H, δ-CH_2), 2.10 (s, 1H, NH), 1.92-1.74 (m, 2H, β-CH_2), 1.60 (m, 2H, γ-CH_2). ^{13}C NMR (D_2O/TFA, ppm): 173.66 (COOH), 160.38 (HNCOO), 138.42 (Ar), 130.72 (Ar), 130.30 (Ar), 129.60 (Ar), 68.85 ($ArCH_2$), 54.42 (αCH), 41.55 (δCH_2), 28.90 (βCH_2), 26.58 (γCH_2).

3.1.5.2.1. N_δ-carbobenzyloxy Z-Ornithine

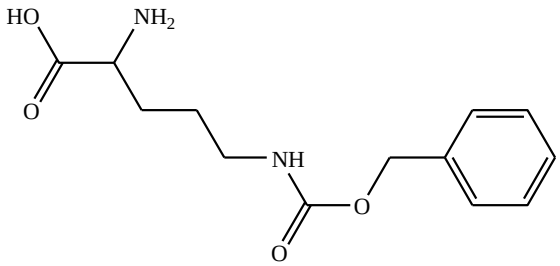

Scheme 3-8 Chemical structure of Z-ornithine.

3.1.5.2.2. N_δ-9-fluorenylmethyloxycarbonyl f-Ornithine

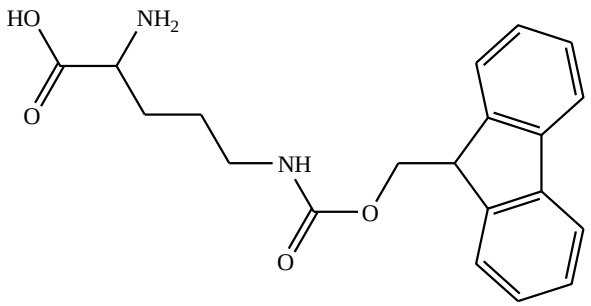

Scheme 3-9 Chemical structure of N_δ-f-ornithine.

The N_δ-f-Ornithine (Scheme 3-9) was prepared using the above-mentioned method at a pH lower than 7 (at higher pH values, the fmoc group was removed). Ethanol was used instead of acetic acid. Yield 95%, ^{1}H NMR (D_2O/TFA, ppm): δ 7.61 – 7.48 (d, 2H, ArH), 7.36 (d, J = 19.6, 2 Hz, 2H, ArH), 7.31 – 7.08 (m, 4H, ArH), 4.28 (m, 1H, αCH), 4.02 – 3.98 (d, 2H, OCH_2), 3.92 – 3.85 (t, 1H, CH), 2.79 (dd, J = 102.2, 82.3 Hz, 2H, δCH_2), 2.00 (s, 2H, NH_2), 1.77 (m, J = 47.0 Hz, 2H, βCH_2), 1.31 (m, J = 61.5 Hz, 2H, γCH_2).

3.1.5.3. Ornithine NCA synthesis

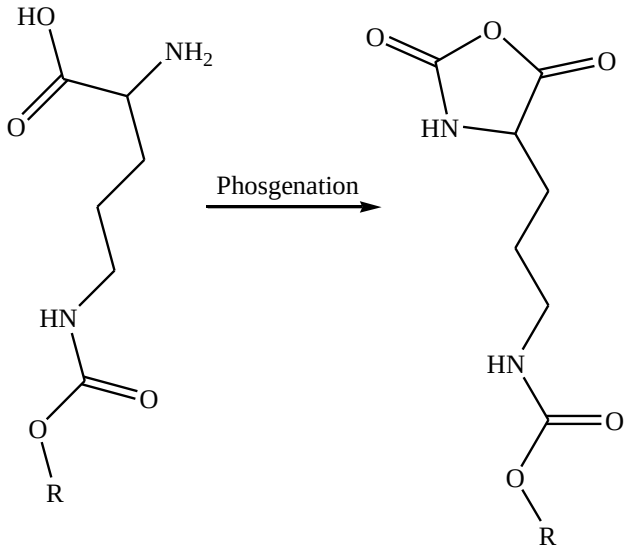

Scheme 3-10 Synthesis of ornithine NCA by phosgenation.

Scheme 3-10 illustrate a general phosgenation synthesis procedure for ornithine NCA derivatives. The NCAs were prepared via triphosgene method as previously described for glycine NCA (See Section 3.1.2).

3.1.5.3.1. Z-Ornithine NCA

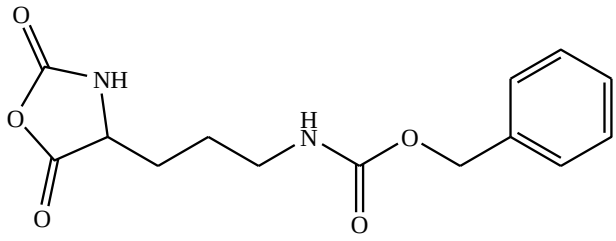

Scheme 3-11 Chemical structure of Z-ornithine NCA.

The chemical structure of N_{δ}-Z-ornithine NCA (Scheme 3-11) prepared via phosgenation method as described for glycine NCA (See Section 3.1.2). Yield 86.8%, ^{1}H NMR (DMSO-d_6, ppm): δ 9.09 (s, 1H, NH), 7.38 – 7.28 (m, 5H, ArH), 5.01 (s, 2H, ArCH2), 4.44 (dd, J = 7.3, 5.2 Hz, 1H, CH), 3.02 (q, J = 6.5 Hz, 2H,d CH2),1.87 – 1.56 (m, 2H, bCH2), 1.55 – 1.27 (m, 2H, yCH2). ^{13}C NMR (DMSO-d_6, ppm): δ 171.58 (CHC(O)C), 156.15 (HNC(O)OCH2), 151.93 (CHNHC(O)O), 137.22 (Ar), 128.35 (Ar), 127.71 (Ar), 65.19 (ArC), 56.87 (CH), 39.64 (δCH_2), 28.51 (βCH_2), 25.06 (γCH_2).

3.1.5.3.2. The f-Ornithine NCA

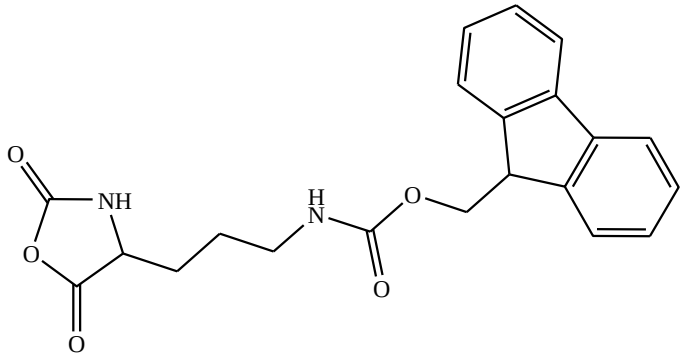

Scheme 3-12 Chemical structure of f-ornithine NCA.

The chemical structure of f-ornithine NCA (Scheme 3-12) prepared via phosgenation method as described for glycine NCA (See Section 3.1.2). Yield 80.6%, ^{1}H NMR (300 MHz, DMSO-d_6): δ 9.10 (s, 1H, NH), 7.88 (d, J = 7.2 Hz, 2H, ArH), 7.68 (d, J = 7.3 Hz, 2H, ArH), 7.44 – 7.29 (m, 4H, ArH), 4.50 – 4.40 (t, 1H, αCH), 4.31 (d, J = 6.8 Hz, 2H, OCH_2CH), 4.24 – 4.17 (t, 1H, CH_2CHCC), 3.00 (dd, J = 12.3, 6.3 Hz, 2H, δCH_2), 1.81 – 1.58 (m, 2H, γCH_2), 1.46 (m, J = 18.4, 13.1 Hz, 2H, βCH_2). ^{13}C NMR (300 MHz, DMSO-d_6): δ 172.04(H CC(O)O), 156.58 ($HNC(O)OCH_2$), 152.39 (HNC(O)OC(O)), 144.37 (Ar), 141.20 (Ar), 128.05 (Ar),

127.50 (Ar), 125.57 (Ar), 120.57 (Ar), 65.64 (C(O)OCH2), 57.33 (αCH), 47.17 (CH), 40.81 (δCH_2), 28.94 (βCH_2), 25.48 (γCH_2).

3.2. Conclusions

Glycine NCA, benzyl aspartate ester and its NCA were successfully prepared according to reported procedures. Basic copper carbonate was utilized for ornithine protection in a process in which copper binds to both the α-carboxyl and α-amino functional groups. Post the protection step, the acylation process was carried out with benzyl chloroformate or fluorenylmethyloxycarbonyl (fmoc) chloride followed by removal of copper with EDTA to yield N_δ-benzyloxycarbonyl (Z) ornithine and N_δ-f-ornithine derivatives respectively.

The direct synthesis of an NCA from the corresponding amino acid-copper complex was reported with phosgenation of the copper-(ε-acylated lysine) complex. Copper chloride precipitate that formed during phosgenation is filtered off, followed by cold aqueous washings of NCA in the organic layer. In this study, copper was removed prior phosgenation, to avoid working with aqueous solutions in the presence of moisture sensitive NCAs and to effect a complete removal of copper.

When thioacetamide and 8-quinolinol were used for removal of copper, the acylated derivative was inseparable from the copper salts. Only small yields were obtained with sodium borohydride when it was employed to remove copper from the copper-amino acid complex. It was observed that these copper sequestrators produce insoluble copper salts, whilst the acylated ornithine derivatives were also insoluble in aqueous solution and in ethanol, therefore the acylated ornithine derivatives were adsorbed in the copper salts. The use of a sequestrator that produces a water-soluble copper salt or complex, leaving the insoluble acylated ornithine out of solution was suggested. Therefore, EDTA was used to reach yields ≥ 95% fmoc ornithine and ≥ 97% Z ornithine. Subsequent synthesis of NCAs of these ornithine derivatives gave yields ≥ 80%.

3.3. References

(1) Thornton, P. D.; Brannigan, R.; Podporska, J.; Quilty, B.; Heise, A. *J. Mater. Sci.: Mater. Med.* **2012**, *23*, 37.

(2) Deming, T. J. *Nature* **1997**, *390*, 386.

(3) Cheng, J.; Deming, T. J. *Macromolecules* **1999**, *32*, 4745.

(4) Deming, T. J. *Macromolecules* **1999**, *32*, 4500.

(5) Obeid, R.; Scholz, C. *Biomacromolecules* **2011**, *12*, 3797−3804.

(6) Collet, H.; Bied, C.; Mion, L.; Taillades, J.; Commeyras, A. *Tetrahedron Lett.* **1996**, *37*, 9043.

(7) Palomo, C.; Aizpurua, J. M.; Ganboa, I.; Oiarbide, M. *Pure Appl. Chem.* **2000**, *72*, 1763.

(8) Leuchs, H. *Chem. Ber.* **1906**, *39*, 857.

(9) Leuchs, H.; Geiger, W. *Chem. Ber.* **1908**, *41*, 1721.

(10) Leuchs, H.; Manasse, W. *Chem. Ber.* **1907**, *40*, 3235.

(11) Noguchi, J.; Fujiwara, Y. *Bull. Chem. Soc. Jpn.* **1970**, *43*, 2515.

(12) Green, M.; Stahmann, M. A. *J. Biol. Chem.* **1952**, *197*, 771.

(13) Bergmann, M.; Zervas, L.; Ross, W. F. *J. Biol. Chem.* **1935**, *111*, 245.

(14) Akssira, M.; Boumzebra, M.; Kasmi, H.; Dahdouh, A. *Tetrahedron* **1994**, *50*, 9051.

(15) Konopińska, D.; Siemion, I. Z. *Angew. Chem., Int. Ed. Engl.* **1967**, *6*, 248.

(16) Katchalski, E.; Ben-Ishai, D. *J. Org. Chem.* **1960**, *15*, 1067.

(17) Ben-Ishai, D.; Katchalski, E. *J. Am. Chem. Soc.* **1952**, *74*, 3688.

(18) Farthing, A. C. *J. Am. Chem. Soc.* **1950** 3213.

(19) Patchornik, A.; Sela, M.; Katchalski, E. *J. Am. Chem. Soc.* **1953**, *76*, 299.

(20) Oya, M.; Katakai, R.; Nakai, H. *Chem. Lett.* **1973**, 1143.

(21) Katakai, R.; Iizuka, Y. *J. Org. Chem.* **1985**, *50*, 715.

(22) Eckert, H.; Forster, B. *Angew. Chem. Int. Ed. Engl.* **1987**, *26*, 894.

(23) Daly, W. H.; Poche', D. *Tetrahedron Lett.* **1988** *29*, 5859.

(24) Habraken, G. J. M.; Peeters, M.; Dietz, C. H. J. T.; Koning, C. E.; Heise, A. *Polym. Chem.* **2010** *1*, 514.

(25) Habraken, G. J. M.; Wilsens, K. H. R. M.; Koning, C. E.; Heise, A. *Polym. Chem.* **2011**, *2*, 1322.

(26) Sela, M.; Berger, A. *J. Am. Chem. Soc.* **1955**, *77*, 1893.

(27) Lundberg, R. D.; Doty, P. *J. Am. Chem. Soc.* **1957**, *79*, 3961.

(28) Senet, J.-P. G. *Chimica Oggi* **2004**, *22*, 24.

(29) Kramer, J. R.; Deming, T. J. *Biomacromolecules* **2010**, *11*, 3668.

(30) Isidro-Llobet, A.; Alvarez, M.; Albericio, F. *Chem. Rev. (Washington, DC, U. S.)* **2009**, *109*, 2455.

(31) Silva, M.; Lara, A. S.; Leite, C. Q. F.; Ferreira, E. I. *Arch. Pharm. (Weinheim, Ger.)* **2001**, *334*, 189.

(32) Silva, M.; Ferreira, E. I.; Leite, C. Q. F.; Sato, D. N. *Trop J Pharm Res,* **2007**, *6*, 815.

(33) Romanski, J.; Karbarz, M.; Pyrzynska, K.; Jurczak, J.; Stojek, Z. *J. Polym. Sci., Part A: Polym. Chem.* **2012**, *50*, 542.

(34) Wiejak, S.; Masiukiewicz, E. b.; Rzeszotarska, B. *Chem. Pharm. Bull.* **2001**, *49*, 1189—1191.

(35) Karbarz, M.; Pyrzynska, K.; Romanski, J.; Jurczak, J.; Stojek, Z. *Polymer* **2010**, *51*, 2959.

(36) Nowshuddin, S.; Reddy, A. R. *Tetrahedron Lett.* **2006**, *47*, 5159.

(37) Sailaja, G.; Nowshuddin, S.; Rao, M. N. A. *Tetrahedron Lett.* **2004**, *45*, 9297.

(38) Hernández, J. R.; Klok, H.-A. *J. Polym. Sci., Part A: Polym. Chem.* **2003**, *41*, 1167.

(39) Kuwata, S.; Watanabe, H. *Bull. Chem. Soc. Jpn.* **1965**, *38*, 676.

Chapter IV: Homopolymerization of *N*-Carboxyanhydrides

Summary

This chapter deals with Ring-Opening Polymerization (ROP) of *N*-Carboxyanhydrides (NCAs) for the preparation of poly(β-benzyl-L-Aspartate), polyglycine, poly(N_δ-Carbobenzyloxy-L-Ornithine) and poly(N_δ-fluorenylmethyloxycarbonyl-L-Ornithine). After preliminary homopolymerizations, in subsequent reactions, the polymerization kinetics were studied via *in situ* ^{1}H NMR spectroscopy. The *in situ* ^{1}H NMR studies were conducted to monitor NCA consumption with time. Monitoring the NCA homopolymerization via *in situ* ^{1}H NMR spectroscopy was essential in developing a protocol that could be applied to study binary copolymerization kinetics as well as a preliminary terpolymerization presented in Chapter V.

Introduction

Ring-opening polymerization of α-*N*-Carboxyanhydrides (NCAs) of amino acids provides a facile synthesis of polypeptides. Synthetic polypeptides play a vital role in the understanding of protein structure in tissue engineering and drug delivery studies. Interest in synthetic polypeptides is increased by their ability to self-assemble, as well as by their biocompatibility and biodegradability. However, synthetic peptides lack sequence specificity and have high dispersity when compared to natural proteins. The invention of living ROP of NCAs offered access to synthetic polypeptides with lower dispersity and properties closer to those of natural proteins. Basically, in these systems, side reactions and unwanted termination reactions are minimized. The details on living ROP systems were discussed in Chapter II.

Termination and side reactions in ROP of NCAs arising from reactions involving solvent(s) and/or high reaction temperatures limit the preparation of polypeptides with complete retention of the ω-amino end (NH_2) groups.[1,2] Kricheldorf *et al.*[3] studied solvent-induced polymerizations of phenylalanine NCA with solvents such as DMF, NMP, sulfolane and dioxane and found that when DMF was used, the chains terminate by forming formamide ω-end groups. Back-biting of DMF-initiated polymer chains resulted in cyclic peptides. The use of both DMF and NMP as solvents in the absence of initiator resulted in solvent-induced polymerizations in contrast to dioxane and sulfolane. The effect of initiator was also studied by employing different initiators that varied according to their nucleophilic character. Aniline is less nucleophilic than *n*-hexylamine and benzyl amine, and as a result it exhibited a slower initiation step which competes with other initiators such as water. Initiation by water yields hydantoic acid end group which were not observed when a highly nucleophilic initiator (*n*-hexylamine) was used.[3]

Polyglycine forms β-sheet structures, which can be used as a simple model to understand protein structure.[4,5] Studies on polyglycine prepared by ROP of its NCA may be limited by its solubility, the low yields obtained upon preparation of glycine NCA and the lack of side chain functionality for further modification. Due to a variety of protecting groups available for the polyornithine side chain moiety, polyornithine has become one of the most studied basic polypeptides after polylysine.[6,7]

Poly(β-benzyl-L-aspartate) is often used as a precursor for water-soluble poly(aspartic acid) or its derivatives. Micelle-forming hybrid block copolymers of poly(aspartic acid) derivatives and polyethylene glycol were prepared by coupling drugs on free carboxyl group-side chains of polyaspartic acid segment which acted as prodrugs.[8,9]

In this study, ROP of NCAs is used to prepare polyglycine, poly(β-benzyl-L-aspartate), poly(N_δ-carbobenzyloxy-L-ornithine) and poly(N_δ-fluorenylmethyloxycarbonyl-L-ornithine) by *n*-butylamine initiation. *In situ* ^{1}H NMR experiments were taken as a first step and build up for *in situ* copolymerization studies.

4.1. Materials

The NCA monomers were prepared and stored as described in Chapter 3. *n*-Butylamine (≥ 99.5%, Sigma-Aldrich), DMF (anhydrous, 99.8%, Sigma-Aldrich), DMSO-d_6 (99.9% atom D, Aldrich) were used as received.

4.2. Characterization techniques

4.2.1. NMR

The ^{1}H NMR and ^{13}C NMR spectra for polymers were Acquired with a 400 MHz Varian Unity Inova spectrometer. DMSO-d_6 and TFA-*d* (for polyglycine) were used as NMR solvents.

4.2.2. SEC

Size exclusion chromatography (SEC) analysis at Stellenbosch University was carried out on a DMAc solvent system using a flow rate of 1.0 mL/min. The instrument setup consisted of a Shimadzu LC-10AD pump, a Waters 717 Plus autosampler, a column system fitted with a 50x8 mm guard column in series with three 300x8 mm, 10 µm particle size GRAM columns (2 x 3000Å and 100Å) obtained from PSS, a Waters 2487 dual wavelength UV detector and a Waters 410 differential refractive index (DRI) detector all in series. 100 µL injection volumes are sampled individually with the oven temperature of the column and DRI detector kept at 40 °C. The solvent was stabilized with 0.05% BHT (w/v) and 0.03% LiCl (w/v), and samples were filtered through a 0.45 µm GHP filter to prevent any impurities entering the system. Calibration was done using PMMA standards (Polymer Laboratories) ranging from 690 to 1.2 x 10^6 g/mol. Data acquisition was done using Millennium[32] software, version 4.

4.3. Experimental procedures

4.3.1. Preparative (offline) homopolymerization

Poly(β-benzyl aspartate), polyglycine and poly(N_δ-carbobenzyloxy-L-ornithine) were prepared by polymerization of the respective NCAs, initiated with *n*-butylamine in DMF at 25 °C (see Scheme 4-1). In a typical polymerization experiment, β-benzyl-L-aspartate (Bz-Asp) NCA (0.50 g, 2.01 mmol) was dissolved in anhydrous DMF (5 mL) and *n*-butylamine (4.0 µL) was added to the NCA solution in a 50 mL pear-shaped flask with a side tap. The reaction mixture was subjected to three freeze-pump-thaw cycles and polymerization was allowed to proceed for 72 hours under vacuum at 25 °C. At 12 hour intervals, the polymerization mixture was subjected to three freeze-pump-thaw cycles. The reaction was stopped by precipitation from distilled diethyl ether. NMR spectroscopy was used to confirm polymer structures and SEC to determine molecular weight.

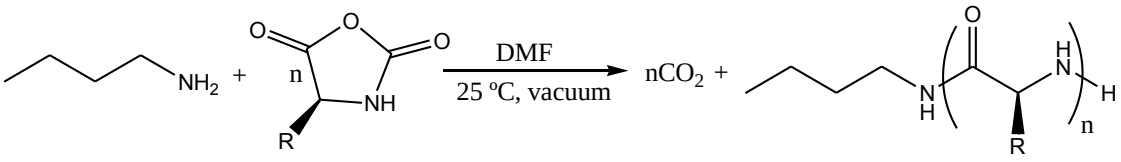

Scheme 4-1 General reaction for ROP of NCA initiated by *n*-butylamine.

4.3.2. Online homopolymerization

4.3.2.1. *In situ* ^{1}H NMR spectroscopy procedure

The ^{1}H NMR spectra were recorded with a 400 MHz Varian Unity Inova spectrometer. The ^{1}H NMR spectra were acquired with 3 μs (40°) pulse width and 4 seconds acquisition time. For the *in situ* experiments, samples were first defrosted, then inserted into the magnet at 25 °C and the magnet shimmed, the first spectrum collected served as reference. Subsequent spectra were collected at 20 or 15 minutes intervals for 14 hours. Phase correction was performed automatically whilst baseline correction and integration were performed manually using ACD Labs 12.0 ^{1}H NMR processor.

4.3.2.2. General procedure for *in situ* ^{1}H NMR monitored NCA homopolymerizations

All the NCA *in situ* homopolymerization experiments were carried out at a monomer concentration of 0.3 M and all other conditions were kept similar. An accurately weighed quantity of NCA was dissolved in DMSO-d_6 then transferred into a Wilmad® quick pressure valve NMR tube that already has the measured initiator. The sample was mixed thoroughly followed by three freeze-pump-thaw cycles. In a typical experiment N_δ-carbobenzyloxy-L-ornithine NCA (0.205 g, 0.701 mmol) was dissolved in 2.4 mL DMSO-d_6. Subsequently, part of the solution was transferred to a Wilmad® quick pressure valve NMR tube with 0.6 μL *n*-butylamine initiator, the reaction mixture was degassed by three freeze-pump-thaw cycles then the ^{1}H NMR *in situ* experiment was started as described in Section 4.3.2.1.

4.4. Results and discussions

4.4.1. Results on Offline homopolymerization

Prior to studying *in situ* homopolymerizations of the NCAs of amino acids, it was necessary to first access offline homopolymerizations of NCAs in order to understand the polymerizability and control of *n*-butylamine-initiated polymerization under specific conditions.

Table 4-1 Chemical structures of *N*-carboxyanhydride monomers and polypeptides that were synthesized in this study.

Amino acid NCAs	Polypeptides
A 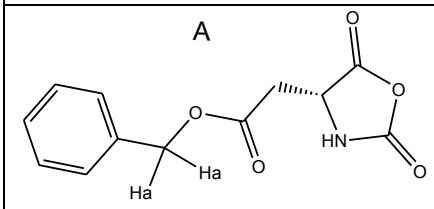 β-benzyl-L-aspartate NCA.	E 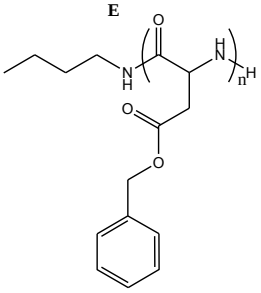 Poly(β-benzyl-L-aspartate).
B 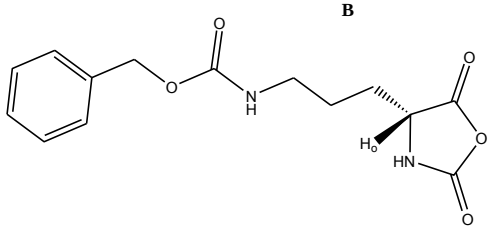 N_{δ}-carbobenzyloxy-L-ornithine NCA.	F 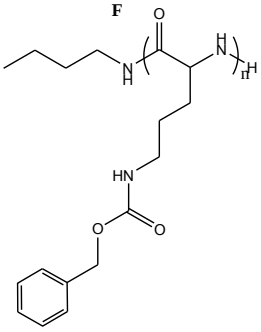 Poly(N_{δ}-carbobenzyloxy-L-ornithine)
C 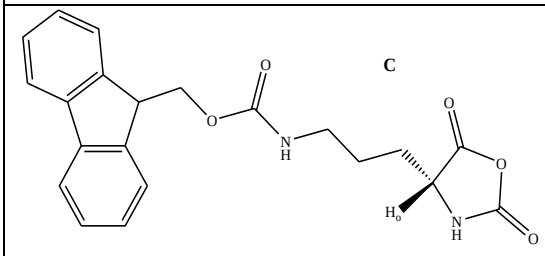 N_{δ}-fluorenylmethyloxycarbonyl-L-Ornithine NCA.	G 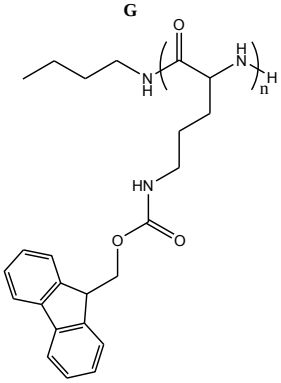 Poly(N_{δ}-fluorenylmethyloxycarbonyl-L-ornithine).
D 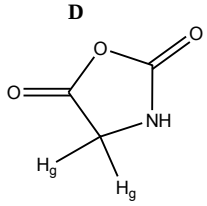 Glycine NCA.	H 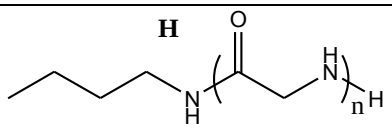 Polyglycine.

Table 4-2 GPC results of polypeptides.

Polymer	$M_{n,}$	M_n (theoretical)	M_w	$Đ$
Poly(Z-Orn)	8848[a]	12415	10059	1.14
Poly(Bz-Asp)	9719[a]	10260	10960	1.13
Poly(Gly)	1941.4[b]	2855	-	-

[a] M_n measured by SEC

[b] M_n measured by ^{1}H NMR

Table 4-2 shows molecular weight data of poly(Z-Orn), poly(Bz-Asp) and poly(Gly) of polypeptides obtained by *n*-butylamine initiated ROP of respective NCAs (see Table 4-1) in DMF at 25 ºC. The number average molecular weights (M_n) obtained were lower than predicted from monomer/initiator ratio of 50 with fairly low $Đ$ (Table 4-2). Polyglycine (**H** in Table 4-1) solubility became a challenge, thus its molecular weight determination was complicated due to insolubility in solvents used for SEC analysis hence it was measured via ^{1}H NMR.

4.4.2. *In situ* homopolymerization results

The offline procedure showed that polymerization of the respective NCA monomers (see Table 4-1) to polypeptides by *n*-butylamine at 25 ºC was feasible. After observing the polymerizability of the NCAs on preparative scale it was therefore necessary to monitor homopolymerization of NCAs at the predetermined experimental conditions for *in situ* ^{1}H NMR copolymerization experiments. All homopolymerization experiments were initiated with *n*-butylamine monomer/initiator ratio of 25 in DMSO-d_6 for 14 hours.

4.4.2.1. Monitoring f-Orn NCA homopolymerization by *in situ* ^{1}H NMR

Figure 4-1 shows an array of spectra [0.5 ≤ δ (ppm) ≤ 9] during *n*-butylamine (labelled I in the spectrum representing the methyl groups) initiated polymerization of f-Orn NCA (structure C in Table 4-1) at 25 ºC in DMSO-d_6 taken with 2 hour intervals for 14 hours.

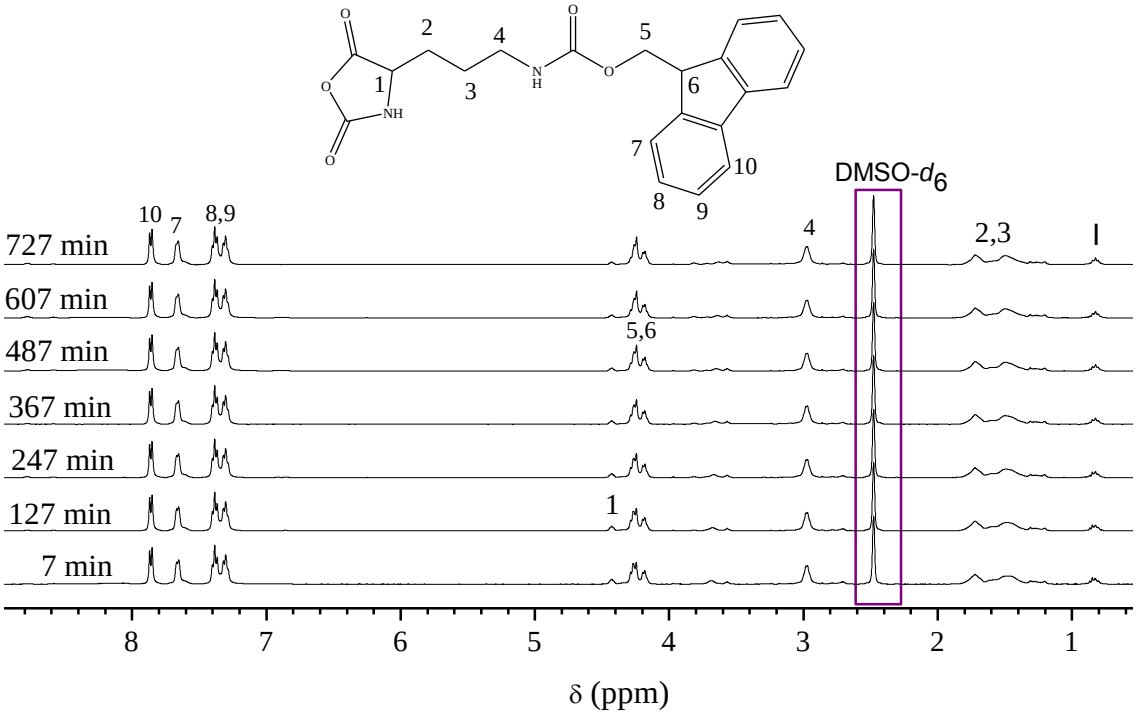

Figure 4-1 ^{1}H NMR spectra as a function of time during *n*-butylamine-initiated homopolymerization of f-Orn NCA conducted in DMSO-d_6 for 14 hours at 25 °C.

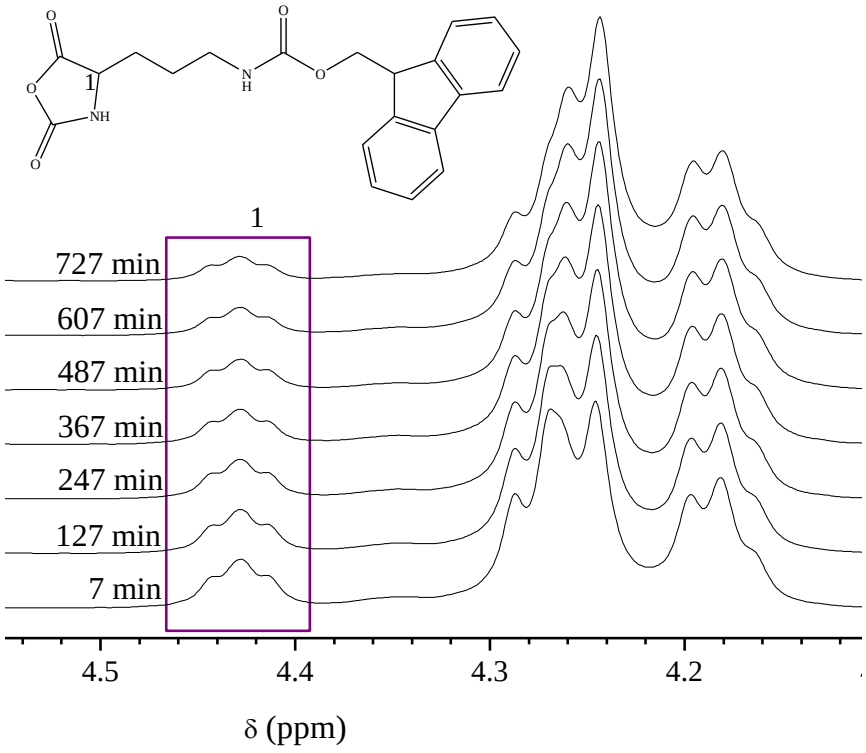

Figure 4-2 Expansion of the region from 4.10-4.56 ppm in Figure 4-1 showing the region of αCH of monomer f-Orn NCA during polymerization at 25 °C in DMSO-d_6.

Figure 4-2 shows the enlarged region from 4.10 ppm to 4.56 ppm of the αCH peak (H_1) used to monitor consumption of f-Orn NCA monomer. The proton signal resonating between 4.50 and 4.35 ppm was observed to be decreasing as a function of time and was therefore used to follow conversion of f-Orn NCA as a function of time as shown in Figure 4-3. The proton used to monitor the NCA consumption is shielded in the polymer and resonate between 4.32-4.20 ppm, overlapping with protons **5**, hence the observed increase in intensity between 4.32-4.22 ppm. The shielding which occurs in α-proton was clearly observed in poly(Z-ornithine) where there is no overlapping from the protection group.

4.4.2.2. Conversion-time measurements of f-Orn NCA

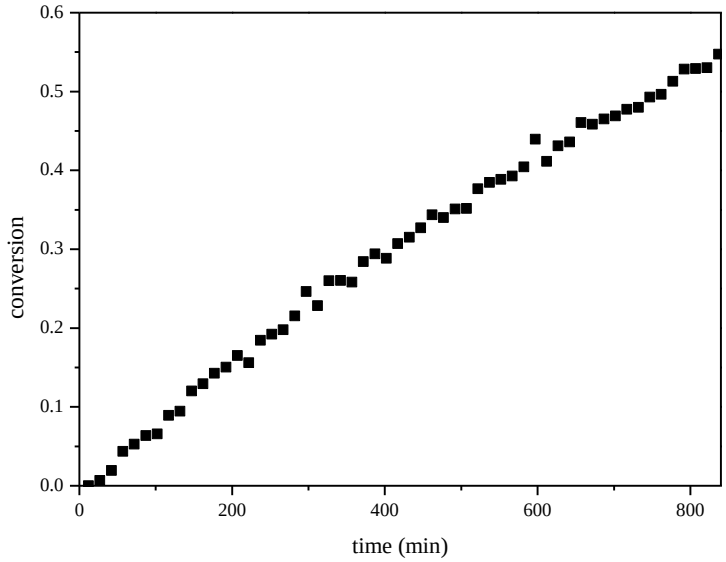

Figure 4-3 Evolution of conversion versus time for *n*-butylamine initiated *in situ* homopolymerization of f-Orn NCA in DMSO-d_6 at 25 ºC for 14 hours.

The conversion vs. time curve for polymerization of f-Orn NCA initiated with *n*-butylamine is shown in Figure 4-3. The conversion-time curve observed for *n*-butylamine-initiated polymerization of f-Orn NCA in DMSO-d_6 at 25 ºC for 14 hours shows a typical first-order rate behaviour, which is confirmed by the linear increase of $\ln([M]_o/[M])$ as a function of time in Figure 4-4.

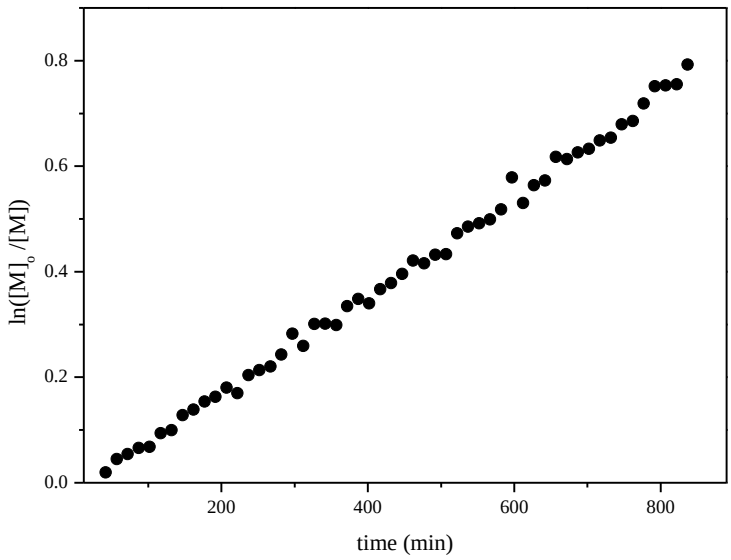

Figure 4-4 Evolution of $\ln([M]_o/[M])$ as a function of time for homopolymerization of f-Orn NCA in DMSO-d_6 initiated by *n*-butylamine at 25 ºC for 14 hours.

4.4.2.3. Conversion-time measurements for Bz-Asp, Z-Orn and Gly NCAs.

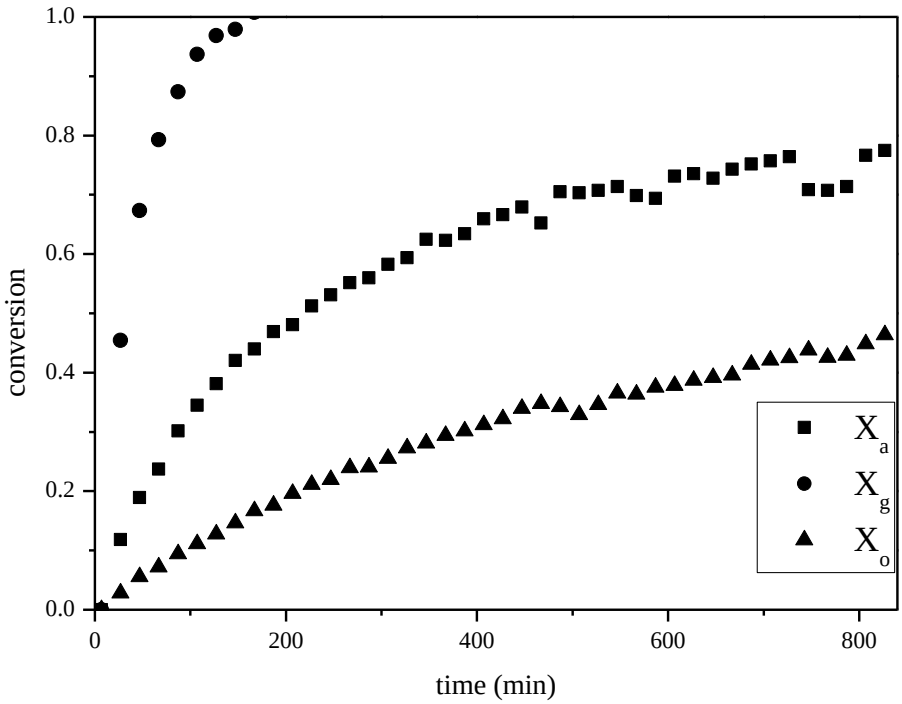

Figure 4-5 Evolution of conversions of the NCAs of Bz-Asp (■, X_a), Z-Orn (▲, X_o) and Gly (●, X_g) as a function of time during *n*-butylamine-initiated polymerization in DMSO-d_6 at 25 ºC for 14 hours.

The conversions of the NCAs as a function of time in Figure 4-5 were monitored with online ^{1}H NMR using the same procedure as specified for f-Orn NCA. Upon polymerization, the intensities of protons attached on to the cyclic αCH of the NCAs decreased with time. This decrease in intensity can be translated to conversion of monomer to polymer as a function of time during polymerization of the NCAs.

Conversion plots of the NCAs are shown in Figure 4-3 for f-Orn and Figure 4-5 for Bz-Asp, Z-Orn and Gly NCAs respectively. Complete conversion was observed for Gly NCA, although solubility of Gly NCA and the corresponding polymer pose a challenge for the polymerization solution. Incomplete conversions were observed for the other NCAs. Low conversions for structures Bz-Asp, Z-Orn and f-Orn NCAs are attributed to steric hindrance from bulky protecting groups that lower the accessibility of the reactive site (steric hindrance) and/or mobility of the propagating amine. Noticeable also, these NCAs have hydrogen bond accepting groups on their side-chains. It can be hypothesized that intrachain hydrogen bonding could decrease the nucleophilicity of the propagating amine chain end.[10,11]

4.5. Conclusions

Homopolymerization reactions of NCAs of glycine, β-benzyl-L-aspartate, N_{δ}-carbobenzyloxy-L-ornithine and N_{δ}-fluorenylmethyloxycarbonyl-L-ornithine were successfully monitored with *in situ* ^{1}H NMR spectroscopy. The low conversions obtained for all monomers except for Gly NCA, can be inferred to either the size of the side chains hindering accessibility of the cyclic electrophilic carbonyl group, or the presence of groups that contribute to hydrogen bonding with propagating amine. The main aim of the *in situ* polymerizations was to find conditions for *in situ* copolymerizations and terpolymerizations of the monomers and this objective was successfully attained.

4.6. References

(1) Vayaboury, W.; Giani, O.; Cottet, H.; Deratani, A.; Schue, F. *Macromol. Rapid Commun.* **2004**, *25*, 1221.

(2) Habraken, G. J. M.; Peeters, M.; Dietz, C. H. J. T.; Koning, C. E.; Heise, A. *Polym. Chem.* **2010**, *1*, 514.

(3) Kricheldorf, H. R.; Lossow, C. v.; Schwarz, G. *Macromol. Chem. Phys.* **2005**, *206*, 282.

(4) Kricheldorf, H. R. *Angew. Chem., Int. Ed.* **2006**, *45*, 5752.

(5) Bykov, S.; Asher, S. *J. Phys. Chem. B* **2010**, *114*, 6636.

(6) Wiejak, S.; Masiukiewicz, E. b.; Rzeszotarska, B. *Chem. Pharm. Bull.* **2001**, *49*, 1189—1191.

(7) Isidro-Llobet, A.; Alvarez, M.; Albericio, F. *Chem. Rev. (Washington, DC, U. S.)* **2009**, *109*, 2455.

(8) Silva, M.; Ferreira, E. I.; Leite, C. Q. F.; Sato, D. N. *Trop J Pharm Res*, **2007**, *6*, 815.

(9) Silva, M.; Lara, A. S.; Leite, C. Q. F.; Ferreira, E. I. *Arch. Pharm. (Weinheim, Ger.)* **2001**, *334*, 189.

(10) Brulc, B.; Žagar, E.; Gadzinowski, M.; Słomkowski, S.; Žigon, M. *Macromol. Chem. Phys.* **2011**, *212*, 550.

(11) Habraken, G. J. M.; Wilsens, K. H. R. M.; Koning, C. E.; Heise, A. *Polym. Chem.* **2011**, *2*, 1322.

(12) Vincent, V. PhD, Universitiet Gent, 2012.

Chapter V: Copolymerization and Terpolymerization of Ornithine, Glycine and β-benzyl-L-Aspartate *N*-CarboxyAnhydrides

Summary

This chapter deals with binary copolymerization of NCAs of glycine, β-benzyl aspartate and ornithines as a build up to a preliminary terpolymerization reaction. Kinetic studies of various binary copolymerizations are conducted in order to determine respective reactivity ratios. Similar to the homopolymerization studies reported in Chapter IV, the binary copolymerizations are initiated with *n*-butylamine in DMSO-d_6 at room temperature under vacuum and the progress of the polymerization is monitored via *in situ* ^{1}H NMR spectroscopy. The protocol achieved in homo- and copolymerization studies was used to monitor a terpolymerization reaction.

5. Kinetic copolymerizations: An Overview

Polypeptides are interesting model compounds for the study of their natural counterparts, *i.e.* proteins. Proteins are composed of at least 20 different natural amino acids linked together in a predetermined order by peptide bonds. The properties of proteins are dictated by the sequence of amino acids along the chain. Synthetically it is challenging to afford polypeptides with a specified order along the chain as observed in natural proteins. The distribution in synthetic polypeptides may be random or blocky depending on the synthetic route. Based on their architecture, random or statistical copolypeptides are better models than other structures.

Random copolymers are prepared by simultaneous polymerization of two or more amino acids or their derivatives. Ring-opening polymerization of two or more amino acid NCAs being the most successful route. Studies on random copolypeptides prepared via ROP of NCAs have been on properties such as conformations[1,2] and proteolytic enzyme degradation.[3,4] Results of degradation studies in most cases showed that proteolytic enzymes (Papain, Bromelain and Ficin) randomly break the peptide bonds along the chains and degradation followed Michealis-Menten kinetics being first order in enzyme concentration.

Work on random copolypeptides has also been devoted to the determination of reactivity ratios of amino acid NCAs.[5] Knowledge of reactivity ratios gives better understanding about distribution of amino acid-units along the polypeptide chain, *i.e.* copolymer composition and sequence distribution. Determination of reactivity ratios proceeds by fitting data from copolymerization reactions to equations derived by manipulating the copolymerization equation (Equation 5-1). The most frequently used techniques utilize instantaneous copolymer composition versus comonomer feed composition and fit those to the equations of relevant copolymerization model. The necessary data to be collected from a copolymer-system is determined by limits or assumptions made when deriving the equation at hand. Equations such as Kelen-Tüdös and Fineman-Ross allow determination of reactivity ratios only at low conversion of about 5-10%. Extended Kelen-Tüdös methods are used for determination of reactivity ratios at higher conversion.

Equation 5-1 Copolymerization equation according to the terminal model.

$$F_1 = 1 - F_2 = \frac{r_1 f_1^2 + f_1 f_2}{r_1 f_1^2 + 2 f_1 f_2 + r_2 f_2^2}$$

On the other hand to prepare copolymers of higher molecular weight in a living polymerization process, copolymerization should be allowed to proceed until higher conversions. During copolymerization, one of the comonomers may preferential add to the growing chain hence there is a composition drift at higher conversion. The instantaneous copolymer composition as a function of conversion can be determined by integrating the copolymer equation.[6] Using the integrated form of the copolymerization equation, reactivity ratios of NCAs were reported at higher conversions.[7,8]

The extent of conversion in copolymerization of amino acid NCAs can be evaluated by monitoring carbon dioxide released during polymerization. The released carbon dioxide can be trapped in benzyl amine solution that is titrated with standard sodium methoxide. In this method the carbon dioxide is pushed from the reaction into the absorbing column solution by a continuous flow of nitrogen gas, therefore the length of the column and flow rate of N_2 affect the accuracy of this method in determining CO_2.[9]

Recently, Zelzer *et al.*[10] developed a method using HPLC to monitor consumption of N_ε-benzyloxy-L-lysine and γ-benzyl-L-glutamate NCAs initiated by *n*-hexylamine under N_2 in DMF. The polymerization samples were quenched by acid hydrolysis (HCl), filtered and analysed by HPLC relying on the UV absorption of the aromatic protection groups at 254 nm for detection of the protected amino acids. The HPLC method provided monomer concentrations at specific time-points during polymerization. When the normalised concentrations obtained from HPLC chromatograms were compared with normalised IR data, the overall shape of the curves matched well from both measurements throughout polymerization. The use of linear graphical methods (Kelen-Tüdös) showed that γ-benzyl-L-glutamate was incorporated more readily in the copolymer.[10]

In this study we developed a method in which copolymerization studies of NCAs are carried out with *in situ* ^{1}H NMR spectroscopy. The copolymerization progress is followed by examining the decrease of signal intensities of protons assigned for each amino acid NCA. These resonances are well separated from each other, which makes it easy to follow the individual NCA kinetics during copolymerization. As a verification of the applicability of the *in situ* ^{1}H NMR protocol achieved in homopolymerization and copolymerization studies, a preliminary terpolymerization reaction was monitored.

Binary copolymerizations of the amino acid NCAs were conducted with the conditions described for *in situ* ^{1}H NMR homopolymerization experiments for the individual monomers in Chapter IV.

General tree diagram for copolymerization of two NCAs initiated by primary amines

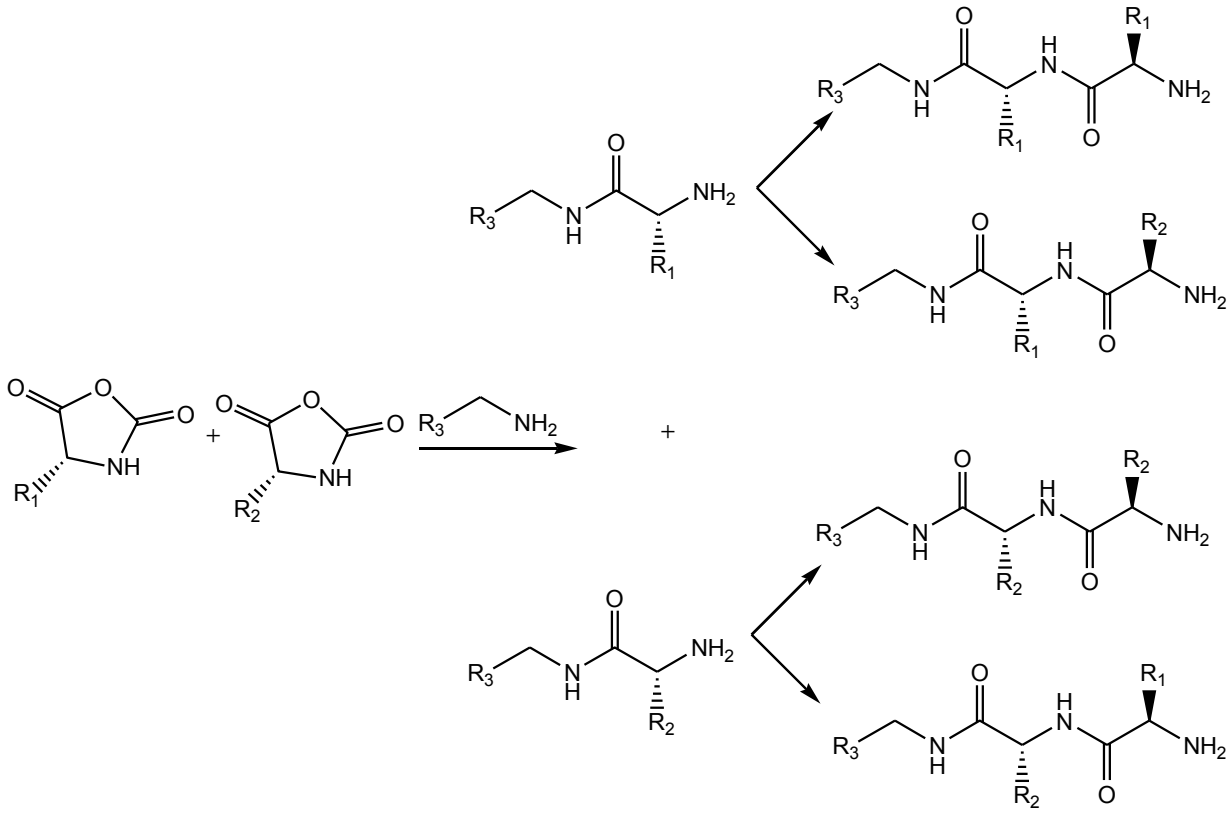

Scheme 5-1 NAM pathway for copolymerization of two NCAs showing the first two monomer additions.

Scheme 5-1 shows a general scheme for binary copolymerization of two NCAs propagating by NAM, in the scheme it is shown that each monomer can either add to its self or cross-propagate during the copolymerization process. The rate of each reaction is influenced by factors such as stereochemical considerations, specificity of the side chain in the NCA[7] solvent and initiator used.

5.1. Experimental

5.1.1. Materials

The NCA monomers were prepared and stored as previously described in Chapter III. *n*-Butylamine (≥ 99.5%, Sigma-Aldrich) and DMSO-d_6 (99.9% atom D, Aldrich) were used as received.

5.1.2. *In situ* ^{1}H NMR spectroscopy procedure

The ^{1}H NMR spectra were recorded with a 400 MHz Varian Unity Inova spectrometer. The ^{1}H NMR spectra were acquired with 3 μL (40°) pulse width and 4 seconds acquisition time. For the *in situ* experiments, samples were first defrosted, then inserted into the magnet at 25 °C and the magnet shimmed, the first spectrum collected served as a reference. Subsequent spectra were collected at 20 or 15 minutes intervals for 14 hours. Phase correction was preformed automatically whilst baseline correction and integration were performed manually using ACD Labs 12.0 ^{1}H NMR processor.

5.1.3. Procedure for *in situ* ^{1}H NMR copolymerization of glycine NCA (Gly) and β-benzyl-aspartate (Bz-Asp) NCA.

Gly NCA and Bz-Asp NCA copolymerizations were followed via *in situ* ^{1}H NMR at 25 ^{o}C and different monomer feed compositions in DMSO-d_6. The total monomer concentration was kept at 0.3 M for *in situ* ^{1}H NMR reactions. Monomers were dissolved in DMSO-d_6 transferred to a Wilmad® quick pressure valve NMR tube that already contained 0.6 μL of *n*-butylamine initiator. The copolymerization mixture in the tube was degassed by three freeze-pump-thaw cycles and copolymerization allowed to run for 14 hours in an NMR instrument after defrosting the content of the tube. In a typical copolymerization experiment of mole ratio 0.1 Gly/0.9 Bz-Asp, Gly NCA (0.0071 g, 0.07 mmol) and Bz-Asp NCA (0.157 g, 0.63 mmol) were dissolved in DMSO-d_6 (2.4 mL) to make a concentration of 0.3 M. Then the NCA solution was transferred to a Wilmad® quick pressure valve NMR tube with 0.6 μL *n*-butylamine. The reaction mixture was degassed by three freeze-pump-thaw cycles after which the progress of the polymerization was monitored via *in situ* ^{1}H NMR spectroscopy as previously described in Section 5.1.2.

5.2. Results and discussion

5.2.1. Monitoring kinetic copolymerization of NCAs of glycine (Gly) and β-benzyl-aspartate (Bz-Asp) system

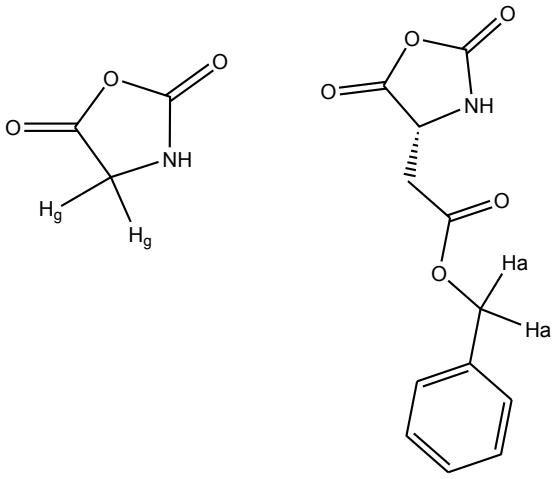

Scheme 5-2 Chemical structures of glycine NCA (H_g) and β-benzyl aspartate NCA (H_a) indicating protons that were used to monitor and construct kinetic profiles.

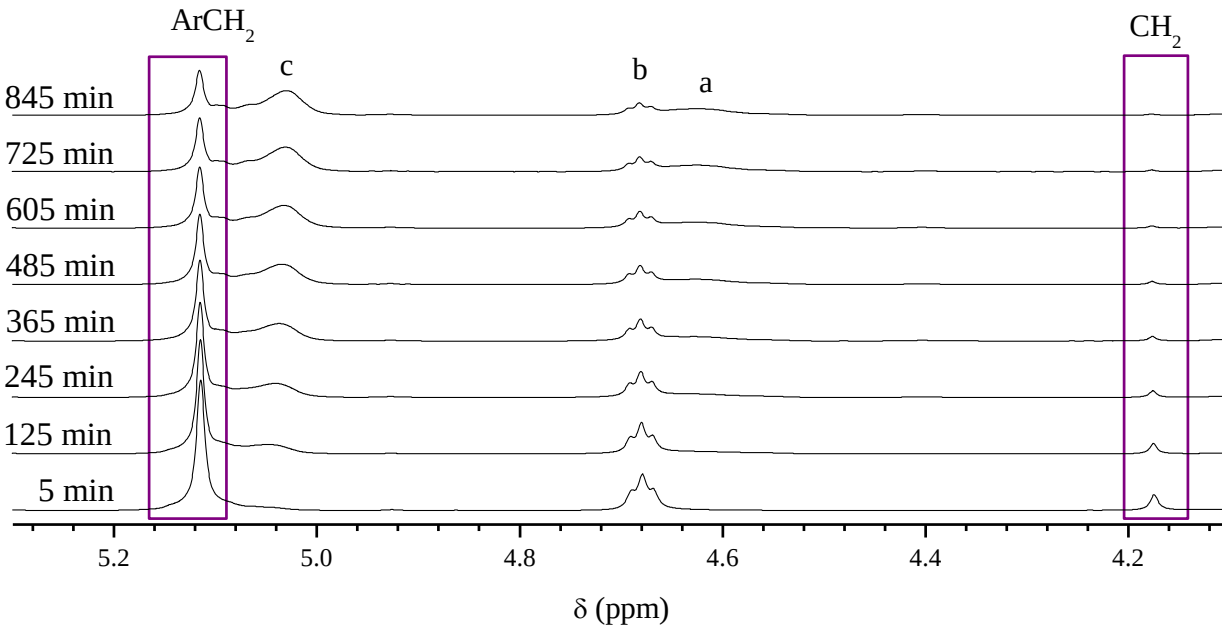

Figure 5-1 ^{1}H NMR spectra at different reaction times illustrating the enlarged region from 4.1 to 5.3 ppm during copolymerization of NCAs of Gly/Bz-Asp in DMSO-d_6 for 14 hours at 25 °C started with f_g^0 =0.10.

Figure 5-1 shows an array of spectra of the enlarged region [4.1 ≤ δ (ppm) ≤ 5.3] during *n*-butylamine-initiated copolymerization of Bz-Asp/Gly NCAs at f_g^0 = 0.10 in DMSO-d_6 at 25 ºC. The peaks labelled CH_2 (αCH_2) and $ArCH_2$ (benzylic CH_2) were used to monitor consumption of NCAs of Gly and Bz-Asp respectively. The peaks c and a represent Bz-Asp in the copolymer, where. c is the benzylic CH_2 and a the αCH. Peak b is the αCH of Bz-Asp in the monomer. Peak b shows a decrease in intensity with time, but at higher Bz-Asp NCA feed compositions it overlaps with a and as a result, the benzylic CH_2 for Bz-Asp that was better resolved, was used in this study. The separation of these two resonance signals enabled the possibility to follow the kinetics of Gly/Bz-Asp NCA copolymerization.

Changes in intensities of $ArCH_2$ and CH_2 protons of Gly and Bz-Asp NCAs respectively, enabled quantification of variation of individual (X_i) and overall conversions (X_t), comonomer fractions in the feed (f_i) and in the copolymer (F_i) using the equations in Section 5.2.1.1.

5.2.1.1. Equations for the Gly/Bz-Asp copolymerization system

Equation 5-2 Glycine NCA conversion as a function of time.

$$X_g = \frac{I\left(CH_2^g\right)_0 - I\left(CH_2^g\right)_t}{I\left(CH_2^g\right)_0}$$

Equation 5-3 β-benzyl-aspartate NCA conversion as a function time.

$$X_a = \frac{I(CH_2^a)_0 - I(CH_2^a)_t}{I(CH_2^a)_0}$$

Equation 5-4 Overall conversion as a function of time.

$$X_t = 1 - \frac{I(CH_2^a)_t + I\left(CH_2^g\right)_t}{I(CH_2^a)_0 + I\left(CH_2^g\right)_0}$$

Equation 5-5 Instantaneous feed composition of Glycine NCA as a function of time.

$$f_g = \frac{I\left(CH_2^g\right)_t}{I\left(CH_2^g\right)_t + I(CH_2^a)_t}$$

Equation 5-6 Overall copolymer composition of Glycine as a function of time.

$$cF_g = \frac{I\left(CH_2^g\right)_0 - I\left(CH_2^g\right)_t}{[I(CH_2^a)_0 + I\left(CH_2^g\right)_0] - [I(CH_2^a)_t + I\left(CH_2^g\right)_t]}$$

Equation 5-7 Instantaneous copolymer composition of Glycine as a function of time.

$$F_g = \frac{I\left(CH_2^g\right)_t - I\left(CH_2^g\right)_{t+d}}{[I(CH_2^a)_t + I\left(CH_2^g\right)_t] - [I(CH_2^a)_{t+d} + I\left(CH_2^g\right)_{t+d}]}$$

Average instantaneous copolymer composition represents changes that were taken at intervals of time, with t_n representing the first data point and the next being t_{n+d}, where d is a common time difference between the points *e.g.* for n = 1 and d = 4, the first data is taken at t_1 and combined with one at t_5, followed by one at t_2 and t_6 and so on. The equations were used taking into account that 2 protons were used for each NCA comonomer also with the

assumption that ≥ 95% of the consumed monomer was incorporated in the growing copolymer.

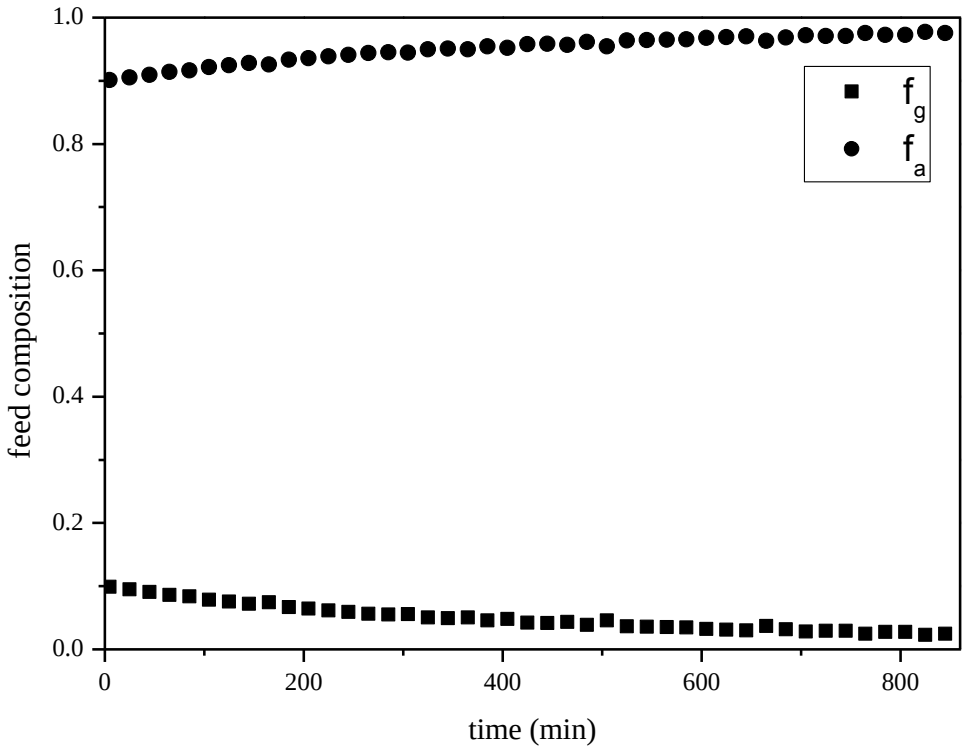

Figure 5-2 The instantaneous feed composition as a function of time, during copolymerization of NCAs of Gly/Bz-Asp, started with $f_g^0 = 0.10$ in DMSO-d_6 at 25 °C for 14 hours.

Figure 5-2 illustrates the change in concentrations (mole fractions) of Gly and Bz-Asp NCAs in a copolymerization with an initial feed composition of $f_g^0 = 0.10$. Gly NCA is consumed faster than Bz-Asp NCA during the copolymerization and as result, the fraction of Bz-Asp NCA in the residual monomer increases with time.

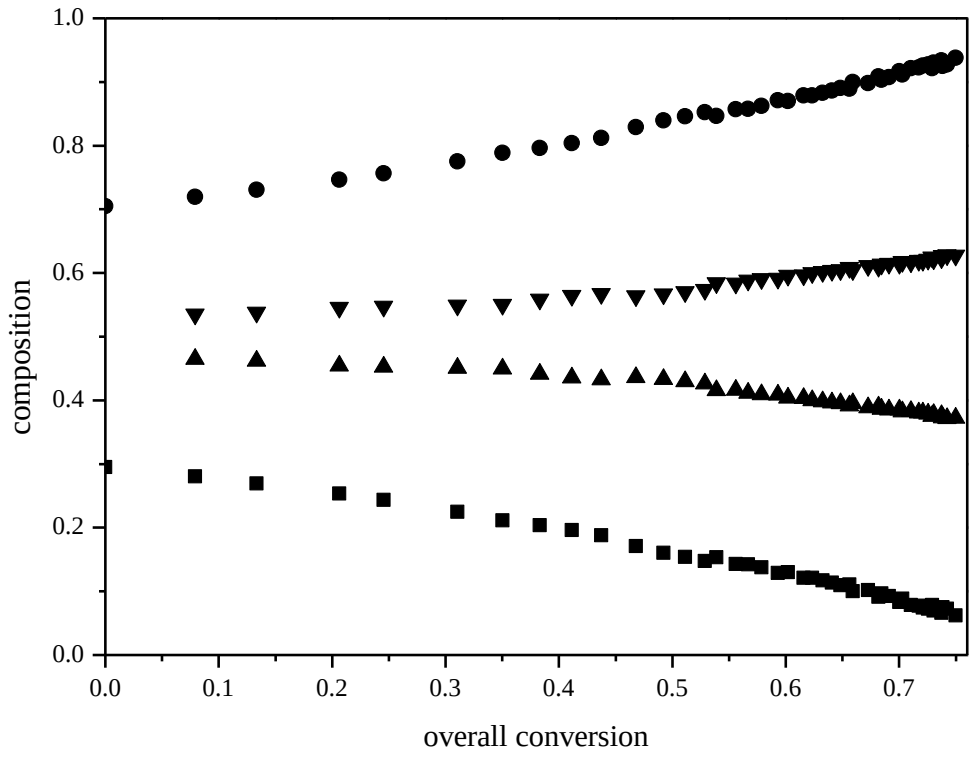

Figure 5-3 Feed composition (■, Gly; ●, Bz-Asp) and copolymer composition (▲, Gly; ▼, Bz-Asp) as a function of overall conversion, during copolymerization of Gly/Bz-Asp NCAs started with $f_g^0 = 0.30$ and $f_a^0 = 0.70$ in DMSO-d_6 at 25 °C for 14 hours.

Figure 5-3 shows the variation of NCA comonomer fractions in the feed (Gly = ■ & Bz-Asp = ●) and overall copolymer (Gly =▲ & Bz-Asp =▼) as a function of overall conversion during a copolymerization started with $f_g^0 = 0.30$ at 25 °C in DMSO-d_6. Gly NCA molar fraction decreases in the feed with increasing conversion, whilst the fraction of Bz-Asp NCA increases in the feed, this behaviour shows the preferential addition of Gly NCA to the copolymer in comparison to its comonomer. The changes are significant at higher overall conversions ≥ 50%. The reactivity of Gly NCA is shown by the higher Gly copolymer content respective to the starting Gly NCA in the feed.

As the degree of conversion increases further, the feed becomes richer in Bz-Asp NCA. This has the consequence that the propagating amino end groups have an increasing probability of reacting with Bz-Asp NCA in comparison to the depleting Gly NCA hence an eventual increase of Bz-Asp NCA in the copolymer. This copolymerization mixture generates lower Bz-Asp in the copolymer ($F_a = 0.54$) relative to its starting composition in the feed which then increases at higher conversion.

5.2.1.2. Copolymerization curve for Gly and Bz-Asp system and assessment of reactivity ratios

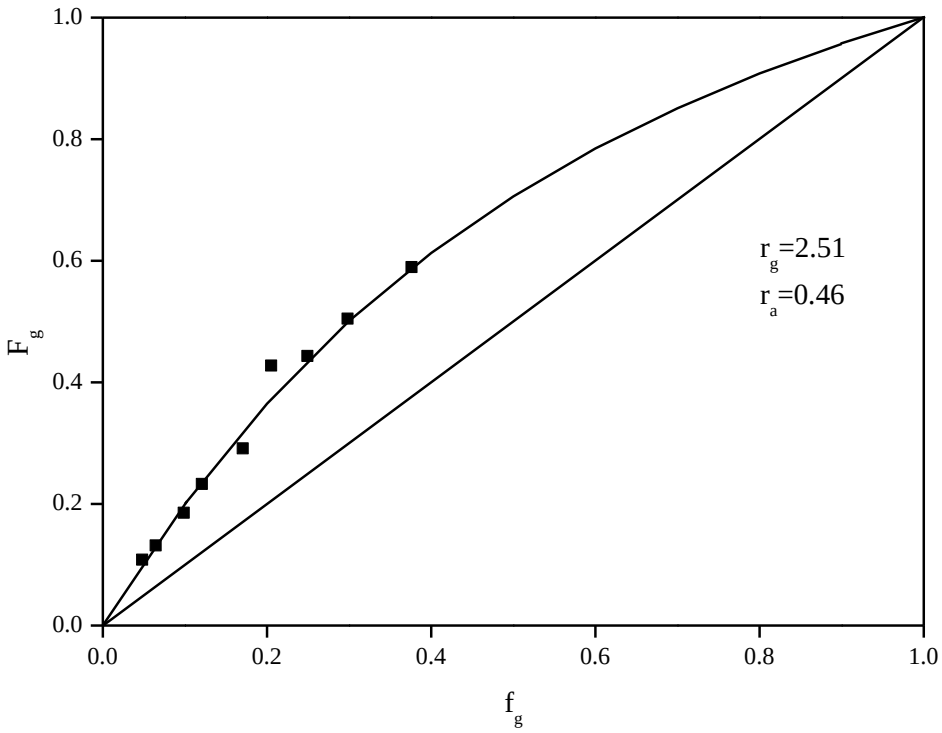

Figure 5-4 Copolymer composition versus feed composition for the three copolymerizations carried of Gly-NCA with Bz-Asp NCA i.e. f_g^0 = 0.10, 0.30 and 0.40. The curve drawn through the experimental data points was calculated with r_g = 2.51 (Gly NCA) and r_a = 0.46 (Bz-Asp NCA).

At higher instantaneous feed compositions, Gly NCA was partly soluble. At 0.3 M total comonomer concentration, it was only soluble up to f_g^0 = 0.40, hence no binary mixtures were determined beyond f_g^0 = 0.40. The three binary copolymerization mixtures with f_g^0 = 0.1, f_g^0 = 0.30 and f_g^0 = 0.40 respectively, were used to construct a copolymerization curve and for the assessment of reactivity ratios (Figure 5-4). Figure 5-4 shows that Gly content in the copolymer was always higher than Bz-Asp for the studied copolymerization mixtures as was expected from Figures 5-2 and 5-3. Therefore Gly tends to be added preferentially to the propagating copolymer amino end groups. Reactivity ratios were calculated with Contour software[11] that uses the nonlinear least squares methodology in conjunction with the terminal model of copolymerization and a constant relative error was chosen in fitting procedure. Inputting the instantaneous feed compositions, copolymer compositions and plotting instantaneous copolymer composition (F_g) vs. feed composition (f_g) for glycine monomer

from the program for the studied copolymerizations, the reactivity ratios were found to be r_g = 2.51 and r_a = 0.46.

5.2.1.3. Contour plot of reactivity ratios: Gly-Bz-Asp system

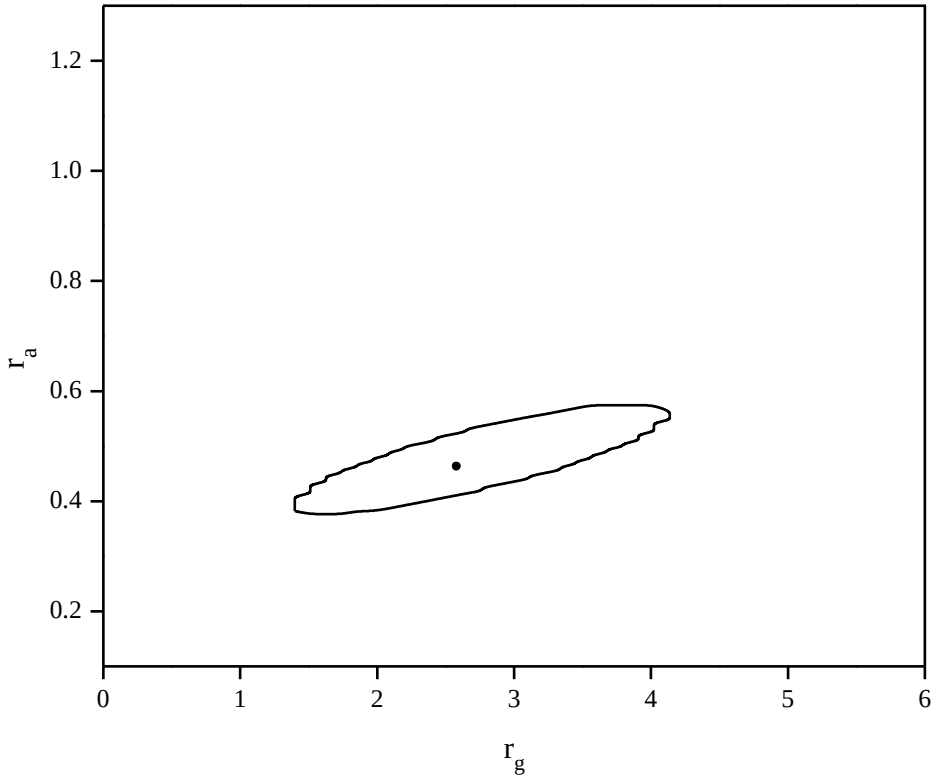

Figure 5-5 The 95% joint confidence interval of reactivity ratios for the Gly (r_g): Bz-Asp (r_a) copolymerization system.

Figure 5-5 illustrates a 95% joint confidence interval of reactivity ratios for the Gly/Bz-Asp system. From Figure 5-5 a broad distribution of possible values for both reactivity ratios is observed.

5.3. Kinetics of the Ornithine-Aspartic acid system

Copolymerization of NCAs allow preparation of side-chain-functional polypeptides that may possess various protecting groups that can be removed under different conditions (orthogonal deprotection). The possibility to selectively remove functional groups may provide access to the synthesis of graft copolypeptides and targeted side group modification on specific amino acid side chains. Hernández *et al.*[12] studied synthesis and polymerization of various lysine NCAs with different protecting groups also exploring the deprotection conditions. It was reported that the Z-group on lysine (1 CH_2 more than ornithine) and the Bz group on glutamate (1 CH_2 more than aspartic acid) can simultaneously be removed by hydrogenolysis (stirring in DMF under H_2 over Pd-C ~, 10% Pd) hence no orthogonal deprotection. On the other hand, the fmoc group on lysine can be removed with 20% (v/v) piperidine in DMF without affecting either the Z group on lysine *i.e*. Lys(f)-*co*-Lys(Z), or the Bz group on glutamate Lys(f)-*co*-Glu(Bz).

Based on the above discussion, this copolymerization system was divided into two copolymerization subsystems based on the protecting groups incorporated on the ornithine side chains, *i.e*. the fmoc-protected and Z-protected ornithine. The difference between these protecting groups is in the stability in terms of deprotection. With fmoc group removed under basic (alkaline) conditions orthogonal to the Bz group of aspartic acid whilst the Z-group in ornithine is removed under acidic or hydrogenolysis conditions, which are the same conditions for deprotection of Bz group in aspartic acid. Orthogonal deprotection is envisaged for eventual modification of ornithine residues without affecting aspartic acid, *i.e*. deprotection of ornithine side chains under conditions that do not affect the Bz group from aspartic acid segments.

It was observed that Gly NCA solubility at higher concentrations became a challenge and ornithine NCAs were slow to copolymerize, if at all, at their low instantaneous feed composition (ca. 20%) mixtures at 0.3 M total monomer concentration. Total monomer concentration was decreased to approximately 0.15 M whilst the conditions and initiator amount were not changed. The procedure described in Section 5.1.2 was followed. ^{1}H NMR was used to monitor the kinetics of copolymerizations of ornithine NCAs with glycine and β-benzyl-L-aspartate NCAs and results are discussed in the following sections.

5.3.1. Monitoring kinetics of N_δ-Fluorenylmethyloxycarbonyl-L-Ornithine (f-Orn) NCA and β-benzyl Aspartate NCA (Bz-Asp) system

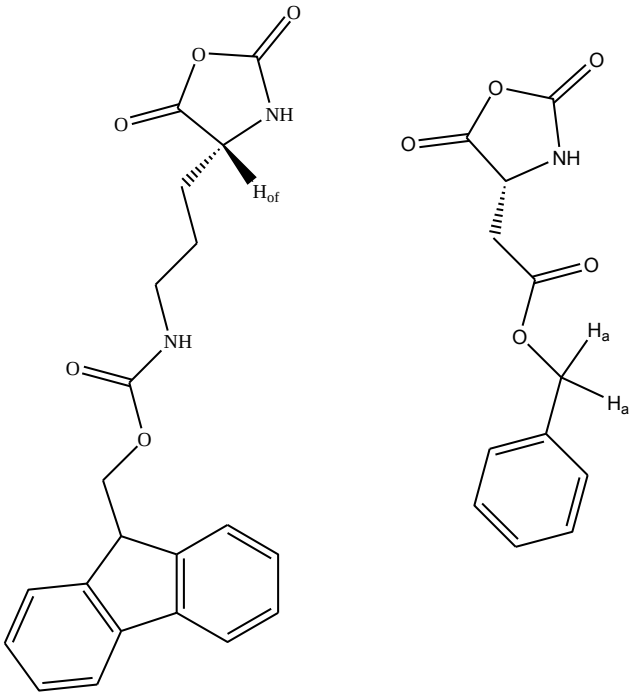

Scheme 5-3 Chemical structures of f-Orn and Bz-Asp NCAs, indicating protons that were monitored during copolymerization.

Scheme 5-3 shows chemical structures of f-Orn and Bz-Asp NCAs, the labelled proton intensities were observed to decrease with time and used to monitor copolymerization kinetics of the respective NCAs. The equations in Section 5.3.1.1 were used to monitor individual and overall conversions, as well as comonomer molar fractions in the feed and in the copolymer as a function of time.

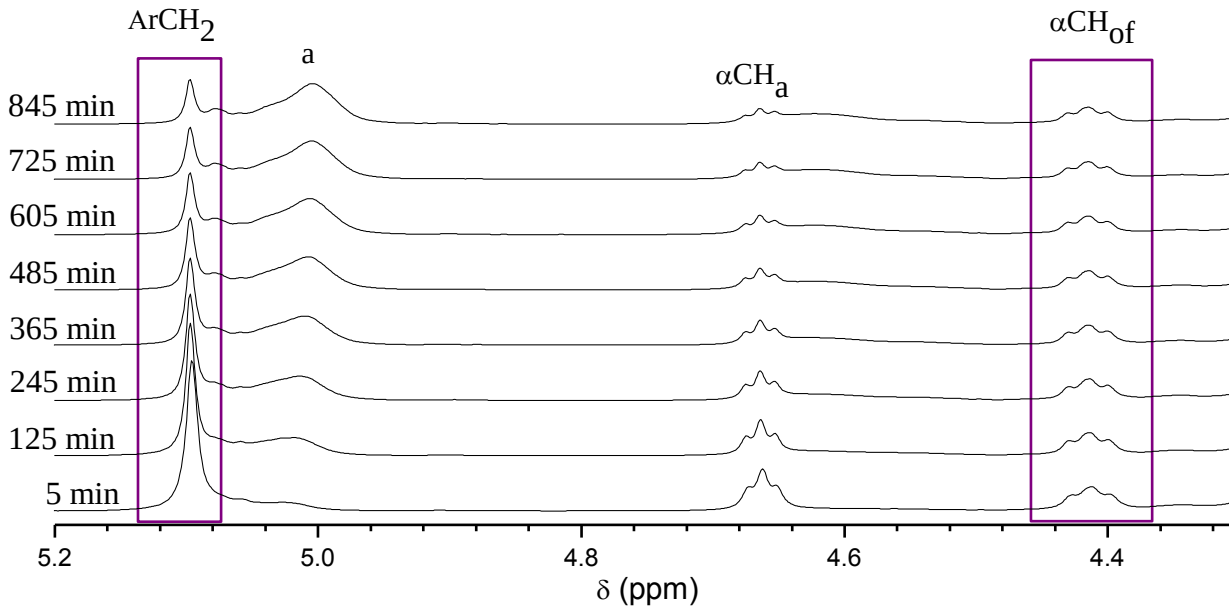

Figure 5-6 ^{1}H NMR spectra as a function of time illustrating the region from 4.3 to 5.2 ppm during copolymerization of NCAs of f-Orn and Bz-Asp conducted in DMSO-d_6 for 14 hours at 25 °C with $f_a^0 = 0.51$.

Figure 5-6 illustrates an array of spectra of the enlarged region [$4.3 \leq \delta$ (ppm) ≤ 5.2] during *n*-butylamine-initiated copolymerization of f-Orn and Bz-Asp NCAs at $f_a^0 = 0.51$ in DMSO-d_6 at 25 ºC. The peaks labeled αCH_{of} and $ArCH_2$ (benzylic CH_2) were used to monitor consumption of NCAs of f-Orn and Bz-Asp with time, respectively. Peak a ($ArCH_2$) represents Bz-Asp in the copolymer and αCH_a of Bz-Asp in the monomer. Using the equations in Section 5.3.1.1, kinetics of f-Orn/Bz-Asp copolymerization system were monitored.

5.3.1.1. Equations for Bz-Asp/f-Orn copolymerization system

Equation 5-8 Conversion of N_{δ}-fluorenylmethyloxycarbonyl-L-ornithine NCA as a function of time.

$$X_o = \frac{I(CH_1^o)_0 - I(CH_1^o)_t}{I(CH_1^o)_0}$$

Equation 5-9 Conversion of β-benzyl aspartate NCA as a function of time.

$$X_a = \frac{I(CH_2^a)_0 - I(CH_2^a)_t}{I(CH_2^a)_0}$$

Equation 5-10 Overall conversion as a function of time.

$$X_t = 1 - \frac{2[I(CH_1^o)_t] + I(CH_2^a)_t}{2[I(CH_1^o)_0] + I(CH_2^a)_0}$$

Equation 5-11 Instantaneous feed composition of β-benzyl aspartate NCA as a function of time.

$$f_a = \frac{I(CH_2^a)_t}{2[I(CH_1^o)_t] + I(CH_2^a)_t}$$

Equation 5-12 Overall copolymer composition of β-benzyl aspartate as a function of time.

$$cF_a = \frac{I(CH_2^a)_0 - I(CH_2^a)_t}{I(CH_2^a)_0 - I(CH_2^a)_t + 2 * [I(CH_1^o)_0 - I(CH_1^o)_t]}$$

Equation 5-13 Instantaneous copolymer composition as a function of time.

$$F_a = \frac{I(CH_2^a)_t - I(CH_2^a)_{t+d}}{I(CH_2^a)_t - I(CH_2^a)_{t+d} + 2 * [I(CH_1^o)_{t+d} - I(CH_1^o)_{t+d}]}$$

Average instantaneous copolymer composition represents copolymer composition changes that were taken at intervals of time, with t_n representing the first data point and the next being t_{n+d}, where d is a common time difference between the points e.g. for n = 1 and d = 4, the first data is taken at t_1 and combined with one at t_5, followed by one at t_2 and t_6 and so on. The equations were used taking into account that only one proton contributes for f-Orn NCA whilst two for Bz-Asp NCA, also with the assumption that all of the consumed monomer

contributes to the build-up of the copolymer chain. The decrease in intensities of these protons was used to monitor changes in comonomer concentration during copolymerization.

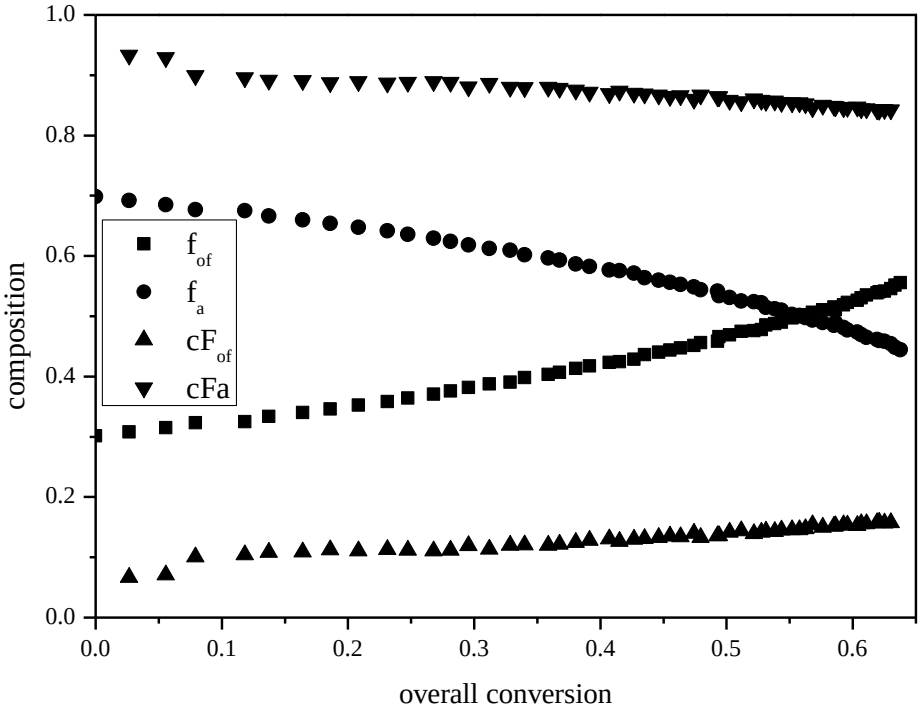

Figure 5-7 Instantaneous feed and copolymer composition as a function of overall conversion during copolymerization of f-Orn/Bz-Asp NCAs in DMSO-d_6 at 25 ^{o}C started with $f_a^0 = 0.70$.

The decrease of signal intensities of $ArCH_2$ for Bz-Asp NCA and endocyclic H_{of} of f-Orn NCA (Scheme 5-3) were monitored as a function of time. On the basis of the equations in Section 5.3.1.1, it was calculated that Bz-Asp NCA (f_a) in the feed decreases with increasing overall conversion. As a result, the residual monomer mixture was increasingly richer in f-Orn NCA (f_{of}) (see Figure 5-7). This implies preferential addition of Bz-Asp NCA to the growing amino end groups of the copolymer in comparison to its comonomer.

5.3.1.2. Copolymerization curve for f-Orn and Bz-Asp system and assessment of reactivity ratios

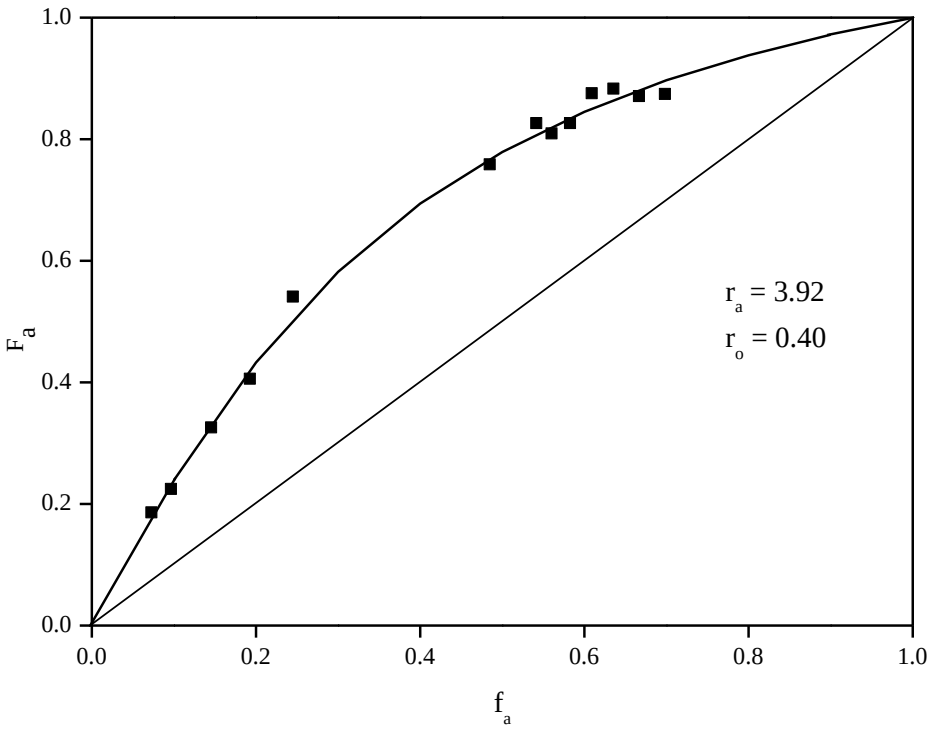

Figure 5-8 Copolymer composition versus feed composition for the copolymerization of f-Orn NCA with Bz-Asp NCA. The curve drawn through the experimental data points was calculated with $r_a = 3.92$ and $r_{of} = 0.40$.

From the binary copolymerization reactions carried out for Bz-Asp/f-Orn, the copolymerization curve in Figure 5-8 was constructed with f_a and F_a representing Bz-Asp composition in the feed and copolymer respectively. Bz-Asp NCA was found to be preferentially incorporated in the copolymer over f-Orn. On basis of F_a versus f_a data, via the nonlinear least squares method, the Contour programme estimated reactivity ratios to be $r_a = 3.92$ and $r_{of} = 0.40$, where a constant relative error was chosen for fitting data in the program. The 95% confidence interval of reactivity ratios obtained for this copolymerization system is shown in Figure 5-9.

5.3.1.3. Contour plot of reactivity ratios: Bz-Asp: f-Orn system

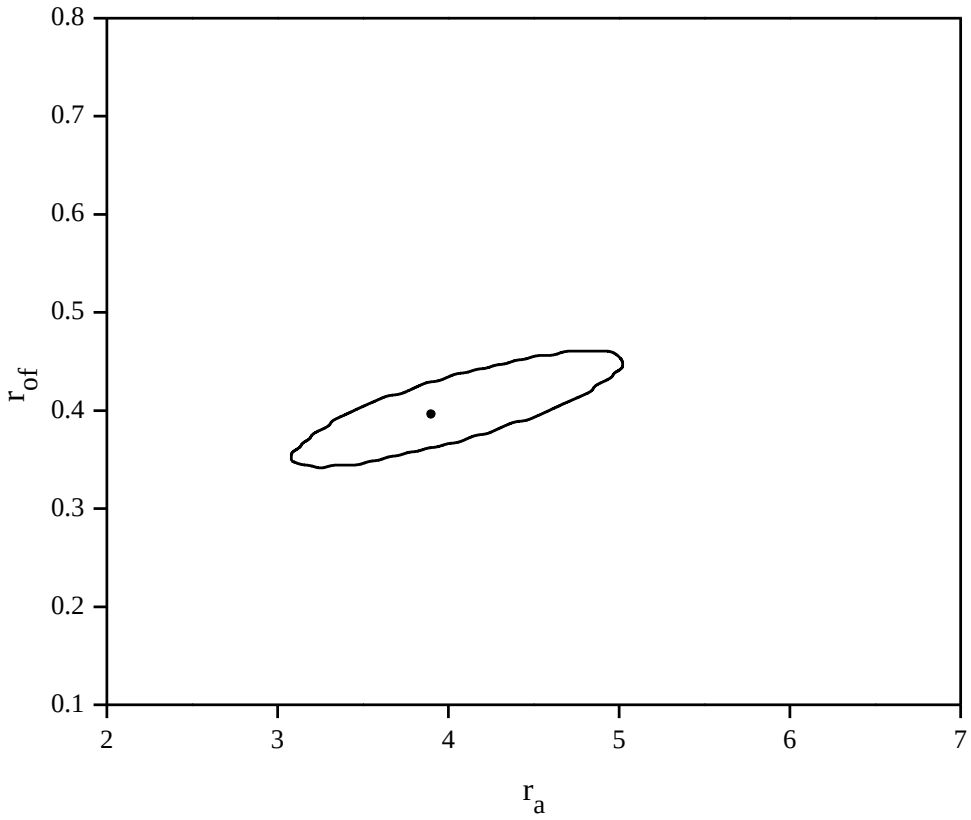

Figure 5-9 The 95% joint confidence interval of reactivity ratios for the Bz-Asp (r_a): f-Orn (r_{of}) copolymerization system.

5.3.2. Monitoring kinetics of N_{δ}-benzyloxycarbonyl-L-Ornithine NCA and β-Benzyl-L-Aspartate NCA system

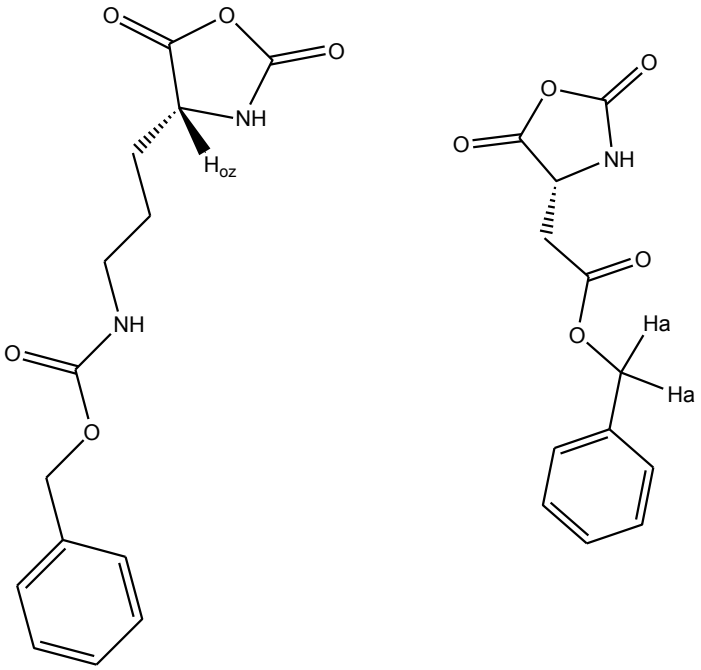

Scheme 5-4 Chemical structures of Z-Orn and Bz-Asp NCAs indicating protons that were monitored for kinetic profiles.

The copolymerization kinetics of the copolymerization between Z-Orn NCA and Bz-Asp NCA were monitored using the same equations as for the f-Orn/Bz-Asp system replacing H_{of} with H_{oz} in Section 5.3.1.1. The H_{oz} for Z-Orn NCA and the two benzylic protons for Bz-Asp NCA were used to monitor comonomer conversion as a function of time. It was observed that the intensities of these protons decreased with increase in time and therefore individual and overall conversions, instantaneous feed and copolymer compositions were monitored as a function of time for each comonomer.

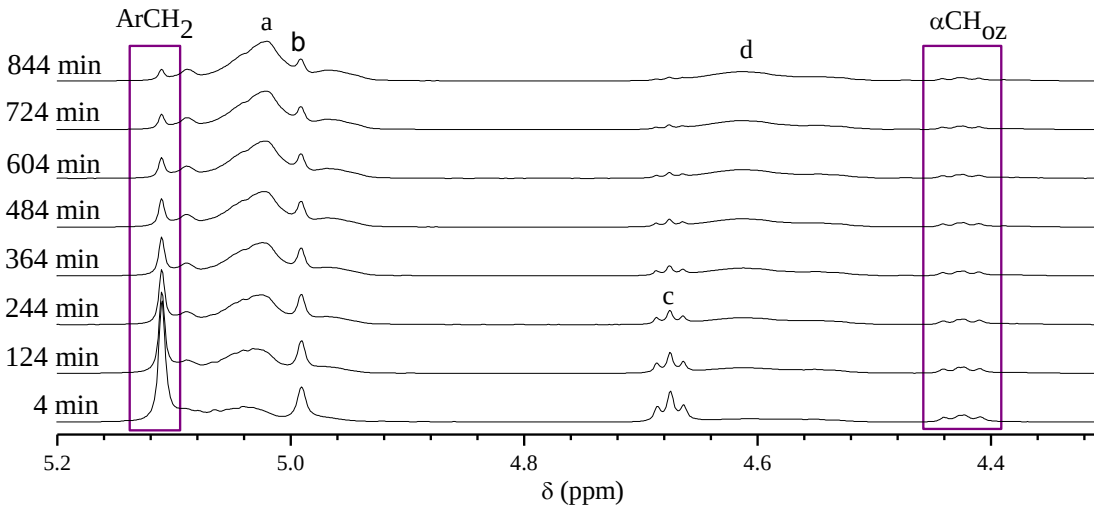

Figure 5-10 ^{1}H NMR spectra as a function of time, illustrating the region from 4.38 to 5.20 ppm during *n*-butylamine-initiated copolymerization of NCAs of Z-Orn/Bz-Asp in DMSO-d_6 for 14 hours at 25 °C started with $f_a^0 = 0.71$.

Figure 5-10 shows an array of spectra of the enlarged region [$4.38 \leq \delta$ (ppm) ≤ 5.2] during *n*-butylamine-initiated copolymerization of Z-Orn/Bz-Asp NCAs at $f_a^0 = 0.71$ in DMSO-d_6 at 25 ºC. The peaks labelled αCH_{oz} and $ArCH_2$ (benzylic CH_2) were used to monitor consumption of NCAs of Z-Orn and Bz-Asp respectively. Peak a ($ArCH_2$) represents Bz-Asp in the copolymer and αCH_a of Bz-Asp in the monomer, with b the $ArCH_2$ from Z-Orn in the copolymer and monomer.

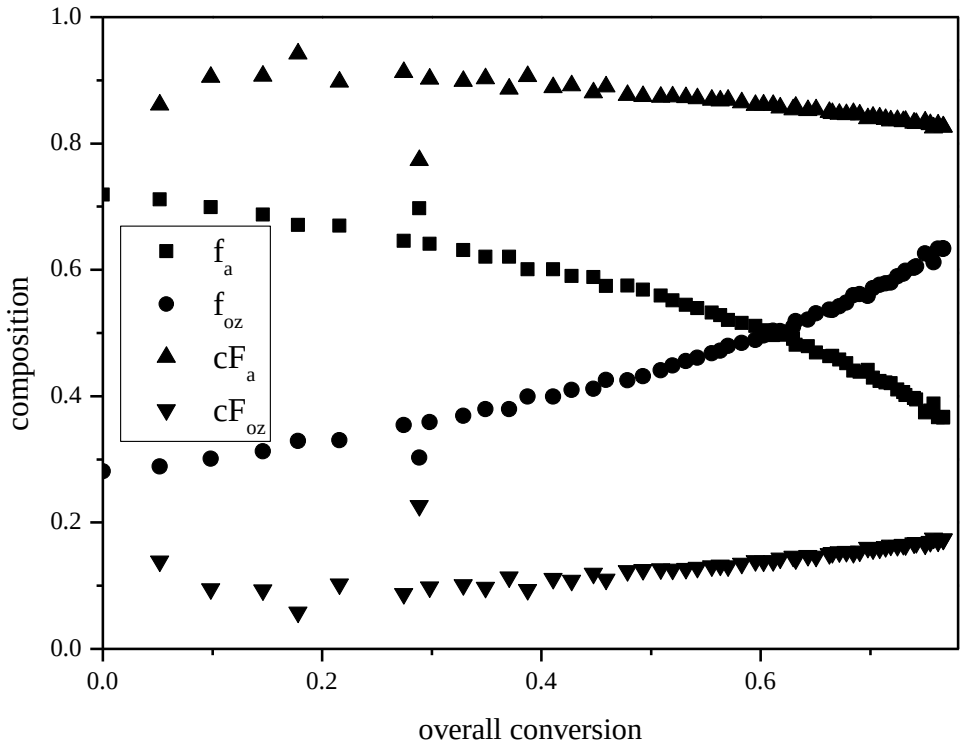

Figure 5-11 Comonomer fractions in the feed and in the overall copolymer as a function of overall conversion during copolymerization of Z-Orn NCA and Bz-Asp NCA in DMSO-d_6 started with $f_a^0 = 0.71$.

Figure 5-11 shows variation of comonomer compositions in the feed (Z-Orn = f_{oz} and Bz-Asp = f_a) and in the overall copolymer (Z-Orn = cF_{oz} and Bz-Asp = cF_a) as a function of overall monomer conversion, during *n*-butylamine-initiated copolymerization of Bz-Asp NCA with Z-Orn NCA started with $f_a = 0.29$. The mole fraction of Bz-Asp NCA in the feed decreases with overall conversion, this explains the tendency of Bz-Asp NCA to add to the growing chain more frequently than Z-Orn NCA and the higher initial Bz-Asp in the copolymer compared to starting molar fraction. With increasing conversion, the feed composition becomes richer in Z-Orn NCA, whilst the copolymer composition initially has higher Bz-Asp composition. As the degree of conversion increases further, the amount of Z-Orn in the copolymer increases as well.

5.3.2.1. Copolymerization curve for Z-Orn and Bz-Asp system and assessment of reactivity ratios

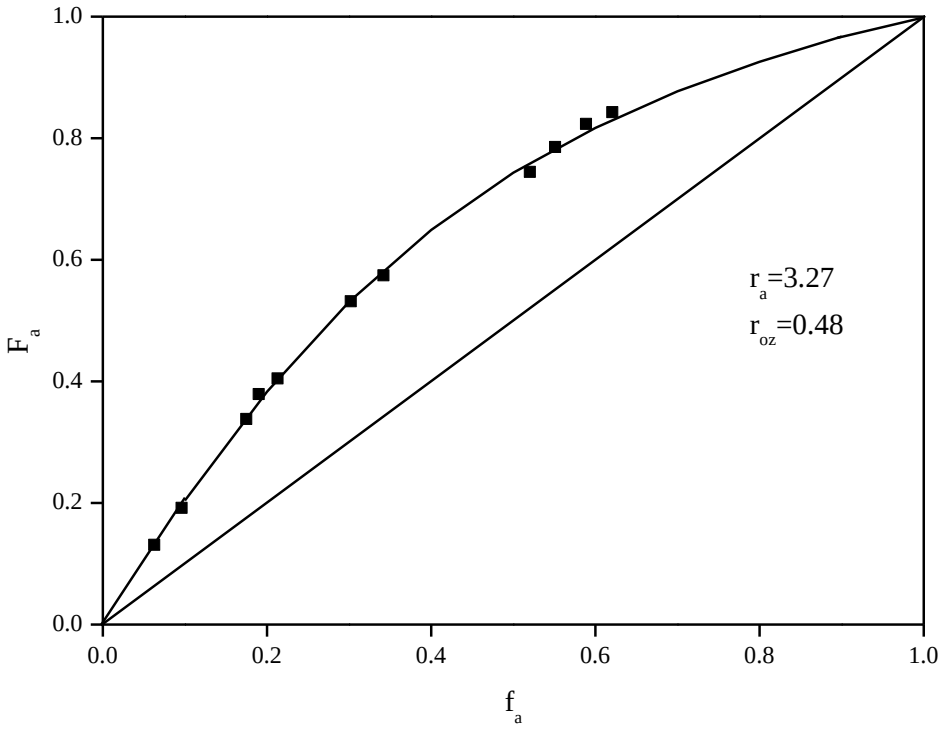

Figure 5-12 Copolymer compositions versus feed composition for copolymerization of f-Orn NCA with Bz-Asp NCA. The drawn curve through the experimental data points was calculated with $r_a = 3.27$ and $r_{oz} = 0.48$.

From the three copolymerization reactions carried out with $f_a^0 = 0.1$, 0.4 and 0.7, a copolymer composition curve was constructed and reactivity ratios estimated to be $r_a = 3.27$ and $r_{oz} = 0.48$. The copolymerization curve in Figure 5-12 was constructed with f_a and F_a representing Bz-Asp composition in the feed and copolymer respectively.

5.3.2.2. Contour plot of reactivity ratios: Bz-Asp: Z-Orn system

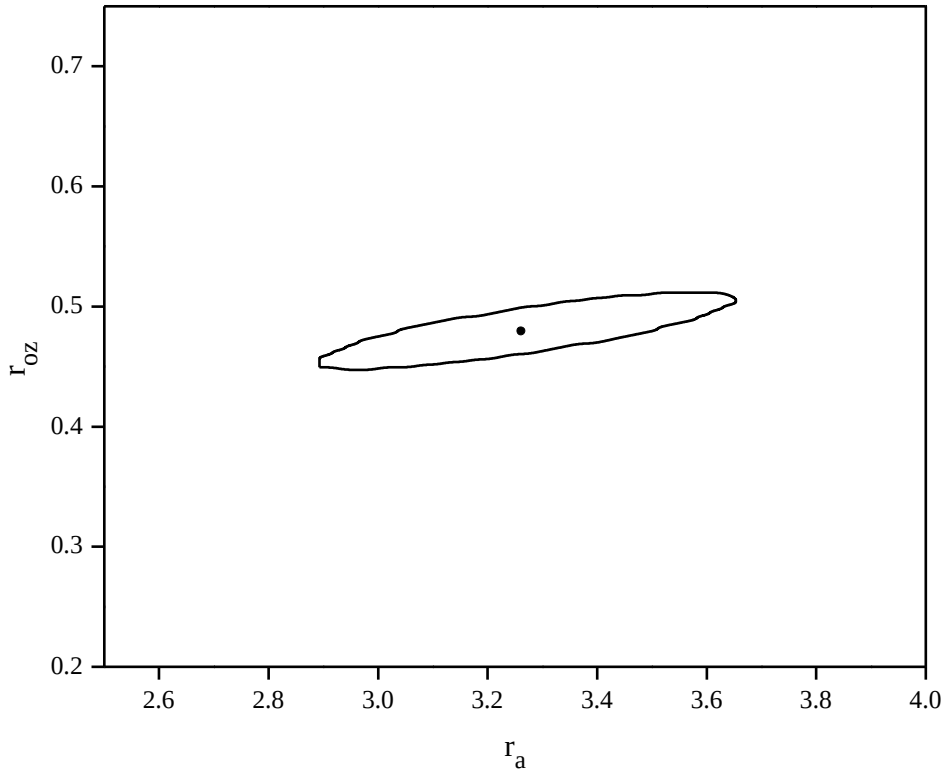

Figure 5-13 The 95% joint confidence interval of reactivity ratios for the Bz-Asp (r_a): Z-Orn (r_{oz}) copolymerization system.

Figure 5-13 illustrates the 95% joint confidence interval of reactivity ratios, again a broad distribution in r_a and narrow distribution for r_{oz} is observed. For all the above mentioned copolymerization systems, the contour plots gave an idea of where the values of reactivity ratios could be found.

5.3.3. Monitoring kinetics of Gly/f-Orn system

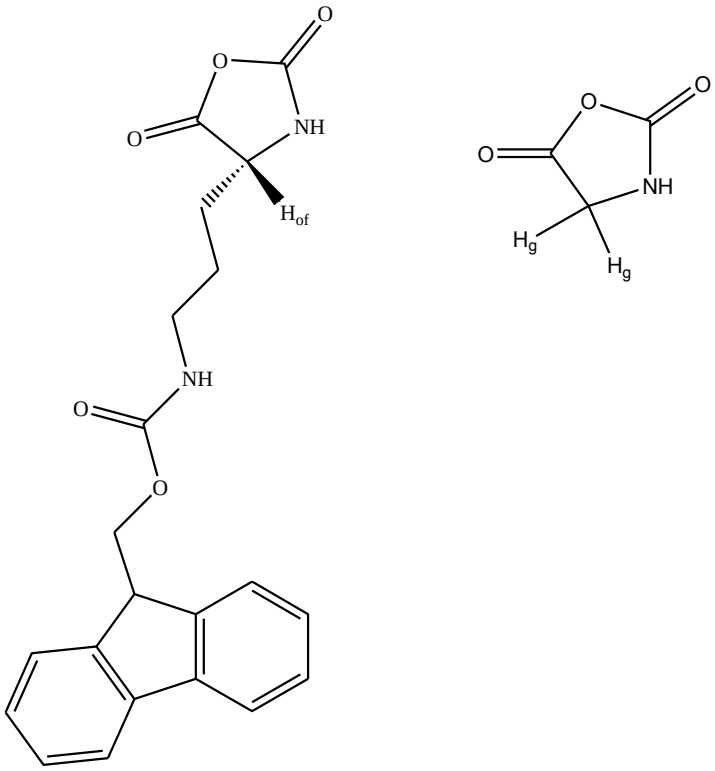

Scheme 5-5 Chemical structures of f-Orn NCA and Gly NCA indicating endocyclic protons that were monitored for kinetic profiles.

A copolymerization reaction mixture with initial feed f_g^0 = 0.43 proceeded in DMSO-d_6 for 14 hours at 25 ^oC. The progress of copolymerization was followed by monitoring the endocyclic αCH$_2$ (H_g) for Gly NCA and endocyclic αCH (H_{o1}) for f-Orn NCA as shown in Scheme 5-5. The signal intensities and the equations in Section 5.3.3.1, allowed the individual and overall conversions, feed and copolymer compositions to be monitored during copolymerization.

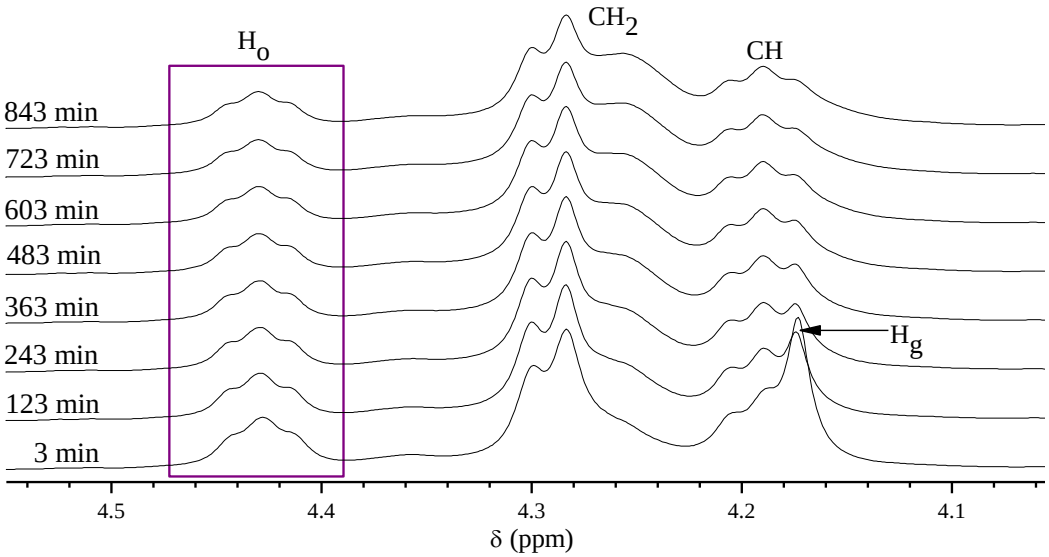

Figure 5-14 ^{1}H NMR spectra as a function of time, illustrating a region from 4.0 - 4.60 ppm during copolymerization of f-Orn NCA and Gly NCA, started with $f_g^0 = 0.57$ in DMSO-d_6 at 25 ^{o}C for 14 hours with 2 hour intervals.

Figure 5-14 illustrates an array of spectra as function of time during copolymerization of Gly NCA and f-Orn NCA for the region [4.0 ≤ δ (ppm) ≤ 4.60]. Protons H_o and H_g (2 protons) were used to monitor copolymerization of Gly/f-Orn, the protons labelled CH_2 and CH are protons from the fmoc moiety of ornithine, from Figure 5-14 the H_g proton used to monitor Gly NCA is overlapping with the CH proton from the fmoc moiety.

5.3.3.1. Equations for the f-Orn/Gly copolymerization system

Equation 5-14 Conversion of N_{δ}-fluorenylmethyloxycarbonyl-L-ornithine NCA as a function of time.

$$X_o = \frac{I(CH_1^o)_0 - I(CH_1^o)_t}{I(CH_1^o)_0}$$

Equation 5-15 Conversion of glycine NCA as a function of time.

$$X_g = \frac{I\left(CH_2^g\right)_0 - I\left(CH_2^g\right)_t}{I\left(CH_2^g\right)_0}$$

Equation 5-16 Overall conversion as function of time.

$$X_t = 1 - \frac{2[I(CH_1^o)_t] + I\left(CH_2^g\right)_t}{2[I(CH_1^o)_0] + I\left(CH_2^g\right)_0}$$

Equation 5-17 Instantaneous feed composition of glycine NCA as a function of time.

$$f_g = \frac{I\left(CH_2^g\right)_t}{2[I(CH_1^o)_t] + I\left(CH_2^g\right)_t}$$

Equation 5-18 Overall copolymer composition of glycine as a function of time.

$$F_g = \frac{I\left(CH_2^g\right)_0 - I\left(CH_2^g\right)_t}{I\left(CH_2^g\right)_0 - I\left(CH_2^g\right)_t + 2[I(CH_1^o)_0 - I(CH_1^o)_t]}$$

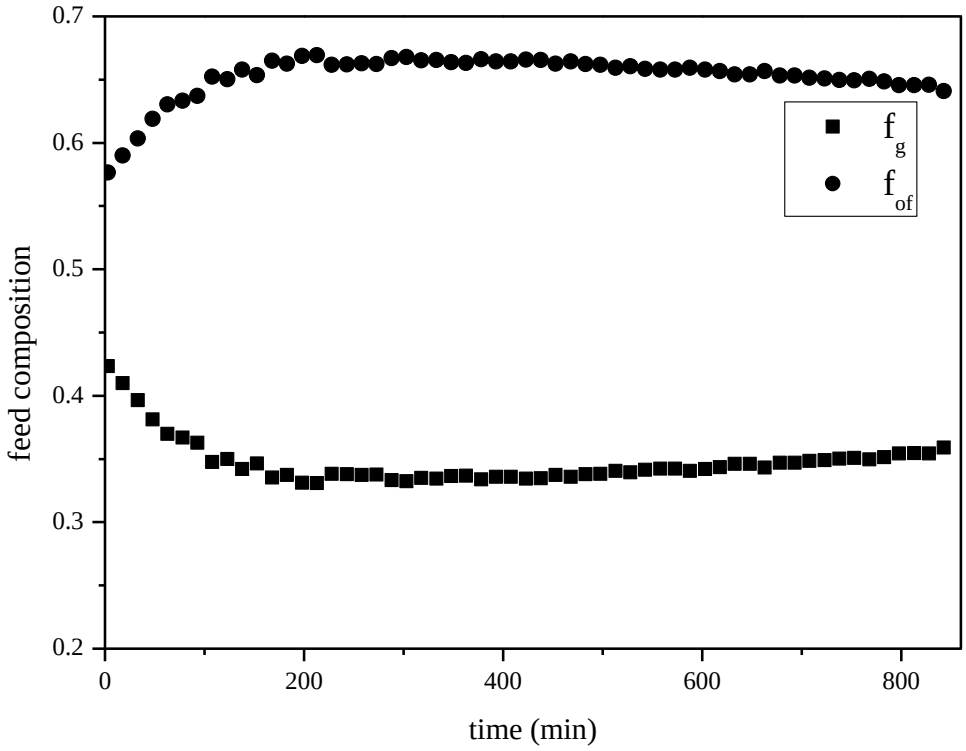

Figure 5-15 Instantaneous feed composition with time for copolymerization of Gly NCA and f-Orn NCA conducted in DMSO-d_6 at 25 ^{o}C.

Figure 5-15 illustrates the variation of feed composition as a function of time for copolymerization of f-Orn and Gly-NCAs started with at f_g^0 = 0.43. The effect of the overlapping peaks can be seen as both comonomer feed compositions are showing changes during the early stages, but as the intensity of Gly peak decreases with time it becomes difficult to track its changes as it is masked by the protons from f-Orn residue. Gly NCA only has αCH_2 that can be used to monitor its kinetics. It was therefore suggested that an ornithine protecting group be used with protons resonating at different chemical shifts.

5.3.4. Monitoring Gly/Z-Orn copolymerization system

Based on the overlapping peaks discussed in Section 5.3.3.1, an ornithine derivative protected with Carbobenzyloxy (Z) group was selected and copolymerization with Gly NCA was monitored as a function of time. The Gly NCA showed rapid consumption upon copolymerization with Z-Orn NCA and its behaviour was identical to the one observed during its homopolymerization. The change in feed composition as a function of time for the comonomers is illustrated in Figure 5-16.

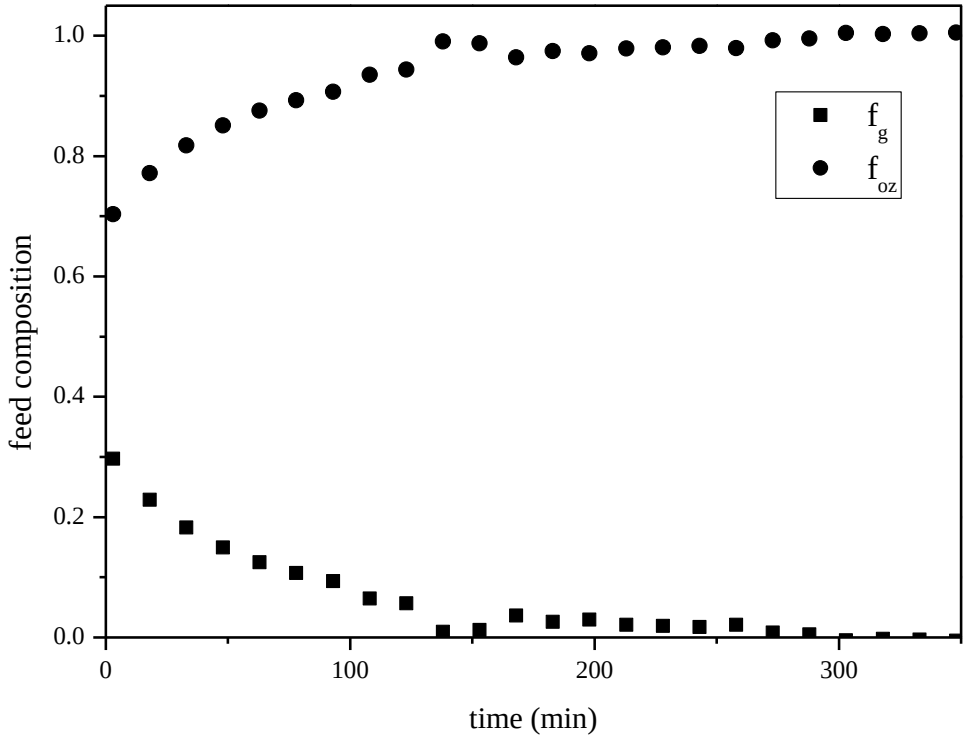

Figure 5-16 Feed composition of comonomers as a function of time during copolymerization of Gly and Z-Orn NCAs in DMSO-d_6 started with $f_g = 0.30$.

Figure 5-16 shows rapid consumption of Gly NCA in the copolymerization mixture. This behaviour of Gly NCA was also observed for this system in all copolymerization mixtures and therefore it was hard to efficiently monitor the kinetics of this system. This behaviour of Gly NCA in this copolymerization system was identical to the one observed during its homopolymerization where it was completely consumed in less than 200 minutes. The conclusion would be that Gly NCA has a high tendency to homopolymerize compared to its cross propagation with Z-Orn NCA.

5.4. Terpolymerization introduction

Terpolymerization involves simultaneous propagation of three different monomers during which they are consumed to generate a terpolymer. The propagation steps are given in a way similar to binary copolymerizations, thus the rate of consumption of monomers and steady state assumptions can be used to derive an equation that correlate comonomer composition and terpolymer composition and therefore it is reasonable to use reactivity ratios obtained from binary copolymerizations in a more complex Alfrey-Goldfinger equation to predict terpolymer compositions.[13,14]

Few terpolymerization studies are documented for NCAs of amino acids.[15,16] Terpolymerization of NCAs of leucine, valine and β-benzyl-L-aspartate initiated by triethylamine in dioxane was reported, reactivity ratios were determined from binary copolymerizations and used to estimate terpolymer compositions using Alfrey-Goldfinger equation for ternary systems, it was reported that there was no statistical difference between calculated terpolymer composition and the actual terpolymer compositions.[16]

In this study, homopolymerization and copolymerization experiments were used to set up conditions for terpolymerization studies, copolymerization studies also gave an idea of how the monomers will behave during terpolymerization based on the reactivity ratios from binary copolymerization. Also, from copolymerization studies, a conclusion can be drawn on which comonomers to use to follow terpolymerization reaction or kinetics, *e.g.* after it was observed that f-Orn NCA cannot be used along with Gly NCA due to overlaps of proton peaks, Z-Orn which can be used with both Gly and Bz-Asp NCAs was employed for terpolymerization. The only difference between Z-Orn and f-Orn is the protecting group that is at a distance far from the reactive site, *i.e.* the NCA ring and therefore its influence on the reactivity of the NCA ring is not expected to be that significant (see Figures 5-7 and 5-11). In a comparison between the copolymerization of Bz-Asp/Z-Orn and Bz-Asp/f-Orn systems, there was no significant difference in their reactivity ratios, hence the reactivity of Z-Orn NCA can be assumed to be very close to that of f-Orn NCA and therefore the latter can be used in terpolymerization studies with reactivity ratios assumed to be identical to those of the former.

5.4.1. Experimental procedure for terpolymerization reaction

The *in situ* ^{1}H NMR procedure was the same as the one used for copolymerization and homopolymerization studies. Terpolymerization kinetics was followed with *in situ* ^{1}H NMR for 14 hours. In a typical terpolymerization experiment: Gly NCA (0.0248 g, 0.245 mmol), Bz-Asp NCA (0.0599 g, 0.240 mmol) and Z-Orn NCA (0.0701 g, 0.240 mmol) were dissolved in 2.4 mL DMSO-d_6. The solution was then transferred into a Wilmad® quick pressure valve NMR tube that already contained *n*-butylamine (0.6 µL, 0.0292 mmol). The monomer to initiator ratio was set to 25. The sample in the NMR tube was subjected to three freeze-pump-thaw cycles and the NMR experiment was carried out as in Section 5.4.1.1 where the reaction was allowed to proceed for 14 hours (overnight) at 25 ^{o}C.

5.4.1.1. *In situ* ^{1}H NMR spectroscopy procedure

The ^{1}H NMR spectra were recorded with a 400 MHz Varian Unity Inova spectrometer. The ^{1}H NMR spectra were acquired with 3µs (40°) pulse width and 4 seconds acquisition time. For the *in situ* experiments, samples were first defrosted, then inserted into the magnet at 25 °C and the magnet shimmed, the first spectrum collected served as reference. Subsequent spectra were collected at 15 minutes intervals for 14 hours. Phase correction was performed automatically whilst baseline correction and integration were performed manually using ACD Labs 12.0 ^{1}H NMR processor.

5.4.2. Results and discussions

5.4.2.1. Monitoring terpolymerization of Z-Ornithine, Glycine and Benzyl-Aspartate NCAs

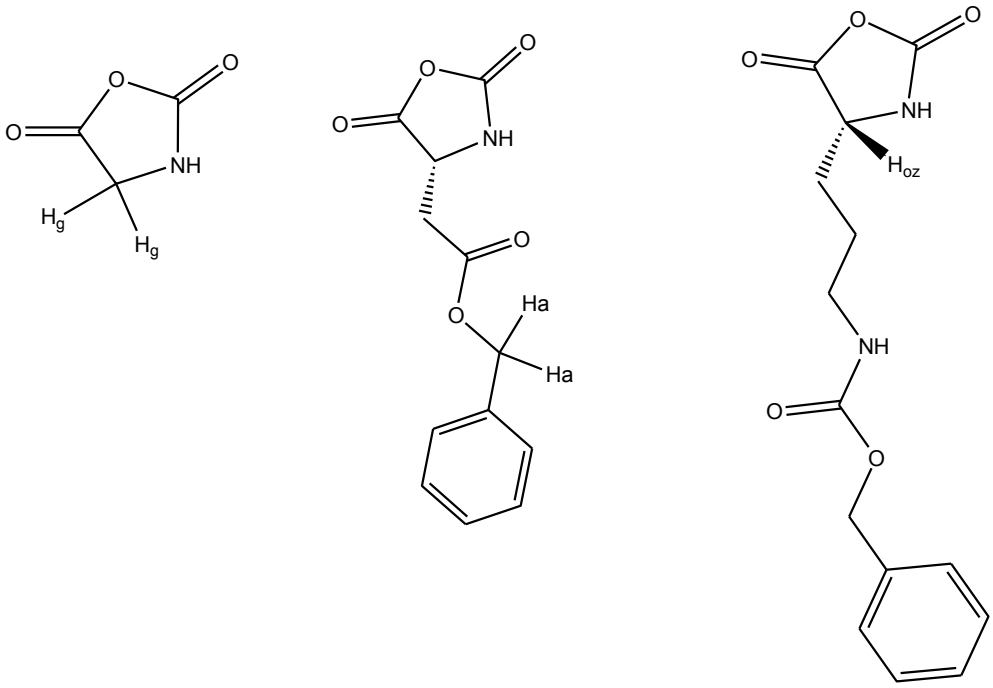

Scheme 5-6 Chemical structures of Gly NCA (H_g), Bz Asp NCA (H_a) and Z-Orn NCA (H_{oz}) indicating protons that were used to monitor kinetic profiles.

Scheme 5-6 shows the chemical structures of the NCAs used for terpolymerization studies, the labelled protons were used to follow consumption of the NCAs as a function of time. These protons resonated at well separated chemical shifts (see Figure 5-17) hence changes in individual and overall conversion, feeds and copolymer compositions were computed during terpolymerization as a function of time.

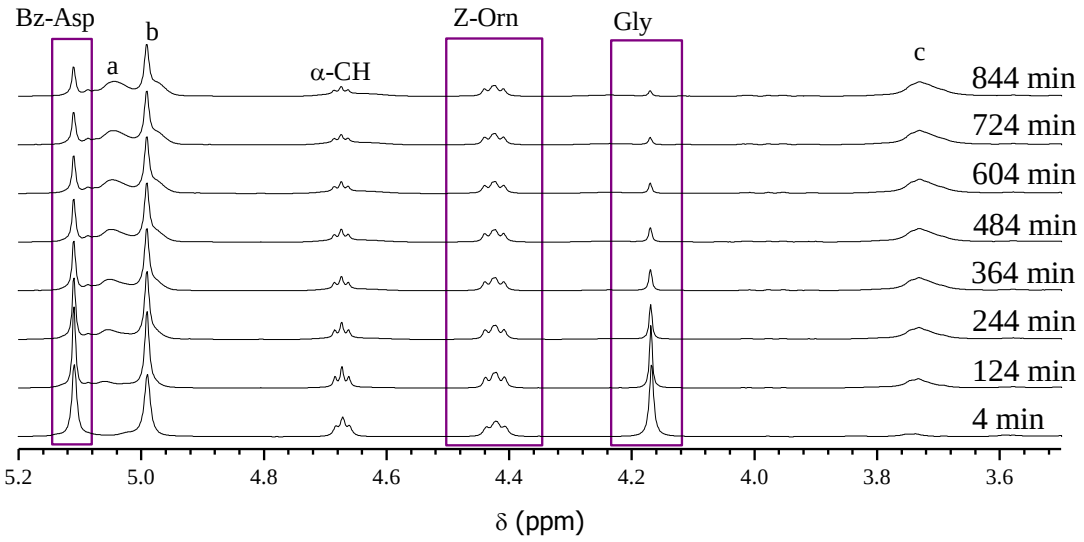

Figure 5-17 ^{1}H NMR spectra at different reaction times illustrating the region from 4.0 to 5.2 ppm during terpolymerization of NCAs of Z-Orn, Bz-Asp and Gly in DMSO-d_6 for 14 hours at 25 °C started with $f_{oz}^{0} = 0.37$, $f_{a}^{0} = 0.33$ and $f_{g}^{0} = 0.30$ respectively.

Figure 5-17 illustrates ^{1}H NMR spectra as a function of time during terpolymerization of Gly, Z-Orn and Bz-Asp NCAs. The peaks labelled Gly, Z-Orn and Bz-Asp were used to monitor consumption of each monomer as a function of time during terpolymerization. The peak assigned a corresponds to the Bz-Asp peak in the terpolymer, b is the $ArCH_2$ of Z-Orn in the terpolymer as well as in the monomer, whilst αCH represents Bz-Asp in the feed with a shoulder appearing at a later stage of the reaction and the peak labelled c was assigned to Gly (Glycine unit) in the terpolymer, however the Z-Orn peak intensity in the terpolymer is very weak for this ternary mixture but is observed to be occurring in the region between 4.3-4.2 ppm (when the scale along the Y axis is increased). Upon recording the intensities of the NCA related peaks as function of time, it was observed that the NCA-proton peaks labelled in Scheme 5-6 decreased with increasing time.

Terpolymerization of a mixture of comonomers occurs with consumption at different conversion rates for each monomer. Thus a shift in the terpolymer mixture will be found from one degree of conversion to another. Therefore composition changes of comonomers in feed and terpolymer can be represented as a function of overall conversion as shown in Figures 5-18 and 5-19.

5.4.2.2. Terpolymer composition changes

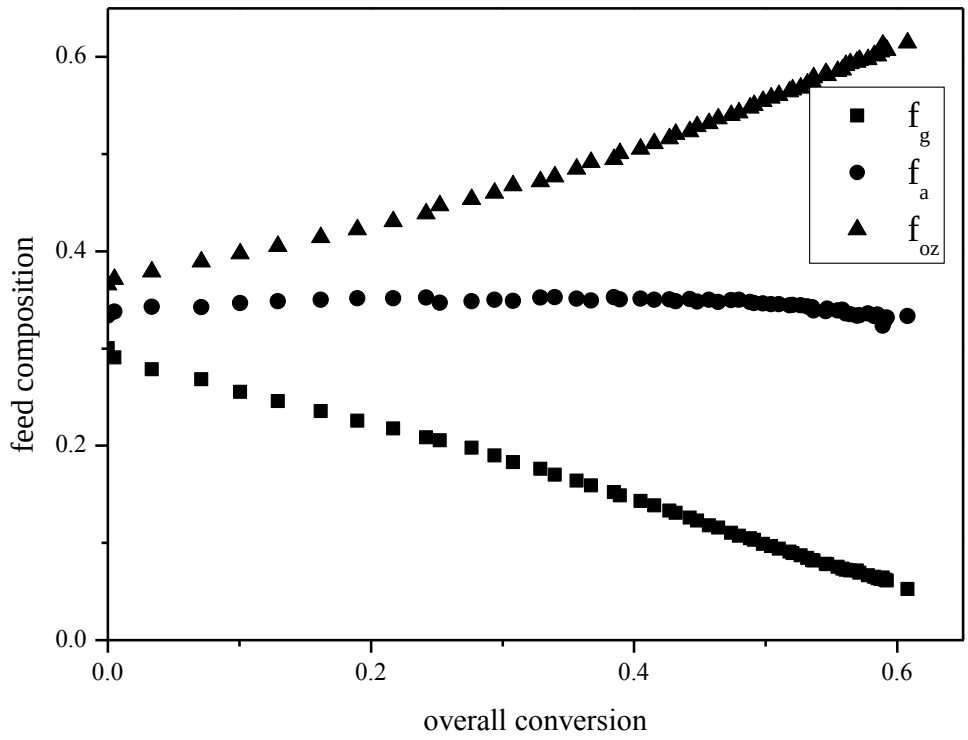

Figure 5-18 Comonomer compositions in the feed (ternary mixture) as a function of overall conversion during terpolymerization of Z-Orn, Gly and Bz-Asp NCAs in DMSO-d_6 started with $f_{oz}^{0} = 0.36$, $f_a^{0} = 0.33$ and $f_g^{0} = 0.31$, respectively.

Figure 5-18 shows variations of comonomer feed compositions of NCAs of Z-Orn (f_{oz}), Bz-Asp (f_a) and Gly (f_g) as a function of overall conversion. At low overall conversion of up to 20%, only small changes are observed in feed composition. As the degree of conversion increases further, significant changes are observed with Gly NCA decreasing significantly in the feed whilst the Z-Orn NCA increases steadily in the feed and only small changes of Bz-Asp NCA. The decrease in Gly NCA is indicative of its preferential addition to the growing terpolymer chain compared to its comonomers, with increasing Z-Orn NCA confirming its low reactivity compared to the other two NCAs and whilst Bz-Asp NCA seems to be the mediator between the two monomers. As overall conversion increases further and feed composition starving of Gly NCA, the feed composition becomes richer in Z-Orn NCA and Bz-Asp NCA implying a tendency of drifting away from a terpolymer with high Gly composition towards a terpolymer richer in segments of Z-Orn and Bz-Asp. This implies that, at very low fraction of Gly NCA in the ternary mixture, a drift towards a terpolymer rich in Bz-Asp and later in Z-Orn will occur.

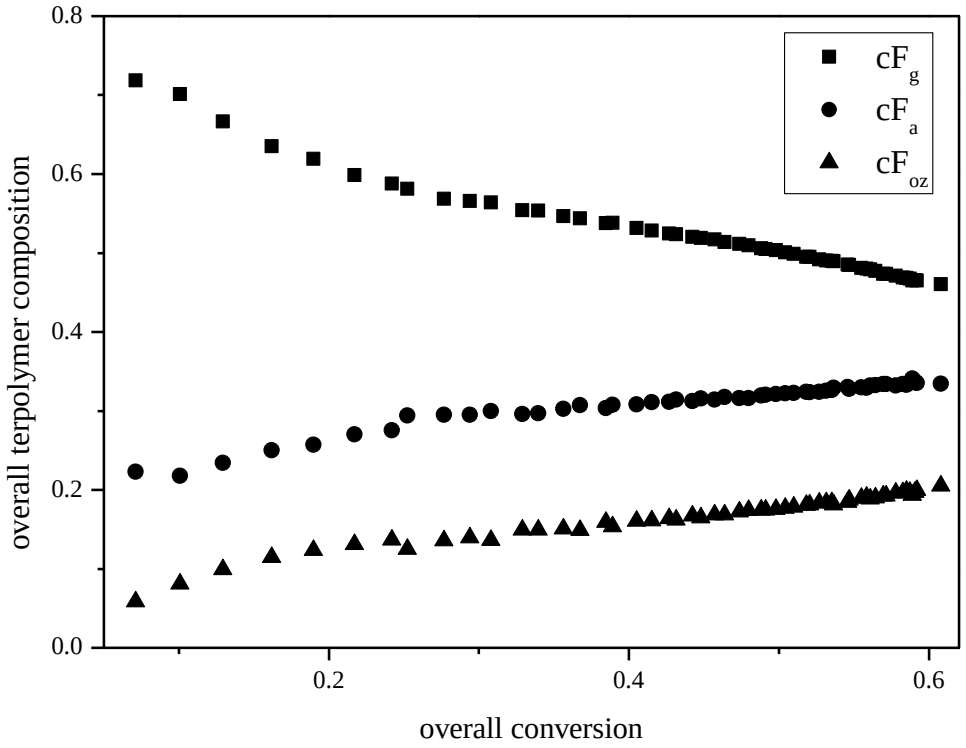

Figure 5-19 Overall terpolymer compositions as a function of overall conversion during terpolymerization reaction of NCAs of Z-Orn, Bz-Asp and Gly in DMSO-d_6 for 14 hours at 25 °C started with $f_{oz}^0 = 0.37$, $f_a^0 = 0.33$ and $f_g^0 = 0.30$, respectively.

The starting ternary mixture of $f_{oz}^0 = 0.37$, $f_a^0 = 0.33$ and $f_g^0 = 0.30$ generates a terpolymer with lower content of Z-Orn ($F_{oz} = 0.080$), and Bz-Asp ($F_a = 0.21$) and richer in Gly ($F_g = 0.71$) (Figure 5-19). Figure 5-19 illustrates changes in overall terpolymer compositions for the comonomers as functions of overall conversion, at low conversion, the terpolymer had very low overall composition of Z-Orn and Bz-Asp in comparison to Gly, but as conversion increases both Z-Orn and Bz-Asp fractions in the copolymer are increasing whilst the fraction of Gly NCA in the ternary mixture decreases (Figure 5-19). As the degree of conversion increases further, the Bz-Asp comonomer recovered its initial feed composition in the terpolymer, as can be seen with $cF_a = 0.33$ at the end of copolymerization. Hence the global terpolymer represents a mixture of terpolymer-chain segments with extreme compositional heterogeneity as we end up with a terpolymer composition of $cF_{oz} = 0.21$, $cF_a = 0.33$ and $cF_g = 0.46$ with both cF_{oz} and cF_a increasing in the copolymer, whilst cF_g decreases.

5.4.3. Table of reactivity ratios

Table 5-1 Monomer pairs and reactivity ratios that were obtained in this study.

	Gly	Bz-Asp	f-Orn	Z-Orn
Gly	-			
Bz-Asp	$r_g = 2.51$ $r_a = 0.455$	-		
f-Orn		$r_a = 3.92$ $r_f = 0.398$	-	
Z-Orn		$r_a = 3.27$ $r_z = 0.481$		-

The overall contour plot of comonomer pairs

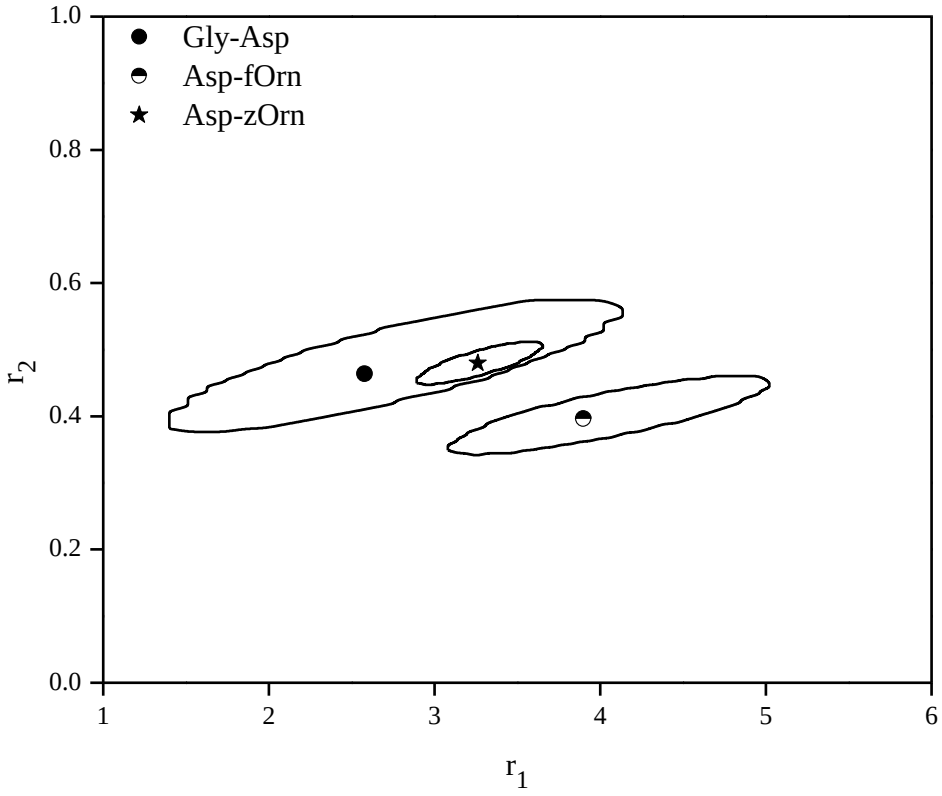

Figure 5-20 Confidence intervals of reactivity ratios for the comonomer pairs obtained in this study.

Table 5-1 compiled binary copolymerizations carried in this study with respective reactivity ratios and Figure 5-20 illustrates their 95% confidence intervals.

5.5. Conclusions

On the basis of reactivity ratios obtained for the binary copolymerizations of NCAs used in this study, the NCAs can be arranged in the following order in terms of reactivity: Glycine > β-benzyl-L-Aspartate > N_{δ}-Fluorenylmethyloxycarbonyl-L-Ornithine ≈ N_{δ}-Carbobenzyloxy-L-Ornithine. The effect of the protecting group on ornithine side chains observed by comparing their reactivity ratios with β-benzyl-L-Aspartate seems to be minimal, but at this stage it is still somewhat premature to draw explicit conclusions. Although binary copolymerization of Glycine NCA with any of the ornithine monomers did not yield reactivity ratios, Glycine NCA can be assumed to have a higher reactivity than ornithine NCAs by comparing the reactivity of these NCAs with β-benzyl-L-Aspartate NCA. With the understanding of binary copolymerizations, reactivity and behaviour of the NCAs, terpolymerization reaction was studied with approximately equimolar fractions of comonomers, although there is an anticipated increase in complexity of propagation with addition of a third monomer in copolymerization, the terpolymerization of NCA in this case did not affect the behaviour of NCAs as all retained their expected reactivity during terpolymerization.

5.6. References

(1) Miller, W. G.; Nylund, R. E. *J. Am. Chem. Soc.* **I965**, *87*, 3542.

(2) Ishiwari, K.; Nakajima, A. *Bull. Inst. Chem. Res., Kyoto Uni* **1976** *54*, 72.

(3) Miyachi, Y.; Jokei, K.; Oka, M.; Hayashi, T. *Eur. Polym. J.* **1999**, *35*, 395.

(4) Miyachi, Y.; Jokei, K.; Oka, M.; Hayashi, T. *Eur. Polym. J.* **1999**, *35*, 607.

(5) Kumar, A. *CPR* **2011**, *1*, 219.

(6) Skeist, I. *J. Am. Chem. Soc.* **1946**, *68*, 1781.

(7) Ishiwari, K.; Hayashi, T.; Nakajima, A. *Bull. Inst. Chem. Res., Kyoto Uni* **1977**, *55*, 366.

(8) Ishiwari, K.; Hayashi, T.; Nakajima, A. *Polym. J. (Tokyo, Jpn.)* **1978**, *10*, 87.

(9) Patchornik, A.; Shalitin, Y. *Anal. Chem.* **1961**, *33*, 1887.

(10) Zelzer, M.; Heise, A. *Polym. Chem.* **2013**, *4*, 3896.

(11) van Herk, A. M. *J. Chem. Educ.* **1995**, *72*, 138.

(12) Hernández, J. R.; Klok, H.-A. *J. Polym. Sci., Part A: Polym. Chem.* **2003**, *41*, 1167.

(13) Walling, C.; Briggs, E. R. *J. Am. Chem. Soc.* **1945**, *67*, 1774.

(14) Tosi, C. *Eur. Polym. J.* **1972**, *8*, 91.

(15) Hull, W. E.; Kricheldorf, H. R. *Die Makromolekulare Chemie* **1980**, *181*, 1949.

(16) Wamsley, A.; Jasti, B.; Phiasivongsa, P.; Li, X. *J. Polym. Sci., Part A: Polym. Chem.* **2004**, *42*, 317.

Chapter VI: Outlook

Summary

This chapter deals with future objectives, *i.e*. discussion on how terpolymer synthesis can be optimized to maximize the frequency of RGD sequences, based on results obtained from copolymerization kinetics. It also went further as to give an idea of how the RGD sequence will be analysed and probably be quantified. Finally, the plans are discussed of how the prepared terpolymers will be immobilized on hydrogels and tested in contact with mammalian cells.

6. Future work and recommendations

On basis of homopolymerization and copolymerization kinetics investigations carried out in this study, the amino acid NCAs can be arranged based on their reactivity as: glycine ≥ β-benzyl-L-aspartate ≥ N_{δ}-x-L-ornithine, where x represent one of the two ornithine protecting groups. This was further corroborated by a preliminary terpolymerization reaction carried out with equimolar feed compositions of the three NCAs, where the carbobenzyloxy (Z) protected ornithine was used. The equimolar ternary feed compositions initially produced a terpolymer with very low content of Z-ornithine and high glycine content relative to β-benzyl-L-aspartate. As overall monomer conversion increased, the glycine fraction in the ternary mixture gradually decreased whilst that of β-benzyl-L-aspartate and N_{δ}-carbobenzyloxy-L-ornithine both increased slowly. This resulted in an eventual increase in overall terpolymer compositions of β-benzyl-L-aspartate and N_{δ}-carbobenzyloxy-L-ornithine whilst that of glycine decreased.

Polypeptides prepared by ROP of NCAs are considered as models for the understanding of proteins. A large amount of research has been devoted to copolypeptides chains composed mainly of one amino acid chain linked to other chains (*e.g*. blocks and graft) or to nonpeptide chains. These polypeptides displayed interesting properties such as secondary structures, self-assembly, hydrogel formation and have potential as carriers for drug delivery devices. Structurally random copolypeptides are closer mimics of natural proteins. ^{13}C NMR and ^{15}N NMR can be used for characterization of terpolypeptides and recently HPLC seems to be a promising technique as it reported individual kinetics for each monomer. In this study an *in*

situ ^{1}H NMR protocol is developed to successfully monitor copolymerizations and a preliminary terpolymerization reaction.

In designing terpolypeptides, a specific amino acid sequence can be targeted for a certain purpose or for a specific function associated with it. However, this requires a background of binary copolymerization studies, where statistical methods based on terminal models are employed for the calculation of triad sequences using only reactivity ratios and monomer feed compositions. In this study, the copolymerization of NCAs of Glycine (Gly), Ornithine (Orn) and Aspartic acid (Asp) was studied. It is recommended that tripeptide sequence (triad) of Orn-Asp-Gly be targeted. The Orn segment in these terpolypeptides can be converted to Arginine segments via a plausible guanidation reaction, hence the conversion of Orn-Asp-Gly sequence to Arg-Asp-Gly basically known as RGD tripeptide sequence.

The RGD tripeptide sequence as a composite of extracellular matrix glycoproteins such as fibronectin and vitronectin was found to be crucial for adhesion of cells, cell growth and cell interaction. These were also corroborated by immobilising short peptides composed of RGD sequence on surfaces. It is recommended that the RGD possessing terpolypeptides be immobilised on hydrogels and tested for cell attachment and cell interaction studies. Hydrogels are recommended for their mechanical and biocompatible properties but mostly these 3D structures can have high water content which mimic body tissues and can permit diffusion of nutrients.

The section below describes in details the context above *i.e*. synthesis of terpolymers and their modification, including immobilization on hydrogels and cell attachment for proposed further study.

6.1. The arginine-glycine-aspartic acid tripeptide sequences

Integrins are cell surface receptors that mediate cell-cell adhesions and cell-extracellular matrix interactions in multicellular organisms. Integrins are heterodimers of two non-covalently associated transmembrane α and β subunits. To date, in mammals 18 α and 8 β subunits are known, these subunits associate to 24 different heterodimers.[1,2] The ligand specificity of integrins is determined by the combinations of the subunits. For example, the $\alpha_{IIB}\beta_3$ integrin binds to vitronectin, fibrinogen, von Willebrand factor, thrombospondin and fibronectin. Some extracellular matrix (ECM) molecules like fibronectin are ligands to several integrins.[2] Cellular recognition studies revealed that of more than 2000 amino acids in fibronectin, the RGD tripeptide sequence is essential for cell interactions. In addition, assessment of an RGDS tetrapeptide sequence found in fibronectin showed that substitution of any of its amino acids beside serine (S) decreases interaction with normal rat kidney cells.[3]

Since the discovery of its cell interaction ability, peptides with RGD sequence have been covalently linked to polymers and embedded on substrates (surfaces, slides or hydrogels), and assessed for cell interactions.[4] The polymers used for ligand coupling are normally biocompatible polyesters or polyethylene glycol.[5,6] These polymers lack functionality. Therefore they are often coupled to functional poly(amino acid)s such as polyglutamate or polylysine, which possess carboxyl and amine functionality, respectively, for RGD peptide coupling. Block copolypeptides can be functionalized with RGD peptides, in a three step approach, by first synthesizing the copolypeptide, then grafting/coupling the RGD peptide onto the copolypeptide, and finally immobilizing the functionalized copolypeptide onto a substrate. This approach is complex, and often results in incomplete incorporation of RGD peptide.[7,8] In addition, the synthesis of RGD peptides is also of complex nature involving sequential peptide synthesis, which often produces low yields and is only feasible for relatively short peptides.[9,10]

6.2. Determination of initial experimental conditions.

The envisaged terpolymerization reaction involves the simultaneous propagation of three monomers to generate a terpolymer with a statistically controlled monomer sequence distribution. The terpolymer composition depends on the relative concentration of comonomers, their reactivity ratios and overall conversion. If the so-called terminal model for copolymerization is assumed to describe the polymerization, reactivity ratios obtained from

the three relevant binary copolymerizations can be used to predict terpolymer composition and there has been little or no observed difference between predicted and experimental terpolymer compositions.[11] Therefore, with the knowledge of reactivity ratios from binary copolymerizations, the probability of occurrence of triad sequences of the comonomers per number of repeating units can be influenced by varying relative initial comonomer compositions as applied in vinyl polymers.[12]

Similarly, reactivity ratios from binary copolymerization were determined and can thus be used to maximize the probability of occurrence of *R*GD triads (where the italic *R* stands for ornithine segments in terpolypeptides which will subsequently be converted to arginine segments) by choosing suitable initial feed compositions of the NCAs of amino acids.

6.3. Experimental verification of theoretical prediction.

Terpolypeptides can be constructed experimentally from predetermined initial feed compositions. The actual probability of *R*GD triads will be analysed using ^{13}C NMR by focusing on glycine centred triads. The application of ^{13}C NMR to determine triads' distribution is used routinely to analyse vinyl polymers[12,13] and in terpolypeptides.[14] Peptide bonds due to different amino acid sequences in statistical terpolypeptides were characterized with ^{15}N NMR.[15] However this approach requires ^{15}N labelled NCAs, and as alternative, the unprecedented ^{14}N NMR can be employed for the characterization of terpolypeptide bonds.

6.4. Modification of terpolymer side chains

In the crude product, the terpolypeptides still possess both side chain protecting groups of aspartic acid and ornithine. The benzyl (Bz) and carbobenzyloxy (Z) protecting groups on aspartic acid and ornithine, respectively, are detached under similar conditions either by acid hydrolysis or hydrogenolysis using a palladium catalyst.[16] Subsequent to deprotection of side chains, guanidation of ornithine segments in the terpolypolypeptides will be the next step. Guanidation is the reaction where the amino groups of amino acids (particularly side chains) are converted to the guanidine group.[17] The most important application of the guanidation reaction is the conversion of ornithine segments in synthetic polypeptides to basic arginine segments. Arginine is difficult to incorporate directly due to complications in the preparation of its precursor NCA monomer. The mostly used guanidating agents are *O*-methylisourea (MIU) and 3,5-dimethyl-1-guanylpyrazole (DMGP) nitrate. The guanidation reaction conditions are mostly room temperature and aqueous medium at pH 9-11. Maximum

conversions are usually achieved by long reaction times (>24 hours) and the use of ionic compounds such as potassium iodide (KI) for conformational purposes.[18,19]

Guanidation of the ornithine segments on terpolypeptides can be used to afford arginine segments. Scheme 6-1 illustrates the guanidation reaction of ornithine to arginine segments using an MIU derivative. In the case of unexpected side reactions of Aspartic acid's carboxyl acid group during the guanidation, the fluorenylmethoxycarbonyl (fmoc)-protected ornithine can be introduced, since its deprotection is orthogonal to that of the Asp protecting group.

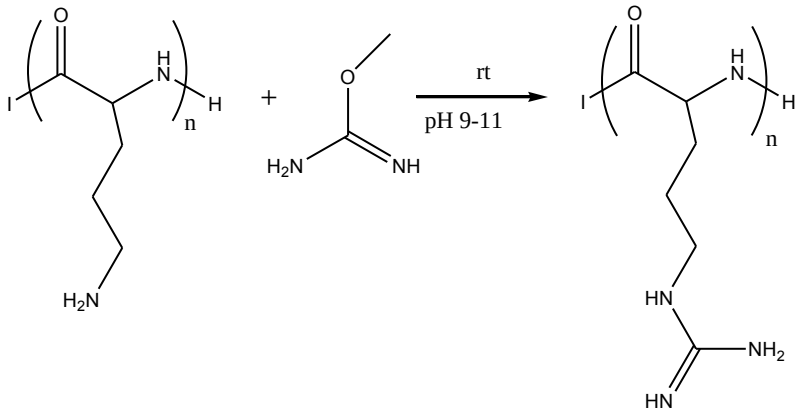

Scheme 6-1 Guanidation reaction of ornithine pendant groups.

6.5. Immobilization on hydrogels

Hydrogels have attracted significant interest as scaffolds in tissue engineering due to their mechanical and biocompatible properties. For example biocompatible poly(ethylene glycol) (PEG) hydrogels provide a highly swollen three-dimensional environment (similar to soft tissues) with high water content, which permits diffusion of nutrients. However, PEG hydrogels lack interaction with body cells. For this reason, RGD peptides are incorporated to PEG hydrogels via amine-carboxylic acid coupling. The procedure involves coupling of RGD peptides to monoacrylated PEG followed by photopolymerization in the presence of photoinitiator and diacrylated PEG to afford hydrogels.[20] Physical hydrogels with activated carboxyl groups for RGD peptide coupling can also be prepared via self-assembling block copolymers.[21]

The terpolypeptides with high probability of RGD will be immobilised by coupling on PEG hydrogels. Since propagation proceeds via the normal amine mechanism, it is believed that a large fraction of the terpolypeptide chains will retain the ω-amino end groups, which are

envisaged for coupling. By selecting the proper conditions, we anticipate that the guanidation reaction will be selective towards the pendant primary amine functionalities of Orn so that the ω-amino end groups will survive the guanidation reaction. If this would turn out not to be feasible, an amine-terminated PEG acrylate can be employed as macroinitiator for NCA terpolymerization, followed by photopolymerization to afford the RGD-functional PEG hydrogel.

6.6. Assessment of cell interactions with terpolypeptides

Interaction of RGD peptides with cells can be influenced by the RGD functionalized surface density, spacing between the RGD motifs and the surface of immobilization, the optimum spacing between RGD peptide and the surface for cell-ligand interactions is observed to be between 11-32 Å. One of the most determining factors in cell interaction studies are affinity and selectivity of integrins. RGD peptides have affinity for cell lines but show selectivity towards integrin type. The type of amino acids flanking the RGD tripeptide and the overall peptide structure (cyclic or linear) can be tuned for specific integrin selectivity. Cells express more than one type of integrin and they adopt to surfaces by upregulating a certain integrin that binds to the offered ligands on surfaces. The mechanism for adhesion of cells by RGD sequences is complex since RGD binds to a number of integrins and the receptor specificity varies among matrix molecules.[22] The selectivity of RGD peptides towards integrins is only essential for applications where certain cell-ligand interactions are targeted for specific purposes. However for cell interaction studies, cells such as human umbilical vein endothelial cells (HUVEC) or mouse fibroblast cells (3T3 or L-929), which are able to interact with a number of different RGD peptides are chosen.[4]

In this study we will be interested on whether the terpolypeptides possessing RGD triads synthesized via statistical terpolymerization interact with cells. HUVEC or mouse fibroblast cells' interactions with the terpolypeptides will be assessed since these cells showed interactions with many RGD peptides. The RGD bearing terpolypeptides tethered on hydrogels maybe applied as scaffolds that promote cell growth and tissue formation in tissue engineering.

6.7. References

(1) Hynes, R. O. *Cell* 2002, *110*, 673.

(2) Mecham, R. P.; Cheresh, D. A. *Integrins: Molecular and Biological Responses to the Extracellular Matrix*; Elsevier Science, 1994.

(3) Pierschbacher, M. D.; Ruoslahti, E. *Proc. Natl. Acad. Sci. U. S. A.* 1984, *81*, 5985.

(4) Hersel, U.; Dahmen, C.; Kessler, H. *Biomaterials* 2003, *24*, 4385.

(5) Jo, S.; Shin, H.; Mikos, A. G. *Biomacromolecules* 2001, *2*, 255.

(6) Tugulu, S.; Silacci, P.; Stergiopulos, N.; Klok, H.-A. *Biomaterials* 2007, *28*, 2536.

(7) Hu, X.; Chen, X.; Xie, Z.; Cheng, H.; Jing, X. *J. Polym. Sci., Part A: Polym. Chem.* 2008, *46*, 7022.

(8) Brandley, B. K.; Schnaar, R. L. *Anal. Biochem.* 1988, *172*, 270.

(9) Aufort, M.; Gonera, M.; Chaignon, N.; Le Clainche, L.; Dugave, C. *Eur. J. Med. Chem.* 2009, *44*, 3394.

(10) Yamada, K.; Nagashima, I.; Hachisu, M.; Matsuo, I.; Shimizu, H. *Tetrahedron Lett.* 2012, *53*, 1066.

(11) Wamsley, A.; Jasti, B.; Phiasivongsa, P.; Li, X. *J. Polym. Sci., Part A: Polym. Chem.* 2004, *42*, 317.

(12) Walling, C.; Briggs, E. R. *J. Am. Chem. Soc.* 1945, *67*, 1774.

(13) Brar, A. S.; Hekmatyar, S. K. *J. Appl. Polym. Sci.* 1999, *74*, 3026.

(14) Wamsley, A.; Phiasivongsa, P.; Jasti, B.; Li, X. *Journal of Polymer Science Part A: Polymer Chemistry* 2006, *44*, 4328.

(15) Hull, W. E.; Kricheldorf, H. R. *Die Makromolekulare Chemie* 1980, *181*, 1949.

(16) Hernández, J. R.; Klok, H.-A. *J. Polym. Sci., Part A: Polym. Chem.* 2003, *41*, 1167.

(17) Maga, J. A. *J. Food Sci.* 1981, *46*, 132.

(18) Konishi, Y.; van Nispen, J. W.; Davenport, G.; Scheraga, H. A. *Macromolecules* 1977, *10*, 1264.

(19) Vincent, V. PhD dissertation, Universitiet Gent, 2012.

(20) Zhu, J.; Beamish, J. A.; Tang, C.; Kottke-Marchant, K.; Marchant, R. E. *Macromolecules* 2006, *39*, 1305.

(21) Zhang, Z.; Lai, Y.; Yu, L.; Ding, J. *Biomaterials* 2010, *31*, 7873.

(22) LeBaron, R. G.; Athanasiou, K. A. *Tissue Engineering* 2000, *6*, 85.